

**GROUNDWATER MANAGEMENT APPROACH
AT KFUPM CAMPUS USING NUMERICAL
SIMULATION**

BY

TAJUDEEN MUHAMMAD IWALEWA

A Thesis Presented to the
DEANSHIP OF GRADUATE STUDIES

KING FAHD UNIVERSITY OF PETROLEUM & MINERALS

DHAHRAN, SAUDI ARABIA

In Partial Fulfillment of the
Requirements for the Degree of

MASTER OF SCIENCE

In

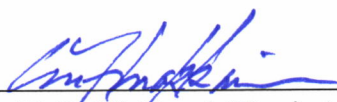
ENVIRONMENTAL SCIENCE

MAY 2012

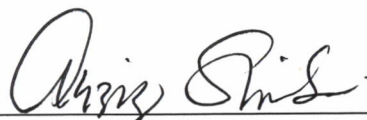
KING FAHD UNIVERSITY OF PETROLEUM AND MINERALS
DHAHRAN 31261, SAUDI ARABIA
DEANSHIP OF GRADUATE STUDIES

This thesis, written by **TAJUDEEN MUHAMMAD IWALEWA** under the direction of his Thesis Advisor and approved by his Thesis Committee, has been presented to and accepted by the Dean of Graduate Studies, in partial fulfilment of the requirements for the degree of MASTER OF SCIENCE.

Thesis Committee




Dr. M. H. Makkawi (Thesis Advisor)



Dr. A. M. Al-Shaibani (Member)




Dr. A. S. Elamin (Member)



Dr. A. M. Al-Shaibani

(Department Chairman)



Dr. S. A. Zummo

(Dean of Graduate Studies)



29/5/12

Date

DEDICATION

I lovingly dedicate
this thesis
to the memory of
my father:
Alhaji Imam Yusuf Iwalewa

ACKNOWLEDGEMENTS

I thank Allah for His limitless help and guidance.

Thanks are due to King Fahd University of Petroleum and Minerals for providing me with excellent computing facilities which aided the successful completion of this work.

I am deeply indebted to Dr. Mohammad Hussein Makkawi, my advisor, for his constant inspiration and guidance in making this work possible. I would like to express my gratitude to Dr. Abdalla S. Elamin, my committee member, for the unconditional support and encouragement I received from him. I would like to thank Dr. Abdulaziz M. Al-Shaibani, my committee member and Chairman of Earth Sciences Department, for his advice and valuable comments. My special appreciations are also due to Dr. Abdulaziz M. Al-Shaibani for making my stay at KFUPM worthwhile by listening to and solving my problems indefatigably.

Sincere and kind cooperations of all members of the Earth Sciences Department, Research Institute, Maintenance Department and Department of Faculty Housing are specially acknowledged.

Wholehearted gratitudes are due to my wife, Khairat Tajudeen-Iwalewa, for her love, patience and understanding which greatly helped in successful completion of this study. Special thanks and appreciations are due to my mother and other family members back home in Nigeria for their love and moral support. I would like to express my deep appreciation to Lateef Kareem for his love and supports.

My sincere appreciations are due to my friends and colleagues for their supports. In particular, constant help and encouragement by Dr. Abeeb Awotunde, Dr. Lameed Babalola, Dr. Balarabe Yushau, Dr. Ayub Adesina, Dr. P. K. Krishnakumar, Mr. Abdullateef Adedigba, Mr. Taiwo Odedairo, Mr. Moshood Kazeem, Jamal Al-Aamri, Mr. Tosin Okeyemi, Mr. Maaruf Hussain, Mr. Musah Ahmed Rufai, Mr. Mufatiu Bello, Mr. Abduljamiu Amao, Mr. Abdulafeez Popoola, Mr. Badie Sadiq Eqnaibi, Mr. Adnan Mubarak, Mr. Abdulafeez Adebiyi and others, too numerous to mention, are especially acknowledged.

TABLE OF CONTENTS

CHAPTER	PAGE
DEDICATION.iii
ACKNOWLEDGEMENTS.iv
LIST OF FIGURES.x
LIST OF TABLES.xiv
ABSTRACT.xv
الملخص.xvii
CHAPTER 1 INTRODUCTION.1
1.1 GENERAL.1
1.2 STUDY AREA.3
1.3 OBJECTIVES.4
1.4 DATA COLLECTION AND ANALYSES.6
1.5 PREVIOUS STUDIES.7
1.6 STATEMENT OF PROBLEM.10
1.7 THESIS OUTLINE.10
CHAPTER 2 GEOLOGICAL AND HYDROGEOLOGICAL SETTINGS.12
2.1 GEOLOGICAL SETTING.12
2.2 STRATIGRAPHY.14
2.2.1 ARUMA FORMATION.16
2.2.2 UMM ER RADHUMA (UER) FORMATION.17

CHAPTER	PAGE
2.2.3 RUS FORMATION.20
2.2.4 DAMMAM FORMATION.21
2.2.5 NEOGENE COMPLEX.24
2.3 KARST.25
2.4 AQUIFER SYSTEM IN THE STUDY AREA.27
2.4.1 UMM ER RADHUMA AQUIFER.27
2.4.2 RUS AQUITARD.36
CHAPTER 3 DEVELOPMENT OF SIMULATION MODEL FOR THE	
STUDY AREA.40
3.1 INTRODUCTION.40
3.2 CONCEPTUAL MODEL.40
3.3 MODELING TECHNIQUE.44
3.3.1 GROUNDWATER FLOW EQUATION.45
3.3.2 FINITE-DIFFERENCE EQUATION.46
3.3.3 INITIAL PIEZOMETRIC SURFACE..50
3.3.4 DISCRETIZATIONS AND BOUNDARY CONDITIONS.51
3.3.5 INITIAL ASSESSMENT OF INPUT PARAMETERS.58
3.3.5.1 HYDRUALIC PROPERTIES.58
3.3.6.2 WELL ABSTRACTIONS.59
3.4 MODEL CALIBRATION.61
3.4.1 STEADY-STATE CALIBRATION.61

CHAPTER	PAGE
3.4.1.1 GROUNDWATER FLOW DIRECTION. .	.66
3.4.1.2 STEADY-STATE WATER BUDGET. .	.66
3.4.2 TRANSIENT-STATE CALIBRATION. . .	.70
3.4.3 VERIFICATION OF THE MODEL.71
3.4.3.1 MODEL RESULTS.71
CHAPTER 4 ALTERNATIVE DEVELOPMENT SCHEMES. .	.81
4.1 INTRODUCTION.81
4.2 ALTERNATIVE SCHEME I.85
4.3 ALTERNATIVE SCHEME II.90
4.4 ALTERNATIVE SCHEME III.	93
4.5 COMPARATIVE ASSESSMENT OF DROP WATER LEVEL IN THE THREE ALTERNATIVE SCHEMES.96
CHAPTER 5 DEVELOPMENT OF SOLUTE TRANSPORT MODEL.	.101
5.1 INTRODUCTION.103
5.2 MODELING TECHNIQUE.105
5.2.1 MODEL FORMULATION.106
5.2.2 PREPARATION OF INPUT PARAMETERS.. .	.106
5.2.3 STEADY-STATE SIMULATION.107
5.2.3.1 STEADY-STATE SOLUTE TRANSPORT CALIBRATION.107
5.2.4 TRANSIENT-STATE SIMULATION.. . .	.111

CHAPTER	PAGE
5.3 PREDICTION OF FUTURE CHANGES IN TDS.113
5.3.1 ALTERNATIVE SCHEME I.113
5.3.2 ALTERNATIVE SCHEME II.113
5.3.3 ALTERNATIVE SCHEME III..116
5.4 COMPARATIVE ASSESSMENT OF TDS LEVEL OF THE THREE ALTERNATIVE DEVELOPMENT SCHEMES.117
CHAPTER 6 HYDROCHEMISTRY.120
6.1 METHODOLOGY.120
6.1.1 GROUNDWATER SAMPLING.120
6.1.2 LABORATORY ANALYSES.122
6.1.2.1 SAMPLE PREPARATION.122
6.1.2.2 GEOCHEMICAL ANALYSIS.122
6.2 HYDROCHEMICAL CHARACTERISTICS.124
6.2.1 PHYSICAL PARAMETERS.124
6.2.2 CHEMICAL AND BIOLOGICAL PARAMETERS.124
6.2.2.1 CALCIUM (Ca^{2+}) AND MAGNESIUM (Mg^{2+}).127
6.2.2.2 SODIUM (Na^{+}) AND POTASSIUM (K^{+}).127
6.2.2.3 BICARBONATE (HCO_3^{-}) AND CARBONATE (CO_3^{2-}).132
6.2.2.4 CHLORIDE (Cl^{-}).132
6.2.2.5 NITRATE (NO_3^{-}).135
6.2.2.6 SULPHATE (SO_4^{2-}).135

CHAPTER	PAGE
6.2.2.7 COLIFORM BACTERIA.138
6.3 WATER QUALITY ANALYSES.140
6.3.1 CLASSIFICATION OF WATER BASED ON HYDROCHEMICAL DATA.140
6.3.1.1 PIPER DIAGRAM.140
6.3.1.2 DUROV DIAGRAM.. . .	.141
6.3.1.3 STIFF DIAGRAM.142
6.4 WATER QUALITY STANDARDS.149
6.4.1 SUITABILITY FOR DRINKING.149
6.4.1.1 HEALTH RISKS.152
6.4.2 SUITABILITY FOR IRRIGATION USE.153
CHAPTER 7 RESULTS AND DISCUSSIONS.157
CHAPTER 8 CONCLUSIONS AND RECOMMENDATIONS.. . .	.158
8.1 CONCLUSIONS..158
8.2 RECOMMENDATIONS..160
REFERENCES.163
APPENDICES.168

LIST OF FIGURES

Figure	Page
Figure 1.1: Map of the Study Area.5
Figure 1.2: Topographic map of the study area.8
Figure 2.1: Tectonic map of the Eastern Province and adjacent region.13
Figure 2.2: Sequence stratigraphy of the Upper Cretaceous to Quaternary sedimentary Succession of the Eastern Province.15
Figure 2.3: Structural contour map of the base of UER Formation in the Eastern Province and adjacent areas (modified after GTZ, 2006).18
Figure 2.4: Isopach map of the UER Formation.19
Figure 2.5: Spatial distribution of the main lithological associations within the Rus succession.22
Figure 2.6: Structural contour map of the base of Rus Formation in the Eastern Province and adjacent areas.23
Figure 2.7: Groundwater head distribution and groundwater flow direction of the Umm Er Radhuma aquifer.31
Figure 2.8: Spatial distribution of hydraulic conductivities from pumping tests conducted in the Eastern Province.34
Figure 2.9: Design of production Well 10 at KFUPM with total depth 120 m.35
Figure 2.10: Top elevation of Umm Er Radhuma aquifer in the study area.37
Figure 2.11: Bottom elevation of Umm Er Radhuma aquifer considered as the productive zone in the model.38
Figure 3.1: Map of the study area denoting the model domain.42
Figure 3.2: Conceptual model of the groundwater system in the study area..43

Figure	Page
Figure 3.3: Finite Difference Block and definition of conductance terms. .	.47
Figure 3.4: Initial piezometric head contour map of the study area. . .	.52
Figure 3.5: Groundwater flow direction in the Umm Er Radhuma aquifer of the study area.53
Figure 3.6: Hydraulic gradient distribution in the study area. . .	.54
Figure 3.7: Finite different grid and boundary condition (steady-state). .	.56
Figure 3.8: Finite different grid and boundary condition (transient-state). .	.57
Figure 3.9: Hydraulic conductivity (K) distribution (in m/d) in the study area.	.60
Figure 3.10: Simulated head in UER of the study area (1967 steady-state). .	.63
Figure 3.11: Calculated versus observed heads in UER of the study area (1967 Steady-state calibration).64
Figure 3.12: Comparison between observed and calculated heads in UER of the study area..65
Figure 3.13: 2-D view of Column No. 20 of the model.67
Figure 3.14: 2-D view of Row No. 10 of the model.68
Figure 3.15: Potentiometric surface contour map at the end of year 2010 (transient state simulation).73
Figure 3.16 (A & B): Hydrographs showing comparison between simulated and observed heads.74
Figure 3.16 (C & D): Hydrographs showing comparison between simulated and observed heads.75
Figure 3.16 (E & F): Hydrographs showing comparison between simulated and observed heads..76

Figure	Page
Figure 3.16 (G & H): Hydrographs showing comparison between simulated and observed heads.77
Figure 3.16 (I & J): Hydrographs showing comparison between simulated and observed heads.78
Figure 3.16 K: Hydrographs showing comparison between simulated and observed heads.79
Figure 4.1: Estimated trend of KFUPM population between 2011 and 2030.	.84
Figure 4.2: Potentiometric surface contour map at the end of 2030 (Alternative I).	.89
Figure 4.3: Potentiometric surface contour map at the end of 2030 (Alternative II)..	.92
Figure 4.4: Potentiometric surface contour map at the end of 2030 (Alternative III).	.95
Figure 4.5 (A – B): Hydrograph showing comparative assessment of drop in water level.97
Figure 4.5 (C – D): Hydrograph showing comparative assessment of drop in water level.98
Figure 4.5 (E – F): Hydrograph showing comparative assessment of drop in water level.99
Figure 4.5 (G – H): Hydrograph showing comparative assessment of drop in water level.100
Figure 4.5 (I): Hydrograph comparing drop in water level.101
Figure 5.1: Upconing in homogenous and isotropic aquifer..104
Figure 5.2: Initial TDS contour map (1967 steady-state condition).108
Figure 5.3: Simulated TDS contour map for year 1967 (steady-state).109
Figure 5.4: Comparison between measured and simulated TDS levels(steady-state).	.110

Figure	Page
Figure 5.5: Simulated TDS contour map for year 2010.112
Figure 5.6: Simulated TDS level for year 2030 (Alternative I).114
Figure 5.7: Simulated TDS level for year 2030 (Alternative II).115
Figure 5.8: Simulated TDS level for the year 2030 (Alternative III).117
Figure 5.9: TDS versus time graph for the three Alternative Schemes.119
Figure 6.1: Sampling of KFUPM Well No. 12.121
Figure 6.2: Calcium concentration (mg/L) variation in the study area.128
Figure 6.3: Magnesium concentration (mg/L) variation in the study area.129
Figure 6.4: Sodium concentration (mg/L) variation in the study area.130
Figure 6.5: Potassium concentration (mg/L) variation in the study area.131
Figure 6.6: Bicarbonate concentration (mg/L) variation in the study area.133
Figure 6.7: Chloride concentration (mg/L) variation in the study area.134
Figure 6.8: Nitrate concentration (mg/L) variation in the study area.136
Figure 6.9: Sulphate concentration (mg/L) variation in the study area.137
Figure 6.10: Distribution of coliform bacteria in the study area.139
Figure 6.11: Piper trilinear diagram for hydrochemical facies.144
Figure 6.12: Piper diagram of groundwater samples collected from the study area. .	.145
Figure 6.13: Index diagram for standard Durov diagram146
Figure 6.14: Durov diagram of the groundwater samples..147
Figure 6.15: Stiff diagram of groundwater samples collected from the study area. .	.148

LIST OF TABLES

Table	Page
Table 3.1: Volumetric budget during steady state.69
Table 3.2: Volumetric budget at the end of the transient state.72
Table 4.1: KFUPM on-campus population trend estimate between 2011 and 2030. .	.83
Table 4.2: Estimated water use per day for an individual.86
Table 4.3: Total water consumption for Alternative Scheme I.88
Table 4.4: Total water consumption for Alternative Scheme II.91
Table 4.5: Total water consumption for Alternative Scheme III.94
Table 5.1: Maximum TDS level for the three alternative development schemes. .	.118
Table 6.1: Methods applied for each parameter in the hydrochemical analyses. .	.123
Table 6.2: Results of hydrochemical analyses and physical parameters.125
Table 6.3: Results of analyses for total coliform and E.Coli..126
Table 6.4: International standards for drinking water.150
Table 6.5: Evaluation of electroneutrality of the groundwater in the study area. .	.151
Table 6.6: Classification of salinity and alkali hazards and magnesium hazard. .	.155
Table 6.7: Measured EC values and the calculated SAR and MH values of water samples in the study area.156

ABSTRACT

Name of Researcher : **Tajudeen Muhammad Iwalewa**

Title of Research Study : **Groundwater Management Approach at
KFUPM Campus Using Numerical Simulation**

Major Field : **Environmental Science**

Date of Degree : **May 2012**

Groundwater abstraction in desert environments results in decline in water level and a corresponding increase in salinity. Groundwater supplies more than 90% of water demand at King Fahd University of Petroleum and Minerals (KFUPM). Rapid development and growing population at KFUPM in the past three decades have led to major increase in water consumption for domestic uses and landscape irrigation, as well as sanitation services. As a result, increase in groundwater pumping from the local Umm Er Radhuma (UER) aquifer has led to decline in water levels and increase in salinity. This study focused on quantitative and qualitative assessments of groundwater resource at KFUPM campus and evaluation of the aquifer system's sustainability for three long-term pumping alternatives. Numerical simulation technique was used to assess the effects of increasing pumping rates on the piezometric surface in the UER aquifer of the area and to predict the future potentiometric levels. A groundwater flow model was developed and calibrated for the area. The simulation spanned 45 years; from 1967 to 2010. The results indicated an increase in total abstraction of 2.4 MCM in 1967 to 13.9 MCM in 2010, a 480% increase, with an average decline in water level of about 8.5 m. Three Alternative Development Schemes were formulated and analyzed to predict future responses of the calibrated

model for the planning period 2011 to 2030. The results showed that Alternative Scheme II, which assumed conservative measures, is the best for long-term sustainability of groundwater resource in the area. A solute transport model was subsequently developed from the flow model and was calibrated to predict future Total Dissolved Solid (TDS) levels of the UER aquifer in the study area. The calibrated transport model was also utilized to predict the TDS levels of the aquifer over a planning horizon of 20 years (2011-2030) under the prescribed pumping alternatives. The results revealed that Alternative Scheme II, which assumed conservative measures, is the best to protect the salinity level of groundwater resource in the area.

Eight groundwater samples from wells in the study area were collected and analyzed for their chemical composition and bacteria content. All the collected groundwater samples have similar chemical signature and can be classified as alkaline water with prevailing sulphate-chloride. The chemical analyses revealed Na+K as the dominant cation. The order of abundance of the anions is $\text{Cl}^- > \text{SO}_4^{2-} > \text{HCO}_3^-$. Hydrochemical assessments by comparison with international and local standards as well as hydrochemical hazard classifications revealed that groundwater in the study area is most likely unsuitable for drinking and irrigation purposes. The results further revealed that salinity is the principal concern in the groundwater of the study area.

The findings presented in this study highlight the need to give priority attention to sustainable groundwater management and preservation of groundwater quality in the study area.

الملخص

اسم الباحث : تاج الدين محمد أيوالوا

عنوان البحث : مقارنة لإدارة المياه الجوفية في حرم جامعة الملك فهد للبترول والمعادن
باستخدام المحاكاة العددية

التخصص : علوم البيئة

تاريخ التخرج : مايو 2012م

إن عملية استخراج المياه الجوفية في البيئة الصحراوية هي سكين ذو حدين: فهي تؤدي إلى انخفاض منسوب المياه وزيادة في الملوحة. تلبي المياه الجوفية أكثر من 90% من الطلب على المياه في جامعة الملك فهد للبترول والمعادن. وقد أدى التطور السريع وتزايد عدد السكان في الجامعة خلال العقود الثلاثة الماضية إلى زيادة كبيرة في استهلاك المياه للاستخدامات المنزلية، وري المسطحات الخضراء، فضلاً عن خدمات الصرف الصحي. ونتيجة لذلك، ازداد ضخ المياه الجوفية من مكن أم الرضمة المائي المحلي مما أدى إلى انخفاض في منسوب المياه وزيادة في الملوحة. وركزت هذه الدراسة على التقويم الكمي والنوعي لموارد المياه الجوفية في حرم جامعة الملك فهد للبترول والمعادن، وتقييم استدامة المكن المائي تحت بدائل ضخ على المدى الطويل. واستخدمت تقنية المحاكاة العددية لتقييم الآثار المترتبة على زيادة معدلات الضخ على السطح البيزومتري في مكن أم الرضمة المائي، وجرى توقع مستويات الجهدية المستقبلية. وتم تطوير ومعايرة نموذج تدفق المياه الجوفية للمنطقة. وجرى عمل المحاكاة لخمس وأربعين (45) عاماً، من 1967 وحتى 2010م. وأشارت النتائج إلى ارتفاع كمية السحب من المياه بما مجموعه 2.4 مليون متر مكعب في 1967 حتى وصل إلى 13.9 مليون متر مكعب في عام 2010، وهو ما يمثل زيادة بحوالي 480%، مع انخفاض في مستوى المياه بلغ متوسطه حوالي 8.5 م. وتم صياغة خطط لثلاث بدائل للتطوير، وجرى تحليلها لتوقع الاستجابة المستقبلية باستخدام النموذج المعايير لفترة تخطيط من 2011 إلى 2030. وأظهرت النتائج أن خطة البديل الثاني، التي تقتض تدابير المحافظة، هي الأفضل على

المدى الطويل لاستدامة موارد المياه الجوفية في المنطقة. وبعد ذلك تم تطوير نموذج انتقال المذابات من نموذج التدفق وجرى معايرته من أجل توقع مستويات الأملاح الذائبة الكلية في مكن أم الرضمة في المستقبل في منطقة الدراسة. وجرى استخدام النموذج المعايير أيضاً لتوقع مستويات الأملاح الذائبة الكلية في المكن المائي لأفق تخطيط لمدة 20 عاماً (من 2011 - 2030) في إطار البدائل المحددة للضخ. وأظهرت النتائج أن البديل الثاني، الذي يفترض تدابير المحافظة، هو أفضل السبل لحماية مستوى ملوحة في مورد المياه الجوفية في المنطقة.

تم جمع عينات من المياه الجوفية من ثماني آبار في منطقة الدراسة، وجرى تحليلها للكشف عن تركيبها الكيميائي والمحتوى البكتيري. وتبين من التحليل أن جميع عينات المياه الجوفية التي تم جمعها متماثلة في بصمتها الكيميائية والتي يمكن تصنيفها على أنها مياه قلوية مع سيادة كبريتات-كلوريد. وكشفت التحاليل الكيميائية أن الكاتيون (Na+K) هو السائد. وأن ترتيب وفرة من الأنيونات هو $\text{HCO}_3^- > \text{SO}_4^{2-} > \text{Cl}^-$. وكشفت التقييمات الهيدروكيميائية بالمقارنة مع المعايير الدولية والمحلية، فضلاً عن تصنيفات الأخطار الهيدروكيميائية أن المياه الجوفية في منطقة الدراسة غير صالحة للشرب وأغراض الري. هذا وكشفت أيضاً أن نسبة الملوحة هي موضع الاهتمام الرئيسي في المياه الجوفية لمنطقة الدراسة.

تسلط النتائج التي قدمت في هذه الدراسة الضوء على الحاجة إلى إعطاء أولوية الاهتمام للإدارة المستدامة للمياه الجوفية، والحفاظ على نوعية المياه الجوفية في كل المناطق الجافة وشبه الجافة.

CHAPTER 1

INTRODUCTION

1.1 GENERAL

The Kingdom of Saudi Arabia is located in an extremely arid zone where the average annual rainfall ranges between 25 to 150 mm in about 80% of the country (MAW, 1988). It is the largest country in the world without natural and perennial rivers running to the sea. Water has always been a scarce resource in Saudi Arabia. Urban life, industry, and above all agriculture, consume far more water than traditional life in the deserts and towns ever required (Beaumont, 1977). Groundwater constitutes the most important natural water source in the Kingdom; hence, its careful management is paramount for the country to minimize long-term adverse changes in water quality and aquifer productivity (Abderrahman et al., 1994).

The limited availability of groundwater resources in Saudi Arabia has been further plagued by enormous developmental projects and agricultural activities in the recent past decades. Groundwater conservation and protection measures have been overlooked in the majority of practices. The dwindling of the limited groundwater resources, coupled with the documented deterioration of groundwater quality requires immediate application of conservation and protection measures.

Groundwater aquifers throughout the Kingdom have been categorized into two types:

(i.) Aquifers (mostly unconfined) found close to the surface and are recharged easily

and quickly by flows into wadis and (ii.) Deep aquifers (mostly confined) that exist within sedimentary formations in the eastern two-thirds of the country. Confined aquifers have been discovered only in the last four decades. Many of the vast agricultural development taking place in the Kingdom, as well as water supplies to urban centers, depend on their water (Al-Hassoun, 1996). Aquifers of the Eastern Province of Saudi Arabia belong to the second category of the aquifers.

The results of hydrogeological studies by Itaconsult (1969), BRGM (1977) and GDC (1980) have indicated the existence of a multi-aquifer system in the Eastern Province. The aquifer system in the Eastern Province consists of three main aquifers separated by semi-confining beds. In ascending order, they are: the Umm Er Radhuma (UER) aquifer, the Rus confining bed (which includes the Midra and Saila Shales and Alveolina Limestone members) the Khobar aquifer, the Alat Marl confining bed, the Alat aquifer and the Neogene aquifer. The Neogene aquifer is absent in the aquifer system of the Greater Dhahran Area. At KFUPM, the aquifer system occurs as an anticline with Dammam aquifer eroded leaving only the UER as the only aquifer in the area and Rus confining bed lying at the top.

The UER aquifer is the most important in the region (Abderrahman et al., 1994). It is the main source of water for industrial, domestic and land irrigation purposes in the urban area of Greater Dhahran. King Fahd University of Petroleum and Minerals (KFUPM), King Abdulaziz Air Base and ARAMCO are all pumping water from this aquifer. In the Greater Dhahran area, there has been drastic increase in groundwater pumping, as well as the number of drilled wells, to meet rising water demands. This has resulted in negative impacts on groundwater levels and quality within the area (KFUPM, 2009; Abderrahman et al., 1994).

1.2 STUDY AREA

The study area covers about 4.8 square kilometers, and is confined between $26^{\circ}17'27.92''$ - $26^{\circ}19'16.80''$ N latitude and $50^{\circ}08'15.96''$ - $50^{\circ}08'59.29''$ E longitude (Figure 1). It is located in the city of Dhahran, which is part of the urban area of Greater Dhahran in the Eastern Province of Saudi Arabia. The climate of the study area is extremely variable (Al Amoudi, 2010). During the summer months (June, July, August), the temperature ranges from 41 to 44 °C. Winter (December, January, and February) is usually mild. Mean monthly temperatures inland lie between 11 and 22 °C. The average annual percentage of sunshine is about 75%. The most frequent direction of prevailing winds is from the west to northwest. These winds decrease by the end of July and the minimum amount of northerly wind occurs during August. These strong winds decrease in frequency during the spring months (March, April, and May). Relative humidity also exhibits considerable variation from place to place and year to year. Relative humidity highs during the winter (December through February) range from 65 to 73 % and relative humidity lows of 37 to 63 % during the summer (June, July, August) are observed along the Arabian Gulf Coast. Precipitation in the study area is scarce, and the rainfall pattern is highly variable. Rainfall records of the Ministry of Agriculture and Water during the years 1952-1978 show an average annual rainfall of about 62 mm in the study area.

The topographic map of the study area is shown in Figure 2. The elevation of the area varies from 55 m to 100 m above mean sea level. Trends of the contours indicate a general eastward dip with the highest elevation at the western part of the area. Average topographic elevation in the study area is estimated at 77 m above mean sea level (amsl). Groundwater is the most important source of water. The area is heavily inhabited and intensively developed due to the presence of KFUPM, King Abdulaziz

Air Base and Saudi ARAMCO. Dammam aquifer has been eroded in the study area, making Umm Er Radhuma (UER) aquifer the only aquifer from which groundwater is sourced in the area.

1.3 OBJECTIVES

The main objective of this study is to carry out quantitative and qualitative assessment of the groundwater resources at KFUPM campus and to evaluate the aquifer system's sustainability for three different pumping alternatives. The overarching aim of this study is to help KFUPM Community in implementing better management of the available and non-renewable groundwater resources.

The specific tasks are:

1. To define the geological and hydrogeological settings of Umm Er Radhuma (UER) aquifer in the study area.
2. To investigate the groundwater quality in terms of major ionic compositions.
3. To investigate the historical changes in groundwater levels of Umm Er Radhuma aquifer system in the area.
4. To develop a groundwater flow model and transport model for the aquifer system in the area, and to use this model to predict the future changes in groundwater levels and quality under three long-term pumping scenarios.
5. To investigate possible environmental and health problems with respect to the hydrochemistry of the groundwater in the study area.

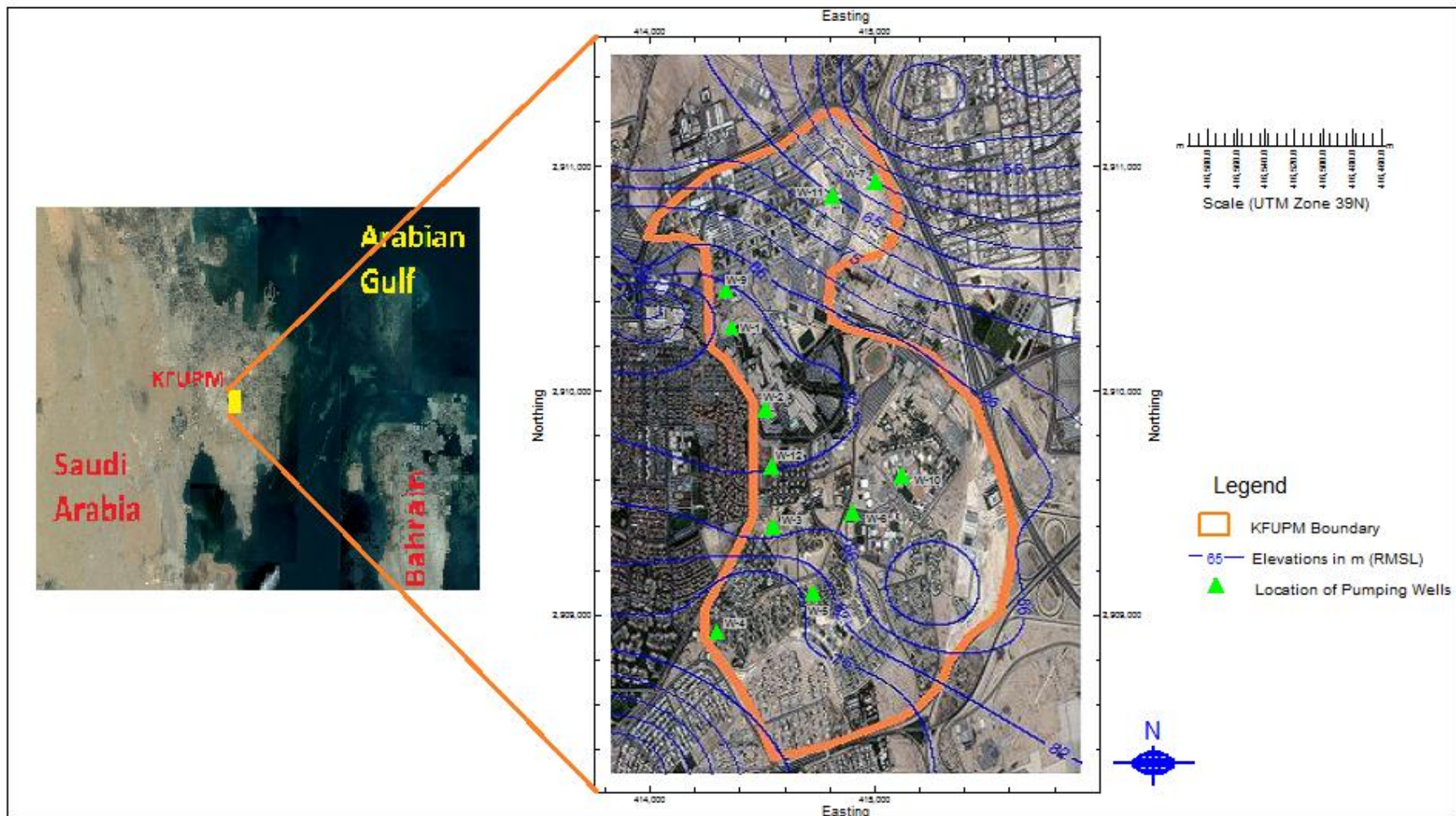


Figure 1.1: Map of the Study Area

1.4 DATA COLLECTION AND ANALYSES

The available regional geological and hydrogeological maps and information about the study area from published and unpublished studies available at KFUPM Maintenance Department and KFUPM Research Institute were used in this study. These sets of information include the coordinates of the study area and well locations, topographic map, pumping rates, historical abstractions, top and bottom elevations of UER aquifer, initial water level, water quality and other parameters such as storativity, thickness of UER aquifer and hydraulic conductivity. Data on KFUPM on-campus population were provided by KFUPM Housing and Faculty Services Department and Student Housing Unit.

A basic study work map was prepared using the collected information. Geographic coordinates were converted to Universal Transverse Mercator (UTM) coordinates. Available information about surface geology, regional water level maps, regional water quality maps, subsurface geology and geological structure were utilized to prepare a surface geological map, hydrogeological structural contour maps (top and bottom elevations of UER aquifer), hydrogeological cross sections, piezometric contour maps and salinity distribution maps of the UER aquifer in the study area.

The defined geological and hydrogeological settings were used to develop the numerical simulation model of the groundwater flow of the aquifer system in the study area. This model is used for prediction of future groundwater flow conditions under three long-term groundwater pumping alternatives.

Data on KFUPM on-campus population were utilized in forecasting the population trend of KFUPM in the next 20 years, hence, the most likely water need. This

information was used in the selection of the most appropriate long-term pumping alternatives.

1.5 PREVIOUS STUDIES

Regional geology and hydrogeology of the Eastern Province have been studied extensively by several researchers and these have been documented in both published and unpublished reports. A groundwater study of North Eastern Saudi Arabia with descriptions of the water potential of the major aquifers and regional investigations on water quality of the aquifers was conducted by Naimi (1965). Powers *et al.* (1966) studied the sedimentary geology of Saudi Arabia covering the entire eastern half of the country. Italconsult (1969) produced reconnaissance regional topographic and water level maps of the Eastern Province at 1: 500,000 scale as part of studies on water and agricultural development for the Eastern Province, Saudi Arabia. A regional hydrogeological investigation of the aquifers of the Eastern Province was carried out in 1977 as part of Al Hassa Development Project by Bureau De Recherche Geologique et Mineres (BRGM). This study involved various pumping tests resulting in regional values of the parameters of the aquifers. A regional study of UER aquifer which involved pumping tests and investigations of the parameters of the aquifer was conducted by Groundwater Development Consultants (GDC) in 1979. The results of the study conducted by GDC are parts of the data utilized in this work. Bakiewicz *et al.* (1982) carried out investigations on the hydrogeology of UER aquifer in Saudi Arabia and provided information on depositional and fossil records of the aquifer. One of the most important preceding studies was carried out by Deutsche Gesellschaft für

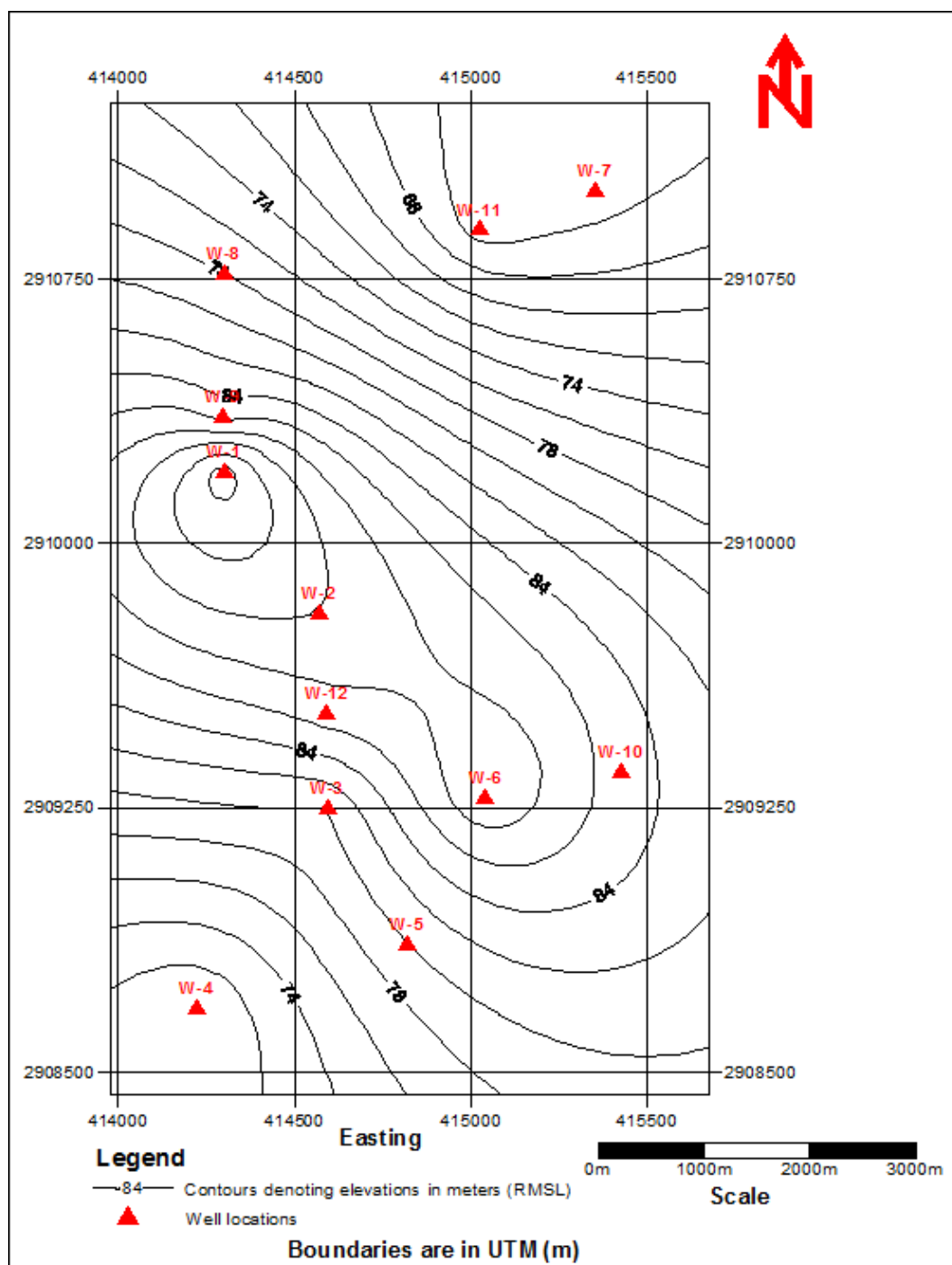


Figure 1.2: Topographic map of the study area

Technische Zusammenarbeit, GTZ, (2006). They developed a mathematical model for Umm Er Radhuma and the overlying aquifers, and provided comprehensive information about the geological and hydrogeological characteristics of the investigated formations of Upper Cretaceous to Quaternary age within the Eastern Province.

In an unpublished M.S. thesis submitted to KFUPM, Rasheeduddin (1988) constructed a numerical quasi-three dimensional groundwater flow model for the multi-aquifer system in eastern Saudi Arabia to determine the hydraulic properties of the system and to evaluate the consequences of various development alternatives. The aquifers modeled were the Alat, Khobar and UER of Paleocene-Eocene age, which are hydraulically connected with intervening aquitards. Abderrahman and Rasheeduddin (1994) used a numerical simulation technique to predict future levels and water quality of UER aquifer in the Greater Dhahran Area under different pumping scenarios. A numerical simulation model of the multi-aquifer system including Dammam and Umm Er Radhuma aquifers was developed by Abderrahman et al. (2007) to assess the behavior of the aquifer system under long-term water stresses in Dammam Metropolitan. KFUPM (2009) developed a numerical simulation model as a prominent part of Groundwater Resources Study for the Dammam-Khobar-Dhahran Metropolitan Area.

All the past groundwater studies in the Eastern Province were regional in scope and therefore are susceptible to lots of approximations of the aquifer systems' behaviour, hence, less reliability. However, this study presents a more focused groundwater study of KFUPM campus, which is an elemental part of the region.

1.6 STATEMENT OF PROBLEM

All previous groundwater studies in the urban area of Greater Dhahran have been regional; there has not been a solitary work on the groundwater system in KFUPM area. Given the population increase experienced by KFUPM between 1967 and 2010 from influx of domestic and international students and increase in the number of staff and faculty members, it becomes apparent that groundwater abstraction from UER aquifer in KFUPM area would have increased drastically within this period. Available pumping data from KFUPM Maintenance Department and KFUPM Research Institute succinctly confirm this. The data revealed an increase in groundwater pumping rates between 1967 and 2010, which is the corollary to the increase in concentrations of the major anions and cations in the water, making a study of the future trend essential.

1.7 THESIS OUTLINE

This section provides the outline of the thesis, chapter by chapter. Chapter 1 provides information on general introduction of this research followed by the descriptions of the study area and explanations of the study objectives. A look into the previous studies in the region where the study area is located is preceded by a summary on data collection and analysis for the research. Justifications on why this study is needed are provided in the statement of problem section.

Chapter 2 contains discussions on the geological and hydrogeological settings of the area. This chapter provides details on the geologic formations in eastern Saudi Arabia, their depositional history and structures. These are followed by elucidation on the aquifer system in the study area.

Development of groundwater model for the study area is contained in Chapter 3. Details on the development of the conceptual model for the study area, modeling technique, discretization and boundary conditions, steady and transient state calibrations are included in this chapter.

Chapter 4 presents analyses on the alternative development schemes. Transient simulation models are developed for each alternative development scheme. Comparisons of water levels between the alternative development schemes for each observation well are parts of this chapter.

Development of solute transport model is the central part of Chapter 5. Prediction of the future changes in Total Dissolve Solids (TDS) for each alternative scheme is also discussed.

In Chapter 6, hydrochemical assessments of the groundwater of the study area are examined. Discussions on environmental consequences of deterioration in water quality of the groundwater in the study area are also contained in Chapter 6.

Conclusions and recommendations are contained in Chapter 7.

CHAPTER 2

GEOLOGICAL AND HYDROGEOLOGICAL SETTINGS

2.1 GEOLOGICAL SETTING

The Kingdom of Saudi Arabia is located in the southern part of the Arabian plate. In Saudi Arabia, the plate comprises a crystalline basement of Precambrian continental crust (about 870 Ma – 550 Ma), and an overlying succession of younger sedimentary rocks, which belong to the Paleozoic (540 Ma – 250 Ma), Mesozoic (250 Ma – 65 Ma), and Cenozoic Eras (65 Ma to present), collectively referred to as the Phanerozoic Eon. The Phanerozoic rocks lie unconformable on the Precambrian basement. They consist of mainly carbonates and clastics, whereas evaporites are also available, but of much less importance. The thickness of the Phanerozoic succession ranges from zero to about 12 km. The youngest deposits of Quaternary age include limestones, unconsolidated silts, sands and gravels, as well as sabkha-, ephemeral lake- and wadi-sediments (Powers et al., 1969).

The sedimentary rocks covering the Precambrian basement accumulated on a stable shelf. During its Phanerozoic history this shelf repeatedly experienced fluctuating marine-to terrestrial conditions. Tectonic movement and cyclic sea level fluctuations resulted in lateral facies shifts across the shelf. These facies shifts left behind systematic patterns within the sedimentary record, known as sedimentary sequences

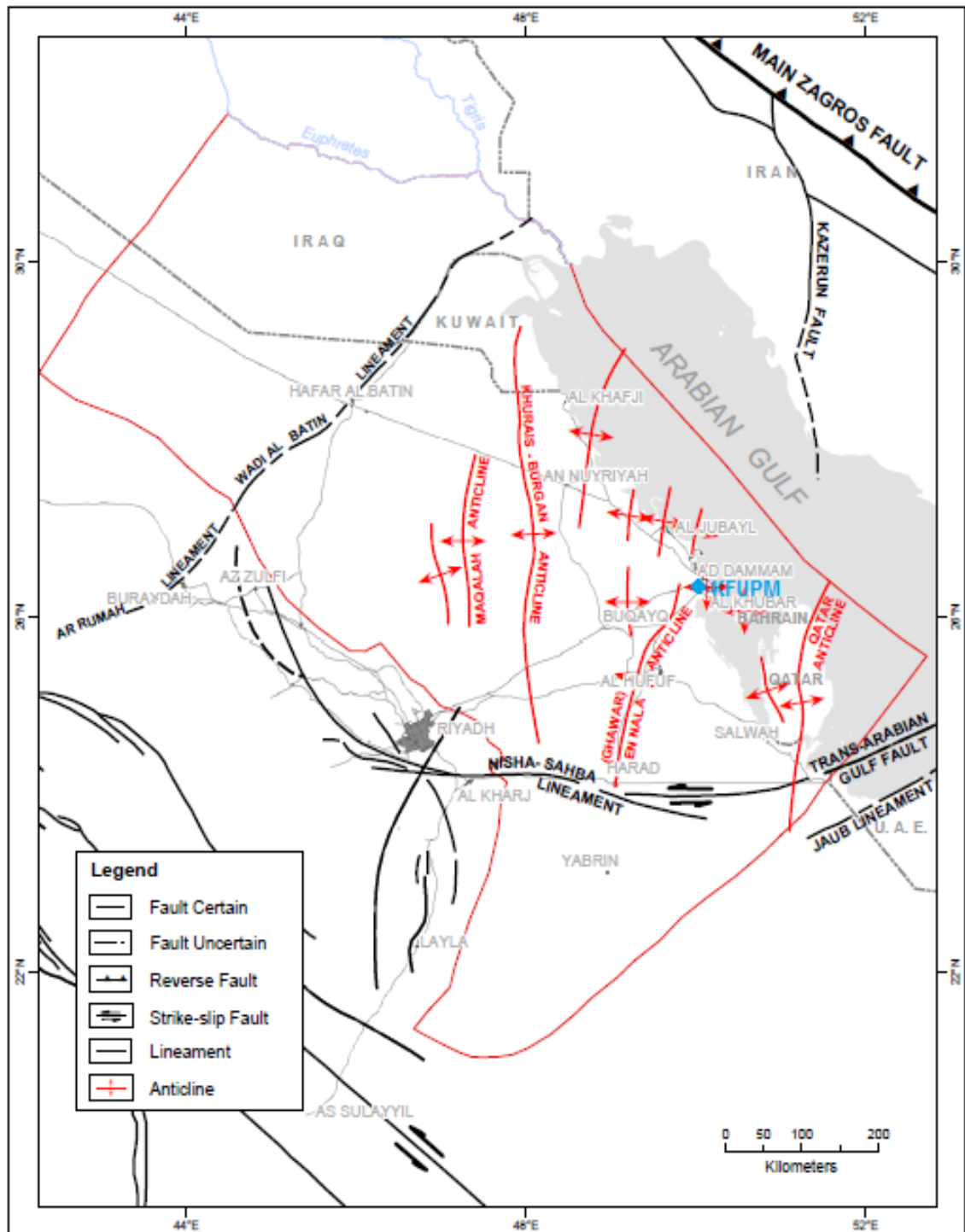


Figure 2.1: Tectonic map of the Eastern Province and adjacent region (modified after GTZ, 2006). The study area (KFUPM) is characterised by north-south trending anticline and syncline

Powers et al., 1969). Apart from some structures, tectonic movements were only of minor importance, especially within the study area. Here the rocks are partly deformed by a series of north-south trending anticline and syncline (Figure 2.1).

2.2 STRATIGRAPHY

According to ARAMCO (1975), the Phanerozoic cover of Central and Eastern Saudi Arabia can be subdivided into eight major divisions:

Early Paleozoic clastic rocks; dominantly coarse sandstones separated by distinctive shale members with some thin carbonate beds at top.

Permian and Triassic clastic rocks; alternating non-marine and marine units, dominantly sandstones with thick calcareous sections, some evaporites occur at the base and in the middle.

Lower and Middle Jurassic clastic and carbonate rocks; marine limestones with interbedded sandstones.

Upper Jurassic and Early Lower Cretaceous carbonate rocks; mainly carbonates, alternating with evaporites.

Late Lower Cretaceous clastic rocks; dominantly coarse sandstones with a thin basal carbonate unit.

Middle Cretaceous clastic rocks; dominantly sandstones.

Upper Cretaceous to Eocene carbonate rocks; dominantly limestones with an evaporate section near the top.

Miocene and Pliocene clastic rocks; dominantly sandy limestones with subordinate calcareous sandstones.

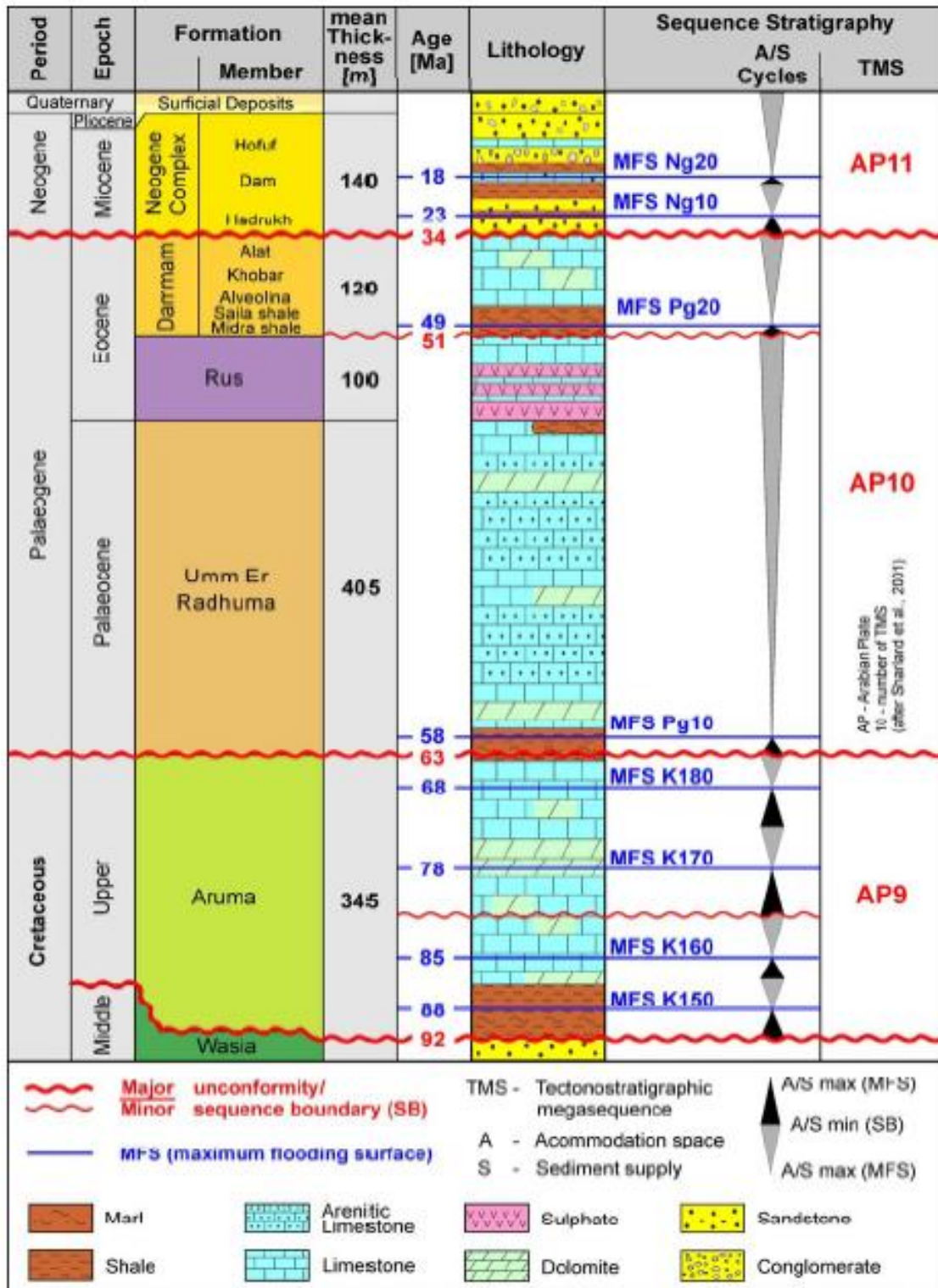


Figure 2.2: Sequence stratigraphy of the Upper Cretaceous to Quaternary sedimentary succession of the Eastern Province (after Sharland et al., 2001)

The generalized stratigraphic column, including local nomenclature and the corresponding hydrogeological units, is given in Figure 2.2.

Concerning this study, only the last two of the divisions stated above are of interest.

The following discussion is limited on those two units.

2.2.1 ARUMA FORMATION

The deposits of the Aruma Formation are of Upper Cretaceous (Coniacian – Maestrichtian) age (El-Asa'ad, 1983a,b). It overlies the Wasia Formation disconformably, where the boundary is termed the Pre-Aruma-Unconformity. The Aruma sediments were deposited under shallow marine conditions, in an arm of the Tethys Sea. They consist of massive limestones, partly dolomitised, and massive dolomites with subordinate shales and marls in the upper part of the formation (Aruma Limestone).

The lithology is laterally uniform except to the extreme southwest and northwest of the Eastern Province, at the margins of the basin of deposition, where it is represented by sandstones. The basal units in the eastern two-third of the Eastern Province consist of dominantly shales (Lower Aruma Shale).

The Aruma Formation is dipping approximately with an angle of $\sim 0.21^\circ$ to the east (Italconsult, 1969). Within the Eastern Province, the thickness of the formation increases from the outcrop area in the west towards the east, where it reaches its maximum of 850 m. The thickness averages about 350 m. The maximum thickness of the upper Aruma, mainly consisting of carbonates (Aruma Limestone) is about 700 m.

The Aruma Formation crops out in a west-facing escarpment located in central Saudi Arabia that courses from the Wadi Dawasir over 1,600 km towards the north, beyond

the Saudi Arabian-Iraqi border. The width of the outcrop increases from 20 km in the south to 200 km in the north of the country (El-Asa'ad, 1983a,b).

2.2.2 UMM ER RADHUMA (UER) FORMATION

The Umm Er Radhuma Formation is of late Paleocene to Early Eocene age and overlies the Aruma Formation unconformably (Powers, 1968; El-Khayal, 1974; Sharland et al., 2001; Ziegler, 2001). The sediments were deposited during a major transgression that spread marine conditions as far as Jordan, Iraq and Yemen. This led to the deposition of a thick succession of carbonate rocks over initial calcareous shales at the base of the formation. The sedimentation occurred on a wide carbonate shelf, which was partly distorted by tectonic movements into a series of deeps and shallows. The resulting palaeorelief determined the type of sediments formed. In the northern part of the Eastern Province, fine limestones, often argillaceous, with intercalated sulphate beds partly showing selenite structures were formed. This succession in general indicates a restricted lagoonal setting, where fine sediments settled out of stagnant waters, and occasionally shallow, hypersaline conditions prevailed. In the centre of the study area the thickness of the Umm Er Radhuma varies. The formation contains thick calcarenite beds and reef type carbonates, which were deposited around palaeohighs. In the south detrital limestones are still predominant, but the thickness is more uniform. In the central and southern area marls and shales are inserted between the carbonate units of the upper part of the formation. Cherts occur sporadically throughout the formation. Syndimentary dolomitisation of the limestone beds led to the formation of dolomitic limestones and massive dolomites of patchy occurrence (Ziegler, 2001). The percentage of sulphates if present averages 9 %, where values can reach up to 23 % of the total Umm Er Radhuma succession.

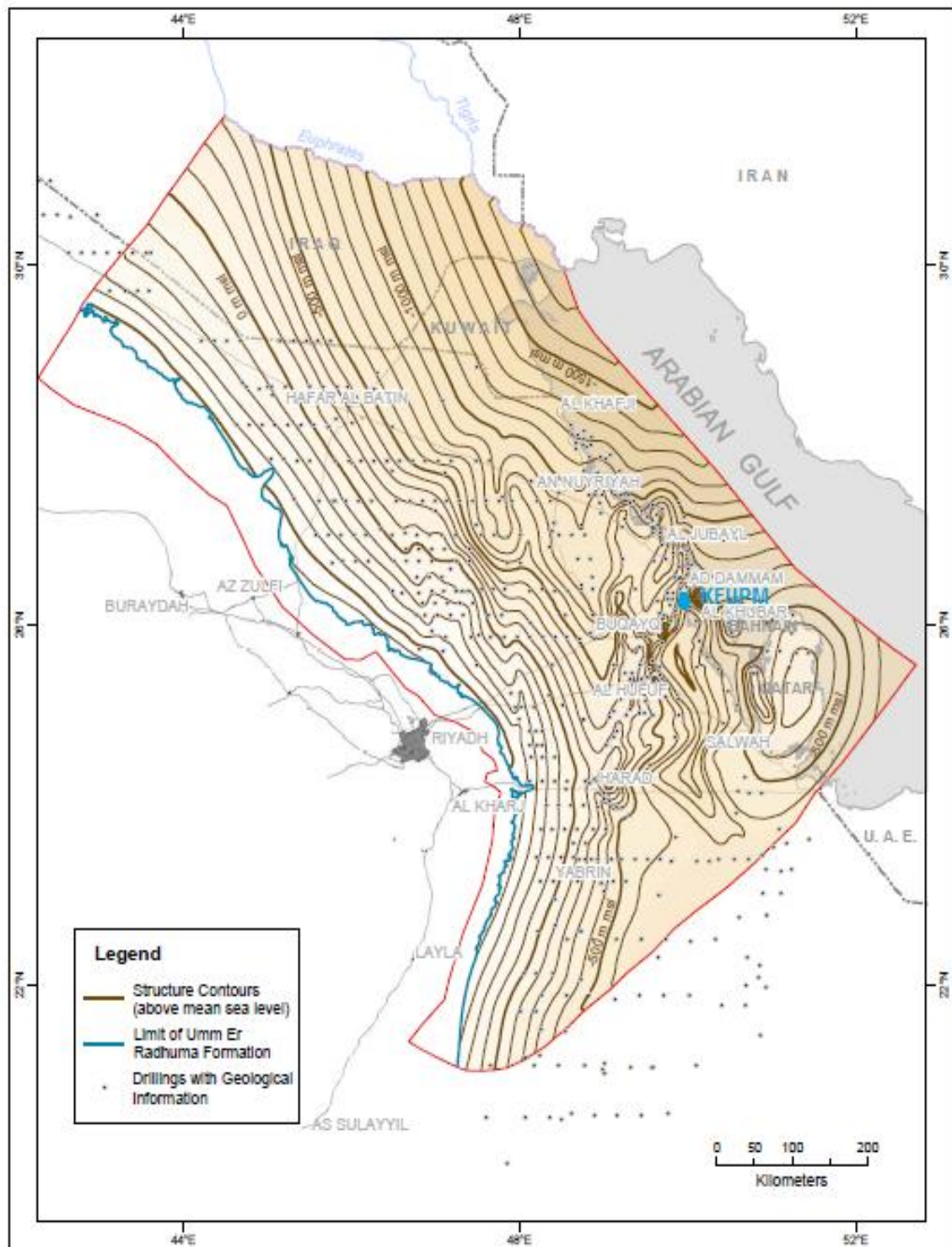


Figure 2.3: Structural contour map of the base of UER Formation in the Eastern Province and adjacent areas (modified after GTZ, 2006)

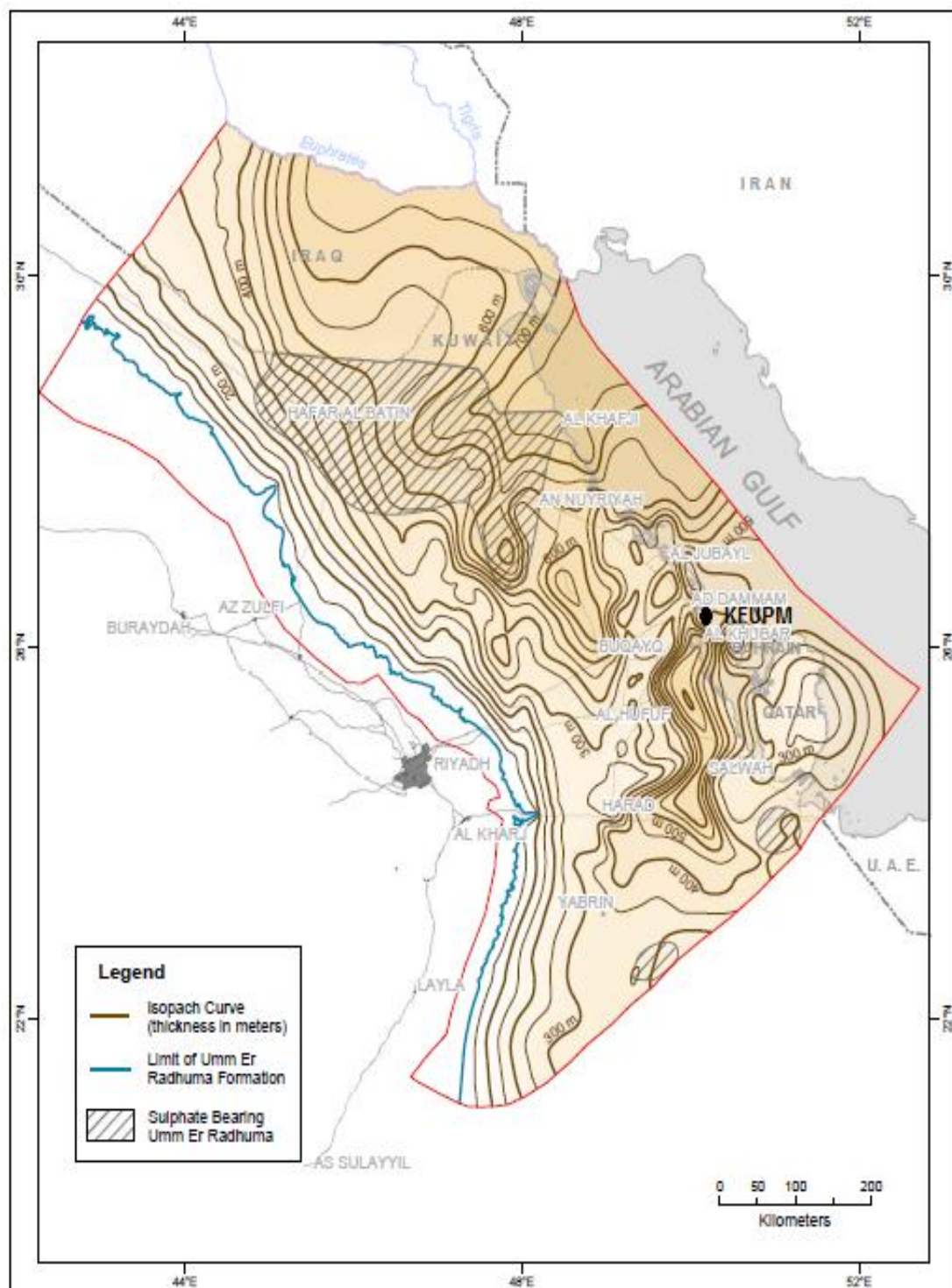


Figure 2.4: Isopach map of the UER Formation; thickness generally increases from west towards the Arabian Gulf, where it reaches about 650 m within the study area (KEUPM). The mean thickness is about 400 m (modified after GTZ, 2006)

The Umm Er Radhuma Formation is gently dipping east towards the Arabian Gulf with an angle of $\sim 0.14^\circ$ (Figure 2.3). The thickness of the formation in general increases from west to east to a maximum thickness of 650 m within the study area (KFUPM), whereas the mean thickness is about 400 m (Figure 2.4).

The Umm Er Radhuma outcrop extends from the Iraqi-Jordan border in a broad band, 50 km to 100 km wide, over 1,200 km south beyond the Wadi Dawasir.

2.2.3 RUS FORMATION

The deposits of the Rus Formation are of Lower Eocene age. The Rus conformably overlies the Umm Er Radhuma Formation. It is composed of soft limestones, dolomitic limestones, chalky limestones, sulphates (gypsum and anhydrite) and shales. The lateral distribution of gypsum and anhydrite is nonuniform (Bakiewicz et al., 1982). They appear primarily in structural depressions. In some areas the absence of sulphates is due to secondary solution processes. In the study area, the Rus is only represented by residual carbonates and in fact shows high similarity to the underlying Umm Er Radhuma carbonate units.

The Rus Formation dips with an angle of approximately 0.14° gently to the east, analog to the underlying strata (Figure 2.5). Within the study area, the Rus Formation occurs as an anticline with thickness of the formation decreasing from west towards the east. The maximum thickness is 65 m and the mean thickness is about 45 m at KFUPM. Regionally, Rus Formation has a maximum thickness of about 270 m and mean thickness of about 100 m (Figure 2.6).

Rus outcrops are limited to small areas. The main outcrop forms a band of about 180 km length to the north of Wadi As Sahba. Further outcrops occur at Dammam, Bahrain and near the Saudi Arabian-Qatar border (GTZ, 2006).

2.2.4 DAMMAM FORMATION

The Dammam Formation is of late Early Eocene to Upper Eocene age (Weijermars, 1999; Ziegler, 2001). The formation is divided into five members, from oldest to youngest: the midra shale, Saila shale, Alveolina, Khobar, and Alat. In the Middle Eocene the evaporitic conditions of the Lower Eocene were terminated by a new marine transgression. This led to the formation of a complex succession of limestones, dolomitic limestones, marls and subordinate shales. In the lower part of the formation (Midra shale, Saila shale, and Alveolina) marls and shales indicate an open-marine depositional setting, while in the Upper part (Khobar, Alat) shallow-marine carbonates prevail.

The Dammam Formation dips approximately in eastern direction with an angle of $\sim 0.11^\circ$ (GTZ, 2006). The maximum thickness of the formation reaches 450 m. In some areas the original thickness of the formation is decreased by subsequent erosion, which led to the formation of the “Pre-Neogene Unconformity”. Around anticlinal structures the primary thickness is less compared to the deeper parts of the basin.

An outcrop of the Dammam Formation is located immediately west of the study area inside Saudi Aramco headquarters. Outcrops are limited to a narrow irregular band, generally less than 5 km wide, north of the Wadi Sabha and scattered patches near the city of Dammam.

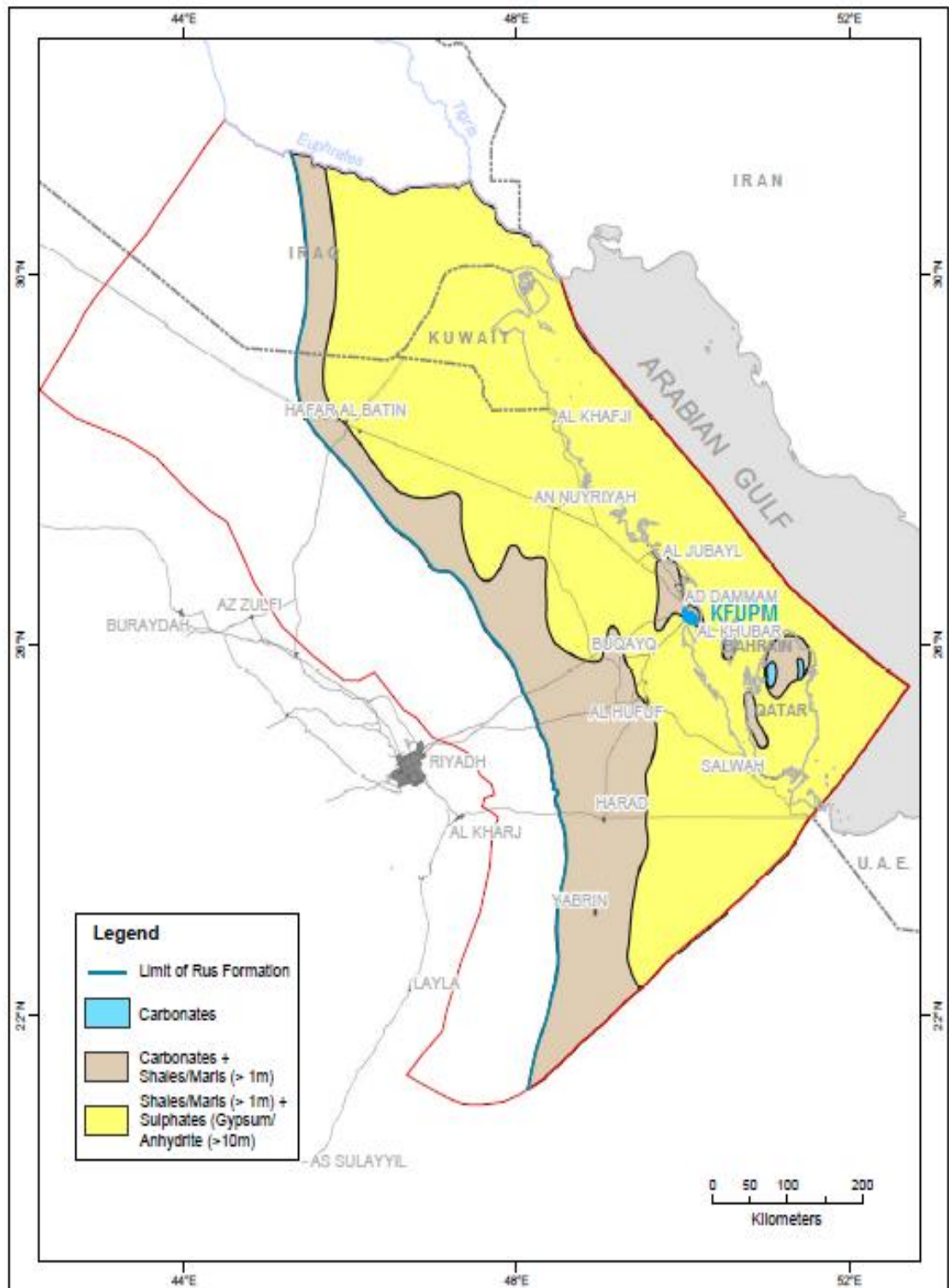


Figure 2.5: Spatial distribution of the main lithological associations within the Rus succession (modified after GTZ, 2006)

2.2.5 NEOGENE COMPLEX

The Neogene complex was deposited during the Miocene (Sharland et al., 2001; Ziegler, 2001). This succession disconformably overlies the older Paleogene sediments (Pre- Neogene Unconformity). Following the deposition of the underlying Dammam Formation a widespread emersion of the whole Arabian Platform occurred, causing the erosion of preexisting rocks. Emerged areas have remained as dry land ever since except for minor ingressions in coastal areas during the Miocene. Nevertheless, marine deposition continued in a series of relic arms of the old sea, while continental sedimentation occurred outside these areas.

The Neogene complex is divided into three formations, from oldest to youngest: the Hadrukh-, Dam- and Hofuf Formations. These formations are only clearly discernable to the east of the study area, where the marine influence was strongest. This succession grades inland, towards the west, into wholly continental units, such as the fluvial and lacustrine Kharj Formation, which is not represented within the study area. The Hadrukh Formation consists of sandstones, marls, sandy marls and sandy limestones, where the measured thickness at the type section at Jebel Al Hadrukh is 84 m. The Dam Formation consists of marls, shales and sandy limestones near the base. The thickness at the type section is 90 m. The Hofuf Formation is of mainly fluvial origin and comprises of sandstones and conglomerates (components of quartz, igneous and metamorphic rocks, and also sedimentary rocks) with intercalations of thin limestones and marls. This formation has a thickness of 95 m at the type section.

The Neogene complex is dipping with an angle of $\sim 0.1^\circ$ approximately to the east, where it reaches its maximum thickness of 500 m within the study area (GTZ, 2006). The mean thickness within the limits of the Eastern Province averages about 140 m.

The Neogene deposits extend over a large area from the Wadi Dawasir northward to the Jordanian border and eastward to the Arabian Gulf. The Hadruk, Dam and Hofuf Formations are exposed near the Gulf coast.

2.3 KARST

Karst phenomena determine the hydrogeological properties of the studied formations of Upper Cretaceous to Quaternary age. They are observable within the carbonate units of the Aruma, Umm Er Radhuma, Rus and Dammam Formations as well as in the sulphates of the Umm Er Radhuma and the Rus. Characteristic karstic features in these formations are sinkholes (dolina), disappearing streams (swallow holes), vertical shafts, and caverns, where surface karst features are mainly restricted to the Aruma and Umm Er Radhuma outcrops. Under the present climatic conditions active karstification is negligible within the eastern part of the Arabian Peninsula. The karst of the studied formations is thought to be mainly the result of palaeo-karstification, developed under wetter climatic regimes in the geological past. Large volumes of clastic sediments deposited during the Neogene indicate the prevalence of fluvial processes under a moist climate (Whybrow & McClure, 1981). Special enhancement of palaeo-karst occurred during the wet “pluvial” epochs in the Middle Pleistocene, where sufficient rainfall was available to develop vegetation and soil covers (Rauert et al., 1988, Edgell, 1990b, Sadiq and Nasir, 2002).

Initial karstification of the Umm Er Radhuma developed shortly after its deposition. A regression in the Lower Eocene led to the exposure of parts of the Umm Er Radhuma at its western extend, e.g. the western part of the As Sulb Plateau (Hoetzel et al., 1993), while to the east marine sedimentation continued and the Rus and Dammam sediments deposited. Although evaporitic conditions were established during the Lower Eocene,

which induced the evaporite precipitation of the Rus sulphates, periodically humid climate prevailed (Hoetzi et al., 1993). This resulted in intense karstification of the exposed Umm Er Radhuma carbonates, which continued throughout the Eocene.

Beside the exposed Umm Er Radhuma on the palaeo-main-land to the west, emerged areas also existed towards the east in Eocene times. During the Paleogene the tectonic uplift movement of the anticlinal structures was renewed. Thereby sporadic emersion of at least one of these structures, the En Nala Anticline (Ghawar), occurred (GDC, 1980). Presumably also positive areas of Qatar were affected by the uplifting (Eccleston et al., 1981). Consequently, erosion of the Rus and karstification of the exposed Umm Er Radhuma was enabled (BRGM, 1976). In addition, the development of karst above the uplifted structures was promoted by the higher degree of fracturing in this zone due to bending of strata. Apart from these zones, GDC (1980) encountered well developed karstic features within the Umm Er Radhuma in the synclinal basin to the west of the En Nala Anticline. They suggested that the post-Umm Er Radhuma emergence was probably more extensive than previously supposed.

In the Upper Eocene this period of temporary emerged land masses was terminated by a rise in relative sea level, which enabled the deposition of the Dammam shales and carbonates across the whole area, whereas parts of the Umm Er Radhuma on the main-land remained sub-aerially exposed until Miocene times (Hoetzi et al., 1993).

Following the deposition of the Dammam Formation, a new regression caused widespread emersion of the Arabian Platform. This led to considerable erosion and intense karstification of pre-existing rocks like the Umm Er Radhuma, the Rus and the Alat limestones of the uppermost Dammam, for example in the eastern part of the As Sulb Plateau (Bayer et al., 1988). Areas emerged have remained as dry land ever since

except for minor incursions of the sea in coastal areas, e.g. in parts of Qatar during Miocene times. Here, karstification reoccurred after the final emergence in the Upper Miocene, where moist and dry conditions alternated. Cavalier (1970) assumed that most of the karstification of the Dammam and Rus carbonates and sulphates in Qatar developed in post-Miocene times and continuous up to present.

2.4 AQUIFER SYSTEM IN THE STUDY AREA

The aquifer system in the study area lies in the Arabian Platform and can be divided into the following hydrogeological units (in ascending order):

- (1.) Umm Er Radhuma (UER).....Aquifer
- (2.) Rus.....Aquitard

The thicknesses of each hydrogeological unit have been determined from the regional information provided in Italconsult (1969), GDC (1980), GTZ (2006) and from local well logs in the study area provided by KFUPM Maintenance Department.

2.4.1 UMM ER RADHUMA AQUIFER

The Umm Er Radhuma aquifer represents a principal aquifer and is the most important aquifer in the eastern part of Saudi Arabia. The lithology of the Umm Er Radhuma Formation is dominated by limestones, arenitic limestones, dolomitic limestones, and dolomites, where subordinate marls and shales occur in the upper part of the formation (BRGM, 1977). In the northern part of the study area and two smaller areas in the south intercalations of sulphate beds are reported from drillings (Figure 2.4). The formation thickness increases from its outcrops in the west towards the east, where it reaches a thickness of about 700 m in the study area and about 800 m in the Arabian Gulf. The mean thickness is about 400 m (Figure 2.4). In general, the Umm Er

Radhuma dips gently towards the east at an angle of about 0.14° (Figure 2.3). The Umm Er Radhuma Formation is considered as one hydrostratigraphical unit.

Aquifer characterisation: The Umm Er Radhuma aquifer can be characterized as a karstified fractured bedrock aquifer. Groundwater movement occurs primarily through secondary openings, such as joints, fractures, and bedding-plane openings, which are often enlarged by solution processes. In areas of mature karst conduits like pipes and caves, as well as dolines, closed depressions and sinkholes are developed. The karstification in vertical and horizontal direction is unevenly distributed leading to large heterogeneities in permeability and storativity (GTZ, 2006). Karstification in the upper units of the Umm Er Radhuma is reported mainly from the central and southern part of the Eastern Province, especially along the En Nala Anticline (Ghawar), whereas in the middle and lower part of the formation fissures and solution features are mainly present in the north-central area (GDC, 1980). Between Ash Shubah and An Nuayriyah and north of it, scarcely any karstic zones are detectable within the Umm Er Radhuma Formation. The distribution of this non-karstified Umm Er Radhuma coincides approximately with the occurrence of sulphates within the formation. In Qatar, karstification of the Umm Er Radhuma is reported from all levels of the formation (Eccleston et al., 1981).

The Umm Er Radhuma aquifer typically exhibits a continuum in groundwater flow ranging from quick flow within solution enlarged fractures and conduits, whereas slow flow occurs through fine fractures and intergranular pores of the carbonates. Quick flow within the aquifer system prevails in outcrop areas in the west. There the rocks are highly weathered and recharge occurs by surface runoff and infiltration via sinkholes. The rapid groundwater movement in these parts diminishes the filtrating capability and influence of the bedrock, resulting in a high vulnerability of potential

drinking water through surface derived contaminations. Slow groundwater flow dominates the aquifer parts towards the east. In these areas the carbonates are overlain by thick successions of younger sedimentary deposits (GTZ, 2006).

Aquifer geometry: Throughout most of the Eastern Province the lower boundary of the Umm Er Radhuma aquifer is formed by marls and calcareous shales, which are located at the base of the Umm Er Radhuma Formation and within the top of the underlying Aruma Formation. In contrast to its lower boundary, the top of the aquifer appears far more complex. In total five different geological upper boundary conditions can be differentiated (GDC, 1979):

1. Umm Er Radhuma overlain by complete Rus Formation predominantly consisting of sulphates,
2. Umm Er Radhuma overlain by non-sulphatic Rus and Dammam (+/- Neogene),
3. Umm Er Radhuma overlain by non-sulphatic Rus (+/- Neogene),
4. Umm Er Radhuma overlain exclusively by Neogene, and
5. Umm Er Radhuma outcrop areas.

The sulphates of the Rus Formation as well as the shales constituting the basal members of the Dammam Formation represent effective aquitards that allow only small leakage, even at high head differences. The study area corresponds to the upper boundary condition number 3, where no sulphates occur in the Rus due to solution processes. Thus, the Rus Formation forms an upward extension of the Umm Er Radhuma aquifer (Figure 2.5). Through the disturbance of strata due to the solution of the Rus sulphates, the confining properties of the shales within the Rus and the shales of the lower Dammam were disrupted, thus the upper boundary of the Umm Er

Radhuma aquifer can be highly permeable in these areas. These zones may serve as hydraulic windows between the Umm Er Radhuma and Dammam aquifers, where a significant exchange of groundwater occurs. In areas where Neogene strata containing marly and clayey beds and directly overlay the Umm Er Radhuma, the vertical groundwater flow is restricted (GTZ, 2006).

Aquifer type: The Umm Er Radhuma aquifer can be described as a leaky unconfined/confined aquifer. Unconfined conditions exist at the outcrop areas and for some distance to the east until the piezometric surface intersects with the confining units of the Rus Formation (Figure 2.8). In the larger part towards the east, the aquifer remains under confined conditions. However, over-pumping of groundwater in the study area has led to a decline in head such that the piezometric level is below the bottom of Rus aquitard. Therefore, Umm Er Radhuma aquifer is unconfined in the study area. Groundwater flow direction within the Umm Er Radhuma aquifer is from the southwest to the northeast (Figure 2.7).

Hydraulic properties: Transmissivity estimates from pumping tests, carried out within the Eastern Province (GTZ, 2006) are in the range of $T = 1 \times 10^{-4} \text{ m}^2/\text{s}$ to $1 \times 10^1 \text{ m}^2/\text{s}$ ($8.64 \text{ m}^2/\text{d}$ to $864000 \text{ m}^2/\text{d}$) (Figure 2.9). The average transmissivity from all pumping tests is $T = 2.0 \times 10^{-3} \text{ m}^2/\text{s}$ ($172.8 \text{ m}^2/\text{d}$). The values of hydraulic conductivity range between $K = 1 \times 10^{-7} \text{ m/s}$ and $1 \times 10^{-2} \text{ m/s}$ (8.64 m/d and 864 m/d , respectively) with an average of $K = 1.6 \times 10^{-5} \text{ m/s}$ (1.3 m/d) (Figure 2.8). Highly permeable zones are due to karstification and appear to be particularly associated with the development of fractures above the anticlinal structures, such as in the study area. The spatial distribution of hydraulic conductivity values is shown in Figure 2.9. Because of the wide range of the values, the diameters of the circles are plotted in logarithmic scale. The storage coefficient obtained from pumping test data ranges

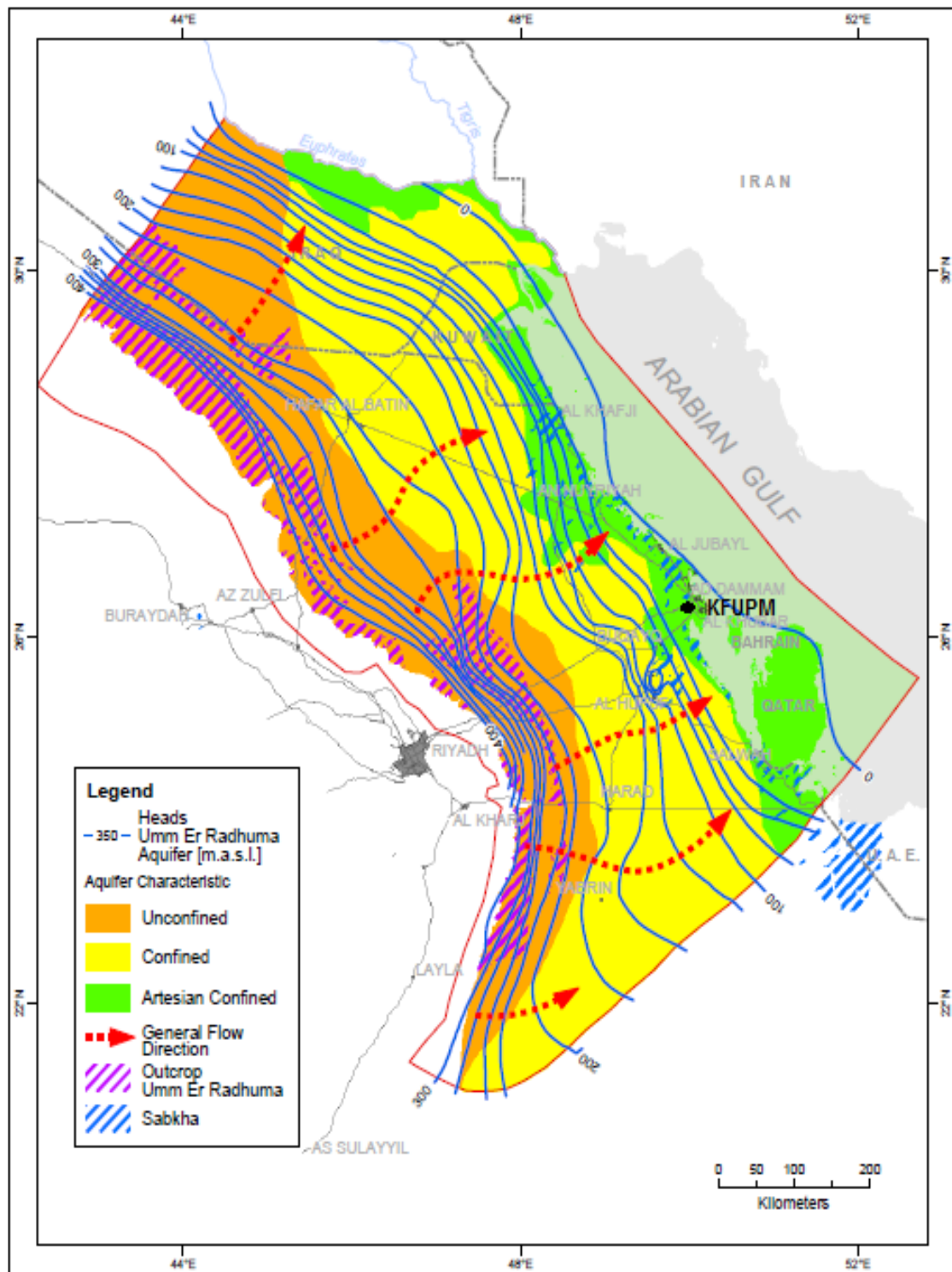


Figure 2.7: Groundwater head distribution and groundwater flow direction of the Umm Er Radhuma aquifer (modified after GTZ, 2006)

mainly from $S = 1 \times 10^{-4}$ to 1×10^{-3} , where the specific storage shows values from $S_s = 1 \times 10^{-8} \text{ m}^{-1}$ to $1 \times 10^{-5} \text{ m}^{-1}$. Values for the specific yield have been determined by pumping tests and range from $S_y = 0.01$ to 0.07 (GTZ, 2006).

Groundwater dynamics: The main groundwater flow of the Umm Er Radhuma aquifer is directed towards the Arabian Gulf and the Euphrates - Tigris Basin, which represents the main discharge areas. The groundwater head contours in general follow the trend of the outcrop in the west and the Arabian Gulf coastline in the east. The values for the groundwater head ranges from 400 (masl) in the outcrop areas down to the sea level of the Arabian Gulf, where the hydraulic gradient is about 0.055° (Figure 2.7). Locally, the drawdown of the Umm Er Radhuma aquifer is conspicuously high in the study area. These locally head declines are due to intense groundwater abstractions at KFUPM over the past three decades. A study conducted by Abderrahman et al. (2007) revealed that some wells near higher populated areas along the Arabian Gulf coastline also show significant drawdown, which is in the range of several meters to tens of meters.

Besides insignificant groundwater recharge through precipitation and infiltration in the outcrop area, additional recharge and discharge occurs by downward- and upward leakage of groundwater from the overlying and underlying aquifers, to which the Umm Er Radhuma aquifer is imperfect hydraulically connected (cross formation flow).

In general, the relatively slow groundwater movement causes long residence times within the aquifer. Therefore, the main portion of the Umm Er Radhuma groundwater is fossil water and is dated through stable isotope analyses with 7,000 years, for example, in Bahrain to over 20,000 years in the Al Hufuf area (Wagner and Geyh,

1999). Present-day recharge is very limited due to the arid climate (Hoetzi, 1995; Hoetzi et al., 1980, 1993; Shampine et al., 1979). Most of the recharge occurred during the last pluvial period, when the climate was more humid. This period ended about 5000 years before present. Since that time, the climate remained similar to the present.

Hydrochemical characteristics: The total salinity of the Umm Er Radhuma groundwater increases from the outcrop and recharge area in the west to the discharge area in the east. The pattern of increasing salinity from west to east is complicated by several tongues of fresh groundwater extending from west to east, which represent paths of preferential groundwater flow (GTZ, 2006). The groundwater under the outcrop and recharge area of the Umm Er Radhuma aquifer has total salinities ranging between 300 mg/l and 1,000 mg/L. In the central part of the Eastern Province, between the outcrop and the Gulf, total salinities range between 1,000 mg/L and 4,000 mg/L and increase in the vicinity of the Gulf to levels ranging between 4,000 mg/l and 10,000 mg/L (GTZ, 2006). The dominant ions change from calcium-bicarbonate in the outcrop area through calcium-sulphate to sodium-chloride in the coastal area. In the north of the study area, around Hafar Al Batin, the proportions of calcium and sulphate increase significantly. This area coincides with the area where the Umm Er Radhuma formation is partly composed of evaporitic layers.

Modeling: Umm Er Radhuma aquifer represents Layer 2 in this work. The design of the wells (Figure 2.9) at KFUPM was taken into consideration in the determination of the productive zone of the UER aquifer in the study area. The top elevation of UER in

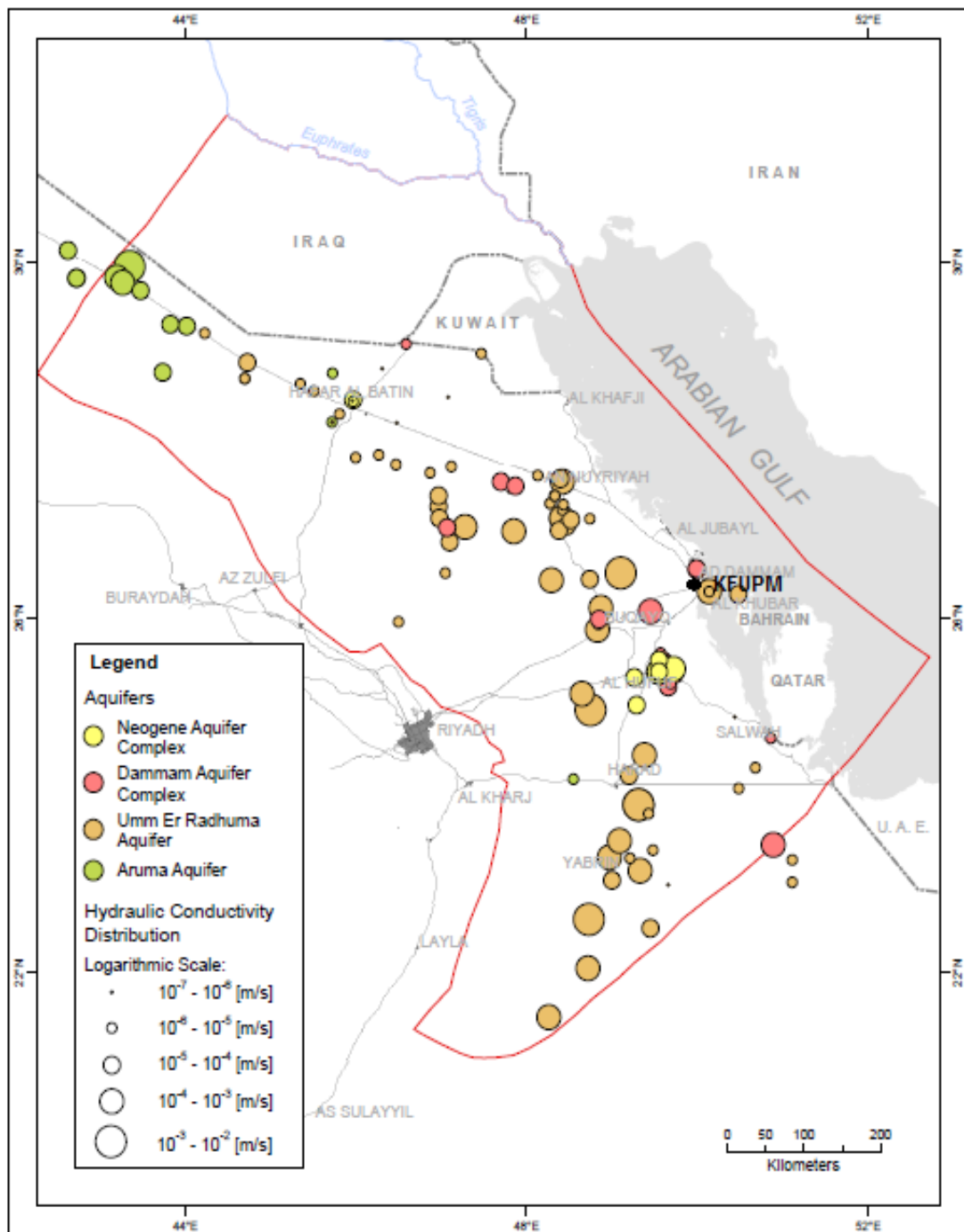


Figure 2.8: Spatial distribution of hydraulic conductivities from pumping tests conducted in the Eastern Province. The UER in the study area (KFUPM) has relatively high hydraulic conductivities (modified from GTZ, 2008)

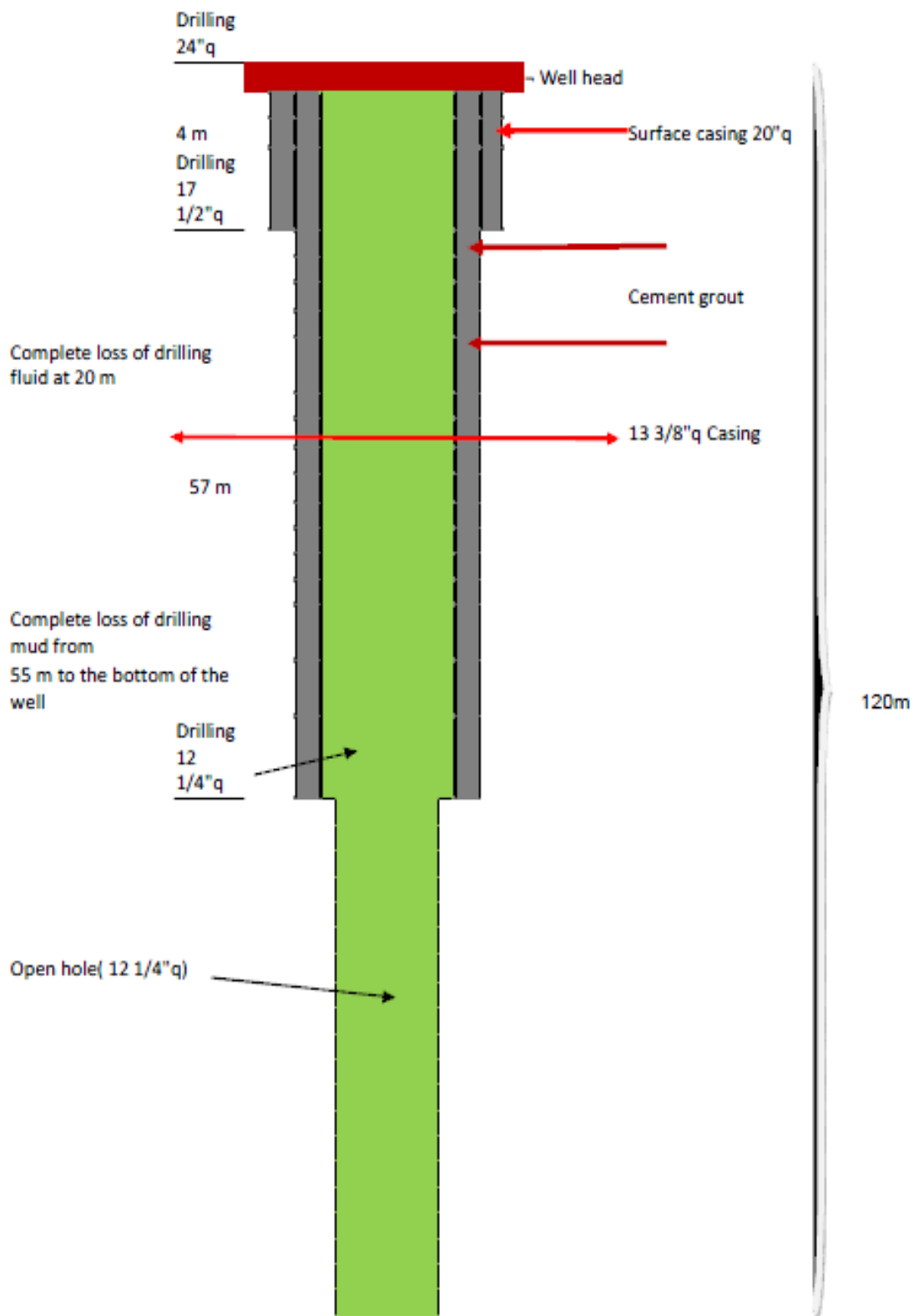


Figure 2.9: Design of production Well 10 at KFUPM with total depth 120 m

the study area (Figure 2.10) corresponds to the bottom of Rus aquitard. Throughout the extent of the UER aquifer in the model domain, the lower boundary (Figure 2.11) corresponds to the lowest depths of the pumping wells. An average thickness of about 85 m was suggested for the UER in the study area and since there is no complete record for the whole study area, this thickness is assumed to be the productive zone during the modeling process.

2.4.2 RUS AQUITARD

The Rus Formation in general represents an aquitard. It consists of soft limestones, dolomitic limestones, chalky limestones, shales and sulphates (gypsum and anhydrite) where present. The lateral distribution of the sulphates is non-uniform (Figure 2.5). They appear primarily in structural depressions and particularly in the north of the Eastern Province. In the study area and some other areas, the absence of sulphates is due to secondary solution processes. Here, the Rus is only represented by residual carbonates and in fact shows high similarity to the underlying units of the Umm Er Radhuma carbonates.

In the study area, Rus aquitard has an average thickness of 35 m. It clearly protrudes concavely at the west-central part of the area than any other part, giving it an anticlinal structure. Lithologically, Rus Formation in the study area is made up of chalky limestones and light colored marl with thin beds of calcarenite at the top. Due to its contact with the UER aquifer, Rus aquitard contains local irregular masses of gypsum partially dolomitized with minor beds of soft limestone at the bottom. There is no complete succession of Rus Formation in the study area since sulphates are absent due to solution.

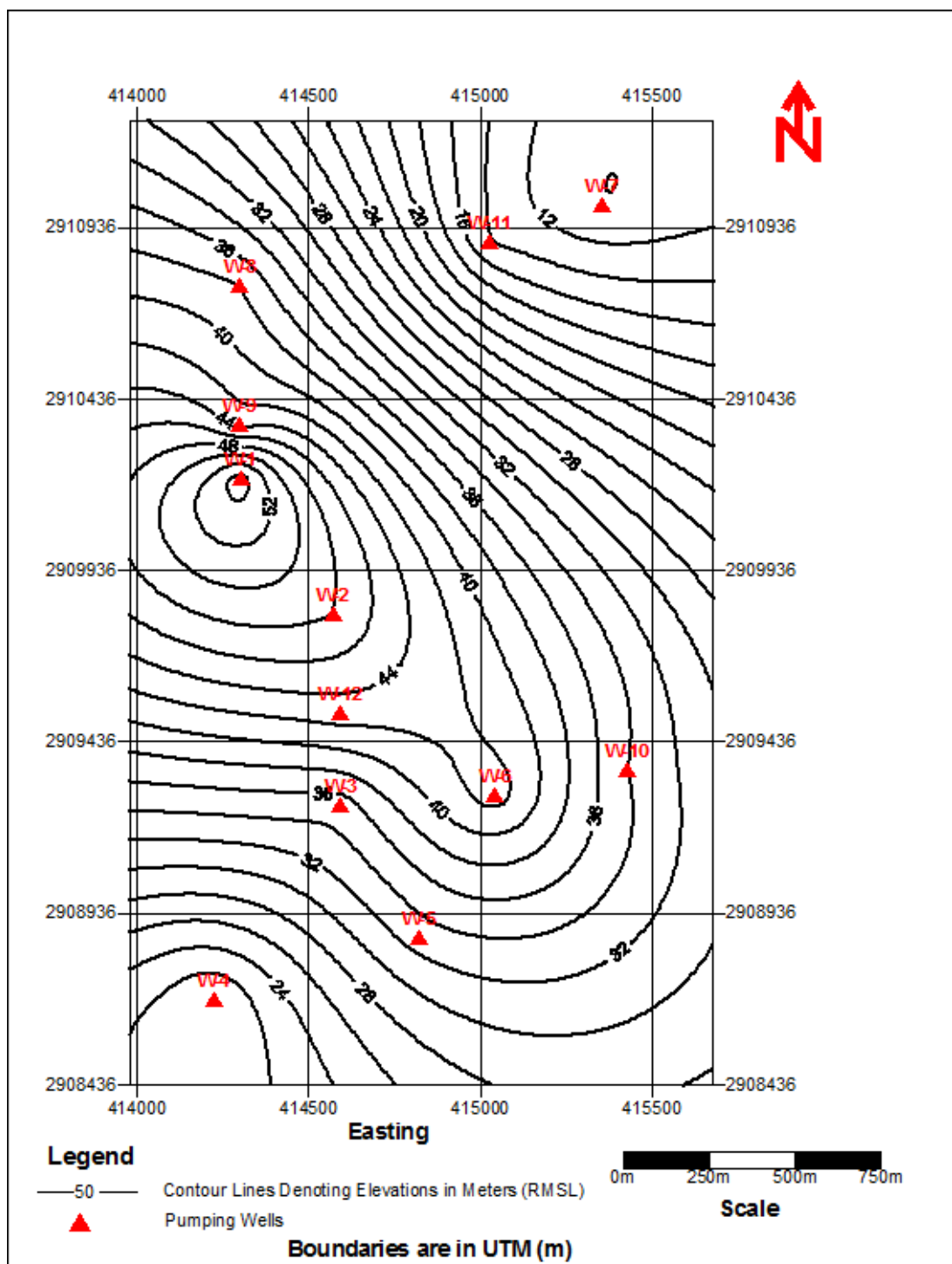


Figure 2.10: Top elevation of Umm Er Radhuma aquifer in the study area

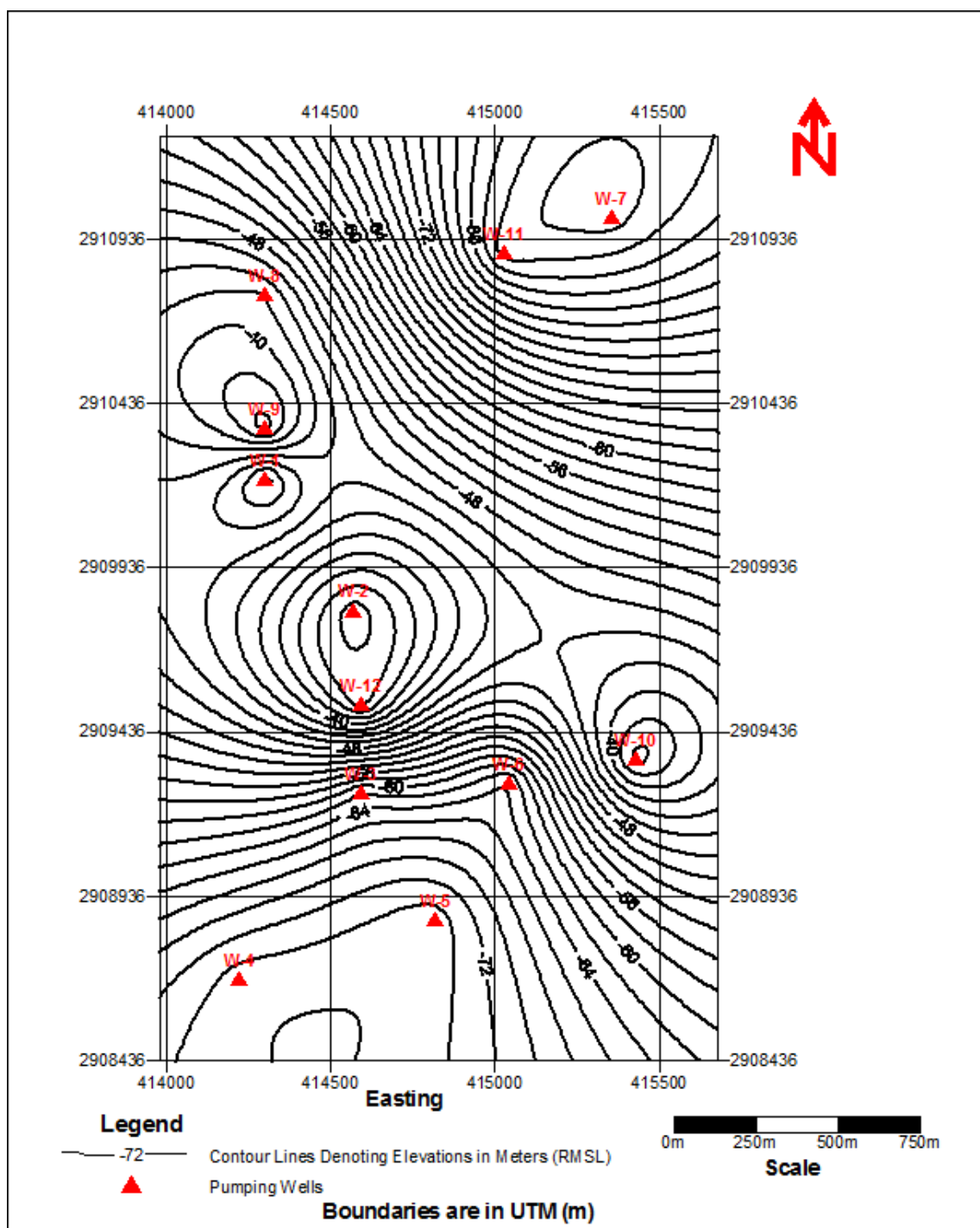


Figure 2.11: Bottom elevation of Umm Er Radhuma aquifer considered as the productive zone in the model

In the model, Rus aquitard represents the Layer 1. Since it is an aquitard, it was not included in the simulation. The top elevation of Rus aquitard corresponds to the ground surface (Figure 1.2) of the study area. The topographic map is one of the most pertinent data used in the model development. The thickness value of 35 m (average) of Rus aquitard in the study area was determined by deducting value of top elevation of UER (Figure 2.10) from the elevation value of the ground surface.

CHAPTER 3

DEVELOPMENT OF SIMULATION MODEL FOR THE STUDY AREA

3.1 INTRODUCTION

Developing a modeling concept is the initial and the most important part of every modeling effort (Kresic, 1997). It requires a thorough understanding of hydrogeology, hydrology and dynamics of groundwater flow in and around the area of interest. The final result is a computerized data base, and simplified map and cross-sections that will be used in model design.

In this chapter, various steps involved in the development of a realistic conceptual model and calibration process of the aquifer system in the study area for an efficient numerical groundwater flow model are explained.

3.2 CONCEPTUAL MODEL

A conceptual model is a simplified representation of the groundwater system. It approximates the field situation. Therefore, it is essential that the conceptual model be a valid representation of the main hydrogeologic conditions present in the area.

Stratigraphic information and understanding of the depositional history is very important in developing a conceptual model. Aquifers and aquitards are identified based on the concept of hydrostratigraphic units (Maxey, 1964) and (Seaber, 1988).

Hydrostratigraphic units consist of geologic units of similar hydrogeologic properties. Several geologic formations may be combined into a single hydrostratigraphic unit or a geologic formation may be subdivided into several aquifers and aquitards in a conceptual model.

In the present study area, the aquifer system comprises an aquitard and a single aquifer. The aquitard (Rus aquitard) lies conformably on the aquifer (UER aquifer). Changes in the vertical flow rates in the aquifer would be induced by head changes in the aquifer system, which would occur in response to changes in pumping patterns. For these reasons, it was necessary to model the groundwater system present in the study area as a single aquifer system representing a full three dimensional flow of a flow system view point as described by Anderson and Woessner (1992).

Based on the geological and hydrogeological settings of the study area, the map of the study area (Figure 3.1) representing the modeling domain was plotted and a conceptual diagram of the simulated aquifer-aquitard system is shown in Figure 3.2. The conceptual model depicts a single aquifer overlain by an aquitard. The Dammam aquifer, also of hydrogeologic significance, is either absent or non-prolific in the study area. Therefore, Dammam aquifer is not included in the present study.

The aquifer-aquitard system as defined for model included the following layers, from top to bottom:

Layer 1: The Rus aquitard

Layer 2: The UER aquifer, which is unconfined throughout the study area

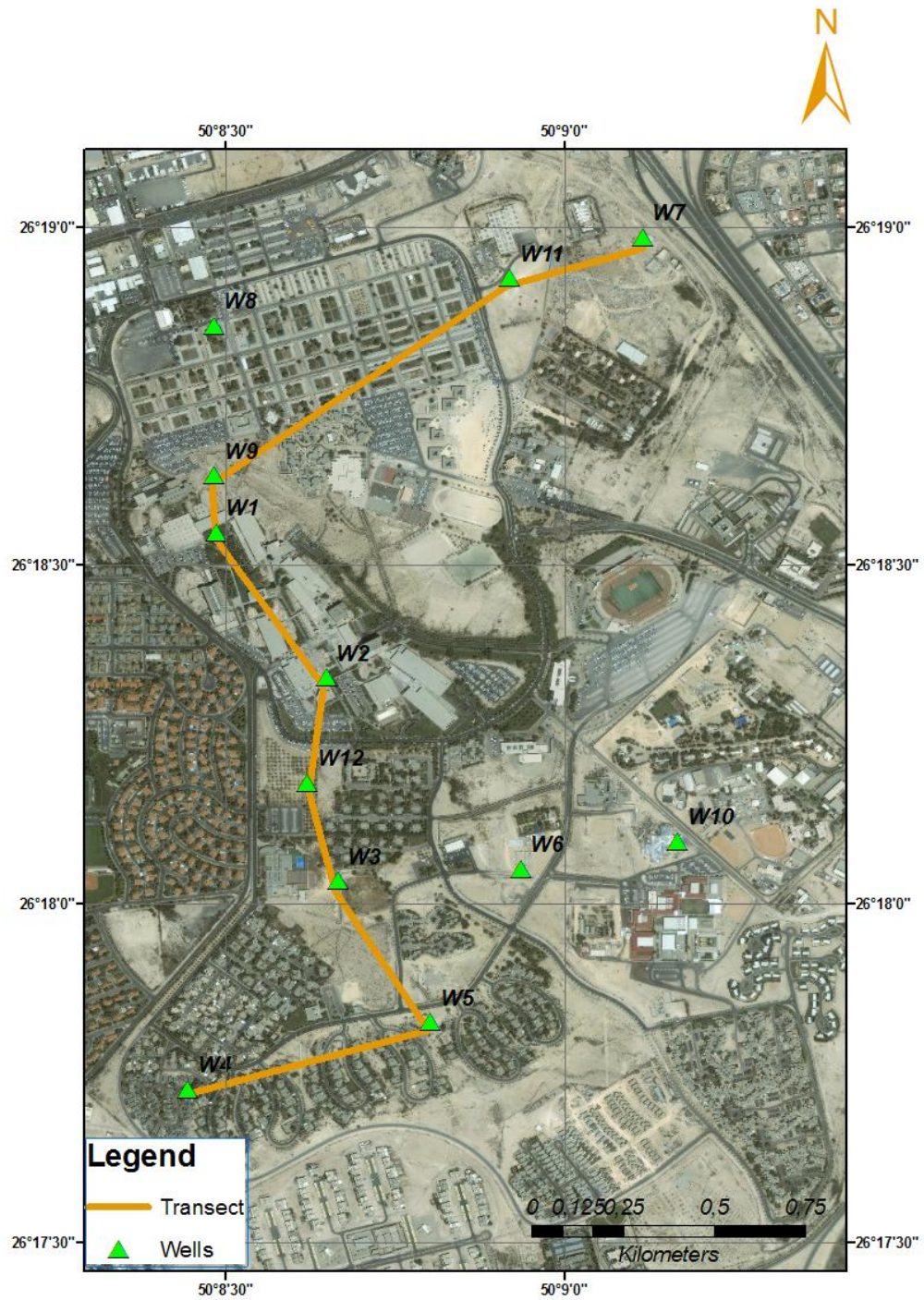


Figure 3.1: Map of the study area denoting the model domain. The transect (inset) and the hydrogeological information of the wells were used in the construction of the conceptual model

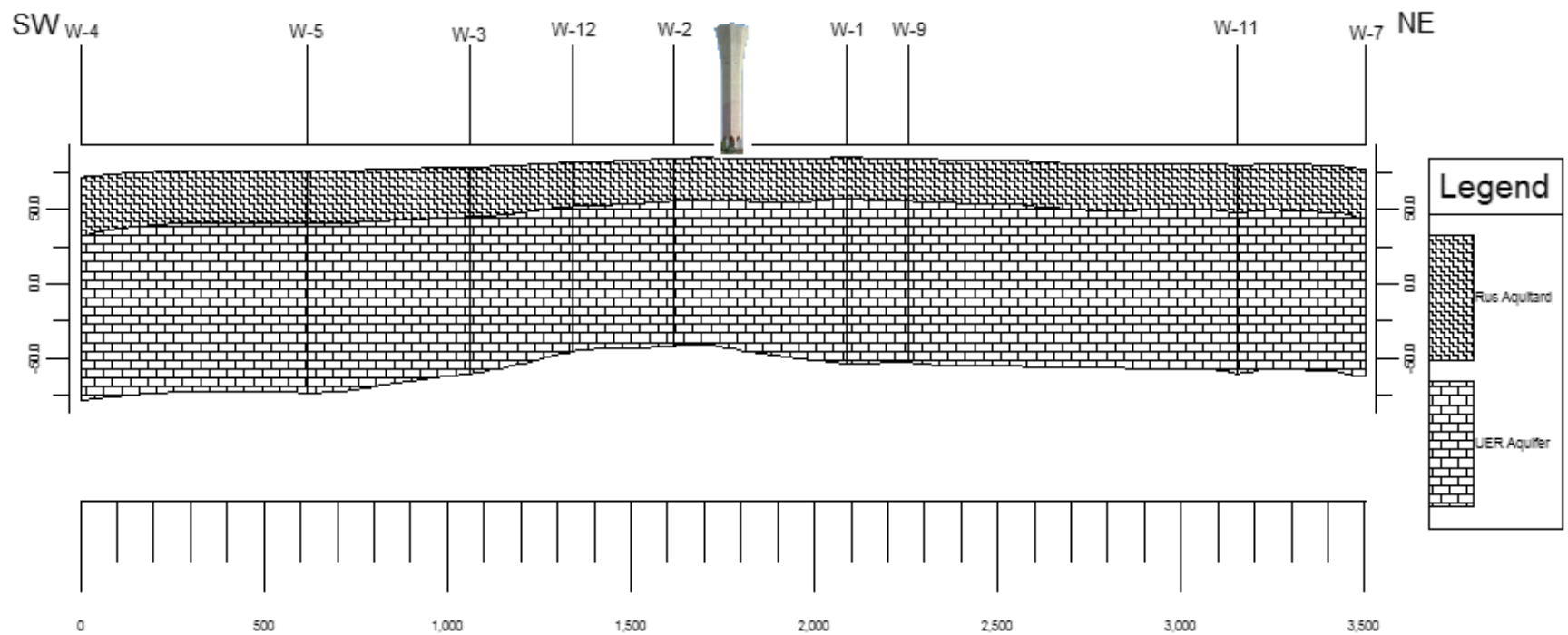


Figure 3.2: Conceptual model of the groundwater system in the study area. The symbolic University Tower is located between Well 2 and Well 1

In the development of the conceptual model, the geographic coordinates of the study area and well locations were converted to Universal Transverse Mercator (UTM). These sets of information were used in constructing a map of the study area that represents the modeling domain. Locations of the wells in the study area are depicted on the map. Information such as well depths, thicknesses of the top and bottom layers for each well and the estimated total elevation of the study area were integrated in the development of the conceptual model. A line of cross-section (transect) was drawn from the southwestern part, where KFUPM Well No. 4 is located, to the northeastern part of the study area, where KFUPM Well No. 7 is located. The transect passed through some of the other wells (Well Nos. 5, 3, 12, 2, 1, 9 and 11) before ending its course at Well No. 7.

The conceptual model clearly shows the anticlinal protrusion of the aquifer-aquitard system in the study area, especially in the middle part. It also reveals that the groundwater flow direction is from the southwest to the northeast.

3.3 MODELING TECHNIQUE

The present study uses a "Visual MODFLOW", which is the MODFLOW of the U.S. Geological Survey (USGS) with an efficient interface for developing three dimensional groundwater flow and contaminant transport models. Visual MODFLOW is an easy to use pre- and post- processor for the MODFLOW. The modular structure of the computer code of MODFLOW (McDonald and Harbaugh, 1988) consists of a main program and a series of highly independent subroutines called modules. These subroutines are grouped into "packages", each dealing with a specific feature of the hydrogeologic system to be simulated. The division of the code into modules makes the program flexible, which permits the user to examine the specific hydrogeologic

feature of the model independently. Numerical modeling is a well-founded and widely used technique in water resources development and evaluation studies. A detailed description of the MODFLOW is out of scope of this thesis, but for completeness of this research, basic theory is included in the following sections.

3.3.1 GROUNDWATER FLOW EQUATION

The general form of the partial differential equation, governing transient, three dimensional flow of groundwater in a heterogeneous and anisotropic aquifer was expressed by Anderson and Woessner (1992):

$$\frac{\partial}{\partial x} \left(K_x \frac{\partial h}{\partial x} \right) + \frac{\partial}{\partial y} \left(K_y \frac{\partial h}{\partial y} \right) + \frac{\partial}{\partial z} \left(K_z \frac{\partial h}{\partial z} \right) = S_s \frac{\partial h}{\partial t} - R^* \quad (3.1)$$

Where:

K_x, K_y and K_z	=	Components of the hydraulic conductivity tensors (LT)
S_s	=	Specific storage of the porous material (LT^{-1})
R^* the	=	Sink/source term that is intrinsically positive and defines the volume of inflow to the system per unit value of aquifer per unit of time to simulate outflow
h	=	Hydraulic head (L)

Equation (3.1), together with specifications of flow and/or head conditions at the boundaries of an aquifer system, and initial head conditions constitute a mathematical model of groundwater flow.

Analytical solutions for (3.1) are difficult, except for very simple systems. Therefore, various numerical methods are employed to obtain approximate solutions. One of such

approaches is the finite difference method, in which the continuous system described by (3.1) is replaced by a finite set of discrete points in space and time, and the partial derivatives are replaced by differences between functional values at these points. The process results in a system of linear algebraic difference equations and their solution yields values of head at specific points and time.

3.3.2 FINITE-DIFFERENCE EQUATION

The finite difference analog of (3.1) can be obtained by applying the rules of differential calculus. However, the approach utilized by McDonald and Harbaugh (1988) simplifies the mathematical treatment and explains the computational procedure in terms of familiar physical concepts regarding the flow system.

Finite-difference formulation of (3.1) involves the discretization of the aquifer system into a mesh of points termed nodes. Conceptually, these points represent prisms of porous material, termed cells, within which the hydraulic properties are constant, so that any value associated with a node or applied to it is distributed over the extent of a cell. A Representative Elementary Volume (REV) is shown in Figure 3.3.

The nodes are referenced with row (i), column (j) and layer (k) index colinear with x, y and z directions, respectively, as in Figure 3.3. The width of cells along the rows is designated as Δr_j for jth column; the width of cells along the rows is designated as Δc_i for the ith row; and thickness of layers in the vertical direction is designated as Δv_k for the kth layer.

Adopting the block-centered grid system, the implicit finite-difference approximation of (3.1) can be written as:

$$\begin{aligned}
& CV_{i,j,k-\frac{1}{2}} h_{i,j,k-1,t} + CC_{i-\frac{1}{2},j,k} h_{i-1,j,k,t} + CR_{i,j-\frac{1}{2},k} h_{i,j-1,k,t} \\
& + \left[-CV_{i,j,k-\frac{1}{2}} - CC_{i-\frac{1}{2},j,k} - CR_{i,j-\frac{1}{2},k} - CV_{i,j,k+\frac{1}{2}} - CC_{i+\frac{1}{2},j,k} - CR_{i,j+\frac{1}{2},k} \right. \\
& + (P_{i,j,k} - S_{i,j,k} \Delta r_j \Delta c_i \Delta v_k) \left. \right] \frac{h_{i,j,k,t}}{\Delta t} + CV_{i,j,k+\frac{1}{2}} h_{i,j,k+1,t} + CC_{i+\frac{1}{2},j,k} h_{i+1,j,k,t} \\
& + CR_{i,j+\frac{1}{2},k} h_{i,j+1,k,t} \\
& = -Q_{i,j,k,t} - S_{i,j,k} (\Delta r_i \Delta c_j \Delta v_k) \frac{h_{i,j,k,t-1}}{\Delta t}
\end{aligned} \tag{3.2}$$

Where:

Δt = Time interval (T);

Δr_j = Width of the cell along row direction in j^{th} column (L);

Δc_i = Width of the cell along column direction in i^{th} row (L);

$CR_{i,j+\frac{1}{2},k}$ and $CR_{i,j-\frac{1}{2},k}$ = Conductance in row direction between nodes (i, j, k) and $(i, j+1, k)$, and (i, j, k) and $(i, j-1, k)$, respectively ($L^2 T^{-1}$);

$CC_{i+\frac{1}{2},j,k}$ and $CC_{i-\frac{1}{2},j,k}$ = Conductance in column direction between nodes (i, j, k) and $(i+1, j, k)$, and (i, j, k) and $(i-1, j, k)$, respectively ($L^2 T^{-1}$);

$CV_{i,j,k+\frac{1}{2}}$ and $CV_{i,j,k-\frac{1}{2}}$ = Conductance in vertical direction between nodes (i, j, k) and $(i, j, k+1)$, and (i, j, k) and $(i, j, k-1)$, respectively ($L^2 T^{-1}$);

$Q_{i,j,k,t}$ = Specified external source/sink at node (i, j, k) during the time interval being considered ($L^3 T^{-1}$);

$P_{i,j,k}$ = Conductance between an external source or sink and node (i, j, k) , ($L^2 T^{-1}$);

$S_{i,j,k}$ = Storativity at node (i, j, k) , (dimensionless);

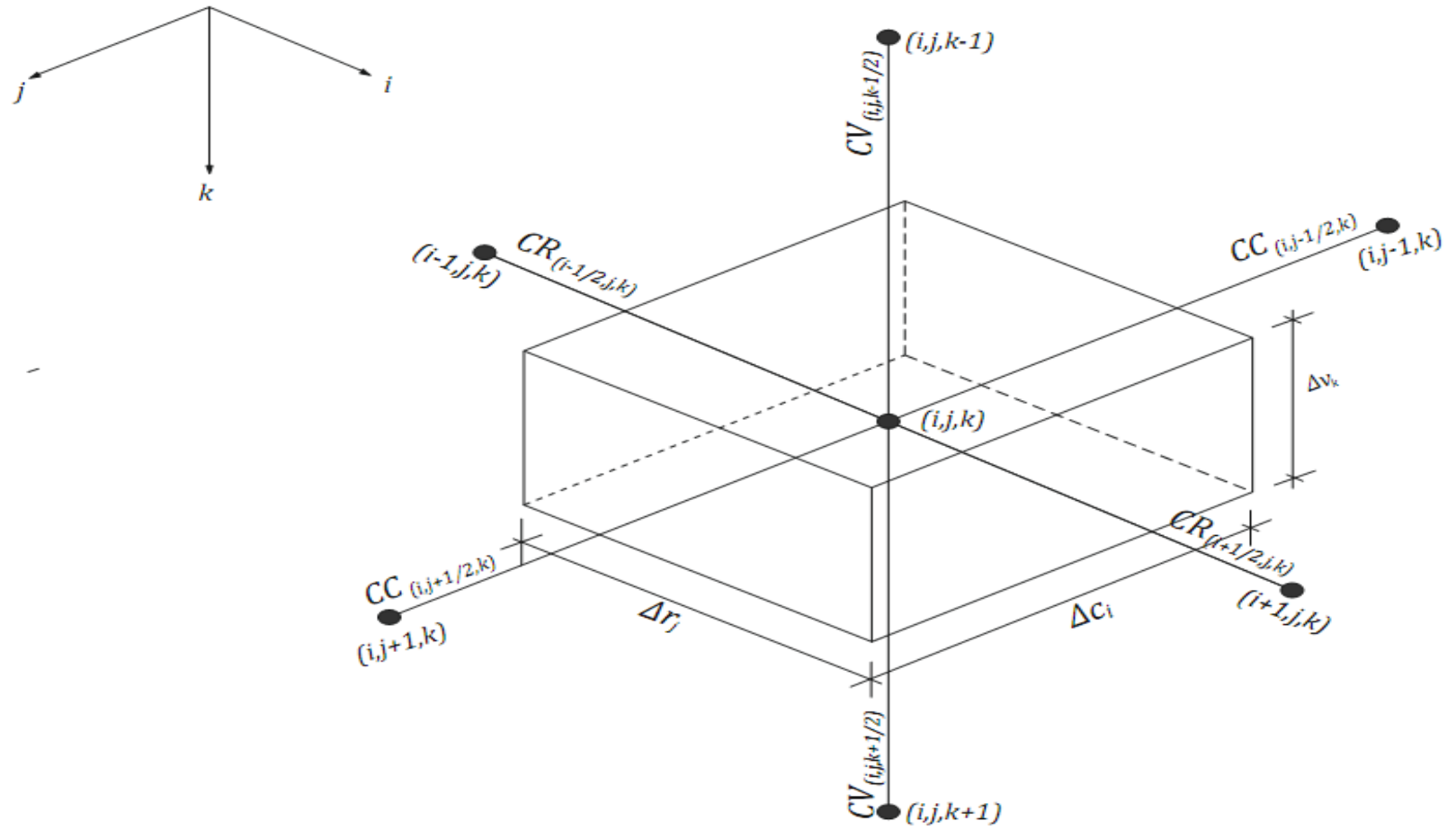


Figure 3.3: Finite Difference Block and definition of conductance terms

$h_{i,j,k,t}, h_{i,j,k-1,t}, h_{i,j-1,k,t}, h_{i-1,j,k,t}, h_{i,j,k+1,t}, h_{i,j+1,k,t}, h_{i+1,j,k,t}$ = Unknown hydraulic heads at indicated nodes at the end of the time interval being considered (i.e., at the end of time t) (L);

$h_{i,j,k,t-1}$ = Hydraulic head at node (i, j, k) at the beginning of the time interval being considered [i.e., at the end of the time $(t - 1)$]. This is known from initial conditions at time $t = 0$.

The finite-difference equation uses the conductance between nodes of adjacent cells, rather than simply the conductance within the cell. The horizontal conductance terms CR and CC between nodes that are adjacent horizontally are calculated using the harmonic mean as follows (McDonald and Harbaugh, 1984):

$$CR_{i,j+\frac{1}{2},k} = 2\Delta c_i \left(\frac{TR_{i,j,k} TR_{i,j+1,k}}{TR_{i,j,k} \Delta r_{j+1} + TR_{i,j+1,k} \Delta r_j} \right) \quad 3.3a$$

$$CR_{i,j-\frac{1}{2},k} = 2\Delta c_i \left(\frac{TR_{i,j,k} TR_{i,j-1,k}}{TR_{i,j,k} \Delta r_{j-1} + TR_{i,j-1,k} \Delta r_j} \right) \quad 3.3b$$

$$CC_{i+\frac{1}{2},j,k} = 2\Delta r_j \left(\frac{TC_{i+1,j,k} TC_{i,j,k}}{TC_{i,j,k} \Delta c_{i+1} + TC_{i+1,j,k} \Delta c_i} \right) \quad 3.4a$$

$$CC_{i-\frac{1}{2},j,k} = 2\Delta r_j \left(\frac{TC_{i-1,j,k} TC_{i,j,k}}{TC_{i,j,k} \Delta c_{i-1} + TC_{i-1,j,k} \Delta c_i} \right) \quad 3.4b$$

Where:

TR and TC are the transmissivities along row and column directions, respectively ($L^2 T^{-1}$).

In model layers or cells which are confined, horizontal conductance will be constant for the whole simulation. However, if a layer or model cell is unconfined or potentially unconfined, new values of horizontal conductance must be calculated as the changes in head takes place. This is done in MODFLOW at the beginning of each

iteration. Initially, the transmissivity is calculated as the product of hydraulic conductivity and saturated thickness; then conductance is calculated from transmissivity and cell dimensions using (3.3) and (3.4).

The finite difference flow equation also requires the conductance between two vertically adjacent nodes. The vertical interval between two nodes (i, j, k) and $(i, j, k + 1)$ may be considered to contain n hydrogeologic units, having vertical conductivities $K_1, K_2, K_3, \dots, K_n$ and thicknesses $\Delta Z_1, \Delta Z_2, \dots, \Delta Z_n$, and the area of the cells around two adjacent nodes is $\Delta r_j, \Delta c_i$. The vertical conductance terms of an individual hydrogeologic layer, g, in this area is given by (McDonald and Harbaugh, 1988):

$$C_g = \frac{K_g \Delta r_j \Delta c_i}{\Delta Z_g} \quad (3.5)$$

Where:

K_g = Vertical hydraulic conductivity of layer, g, (LT^{-1});

ΔZ_g = Thickness of the layer 'g' (L)

3.3.3 INITIAL PIEZOMETRIC SURFACE

Initial piezometric surface contour map of Umm Er Radhuma aquifer in the study area was constructed using the regional water level maps and data from previous investigations. Pseudo-steady-state conditions for the study area were developed as shown in Figure 3.4, which represents the pre-1967 conditions.

Analysis of the piezometric surface map of UER aquifer in the study area shows a general flow pattern from the southwest to the northeast of the study area (Figure 3.5).

The velocity of flow varies between 0.00014 m/s and 0.00074 m/s, with the highest occurring at the central (anticlinal) part of the study area. This flow pattern may be affected by local structural factors. The gradient (Figure 3.6), calculated downhill, varies from 1.2×10^{-4} to 5.0×10^{-4} with an average of 2.8×10^{-4} . The hydraulic gradients are higher at structural highs than at slopes. This reflects changes in transmissivity, possibly caused by karstification, facies and thickness variations. The general piezometric pattern, the flow pattern and the hydraulic gradient distribution in the study area are consistent with the regional hydrogeologic, structural and lithologic information shown in Figure 2.7.

3.3.4 DISCRETIZATIONS AND BOUNDARY CONDITIONS

The study area was discretized into a non-uniform square grid, comprising 50 rows and 34 columns in the steady-state (Figure 3.7), and 69 rows and 52 columns in the transient-state (Figure 3.8), with a grid spacing of approximately 65 m in cells where pumping wells are absent and approximately 33 m in cells surrounding the pumping wells. The total number of cells is 1700 in the steady-state and 3588 in the transient state. The model covers a total area of 4.8 km^2 . The grid spacing was judged in view of the available data and computational time. The present study has a finer mesh than all previous studies in Eastern Province of Saudi Arabia.

The boundaries of the model were determined after critical review of the available hydrogeological data and trends of the piezometric levels in the aquifer. Figures 3.7 and 3.8 show the boundary conditions assigned for Layer 2 (UER aquifer) in the steady-state and transient-state conditions, respectively. Boundary of Layer 1 (Rus aquitard) was assigned inactive throughout the modeling.

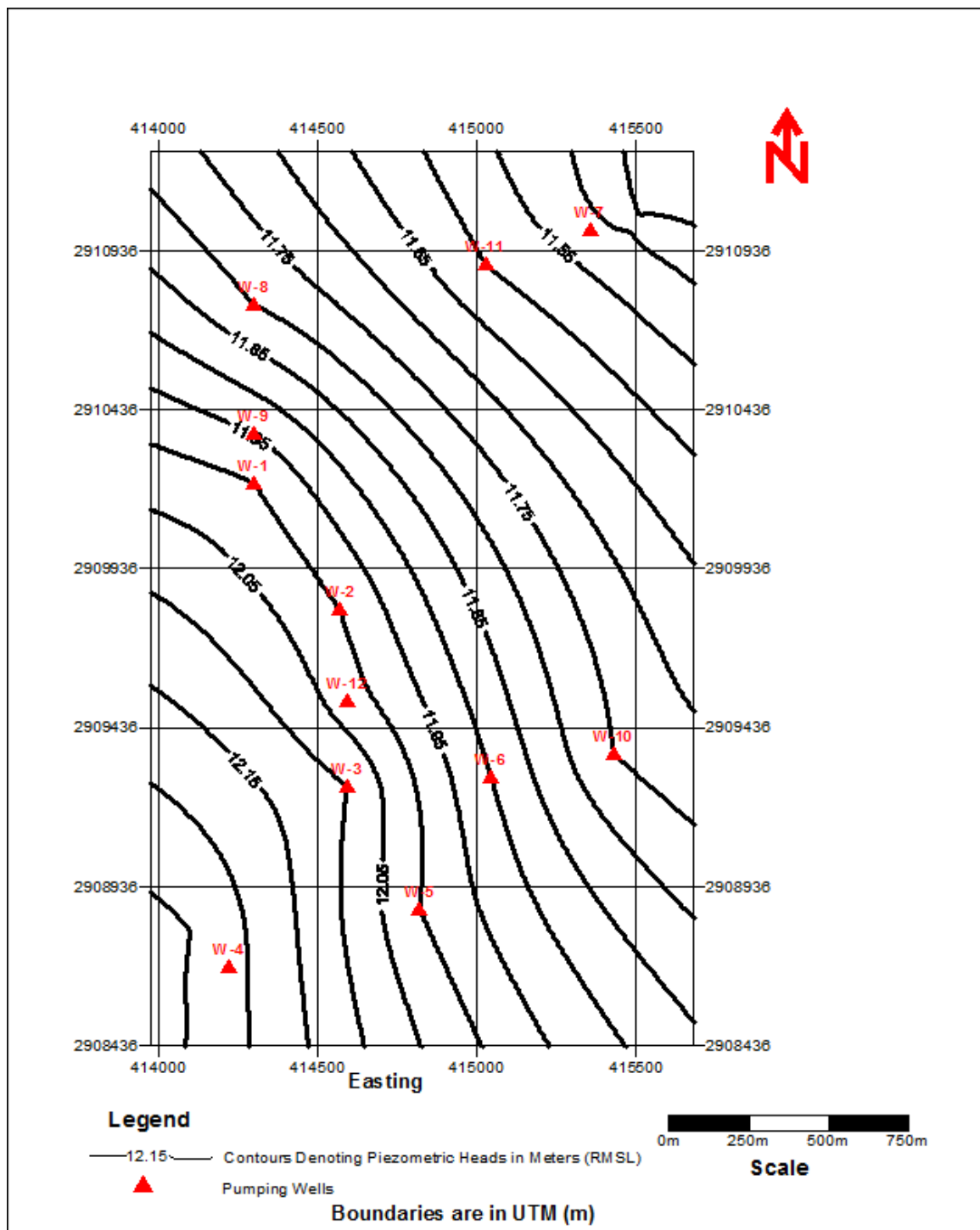


Figure 3.4: Initial piezometric head contour map of the study area (1967 steady-state conditions)

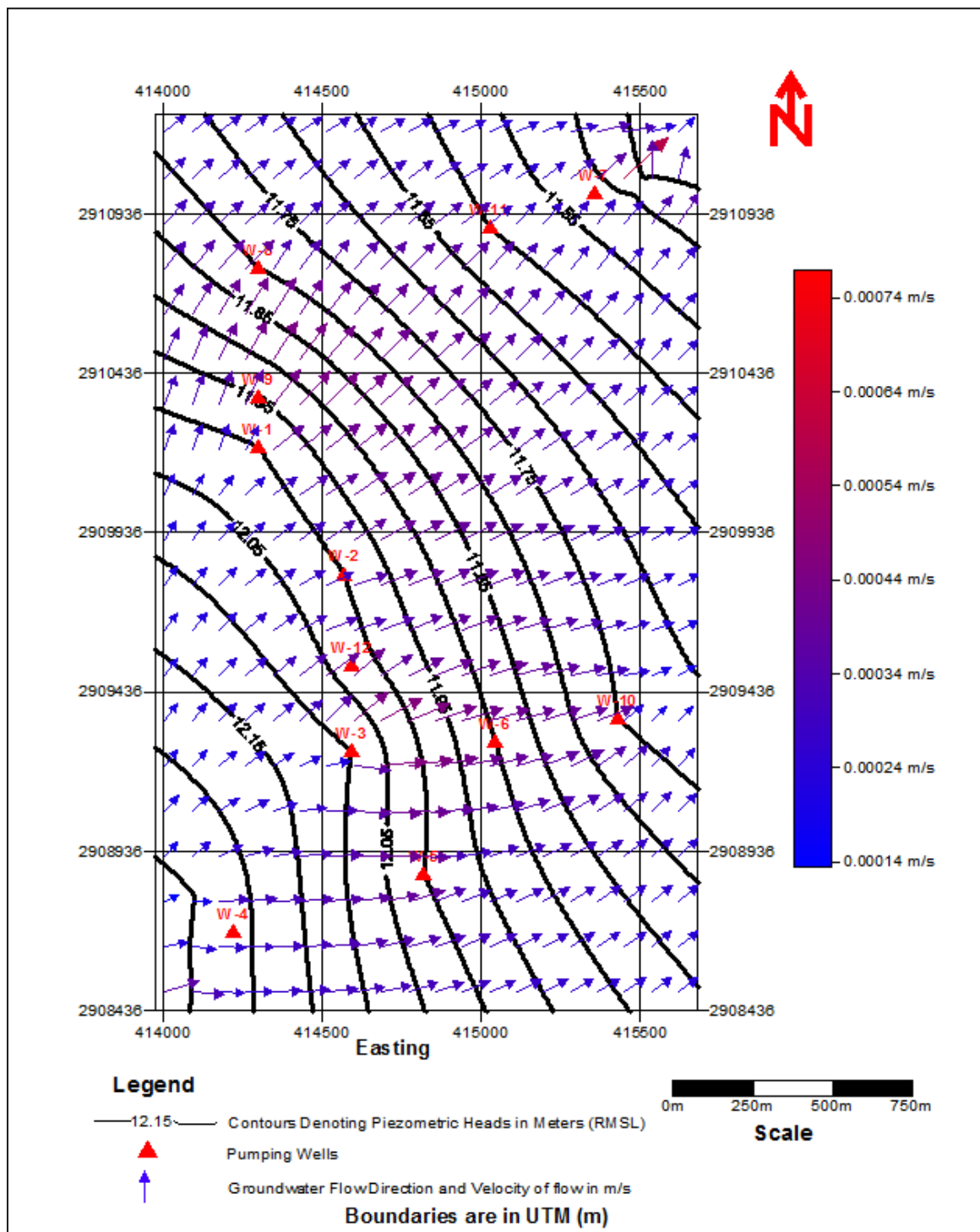


Figure 3.5: Groundwater flow direction in the Umm Er Radhuma aquifer of the study area. This flow pattern is consistent with the regional flow pattern shown in Figure 2.8

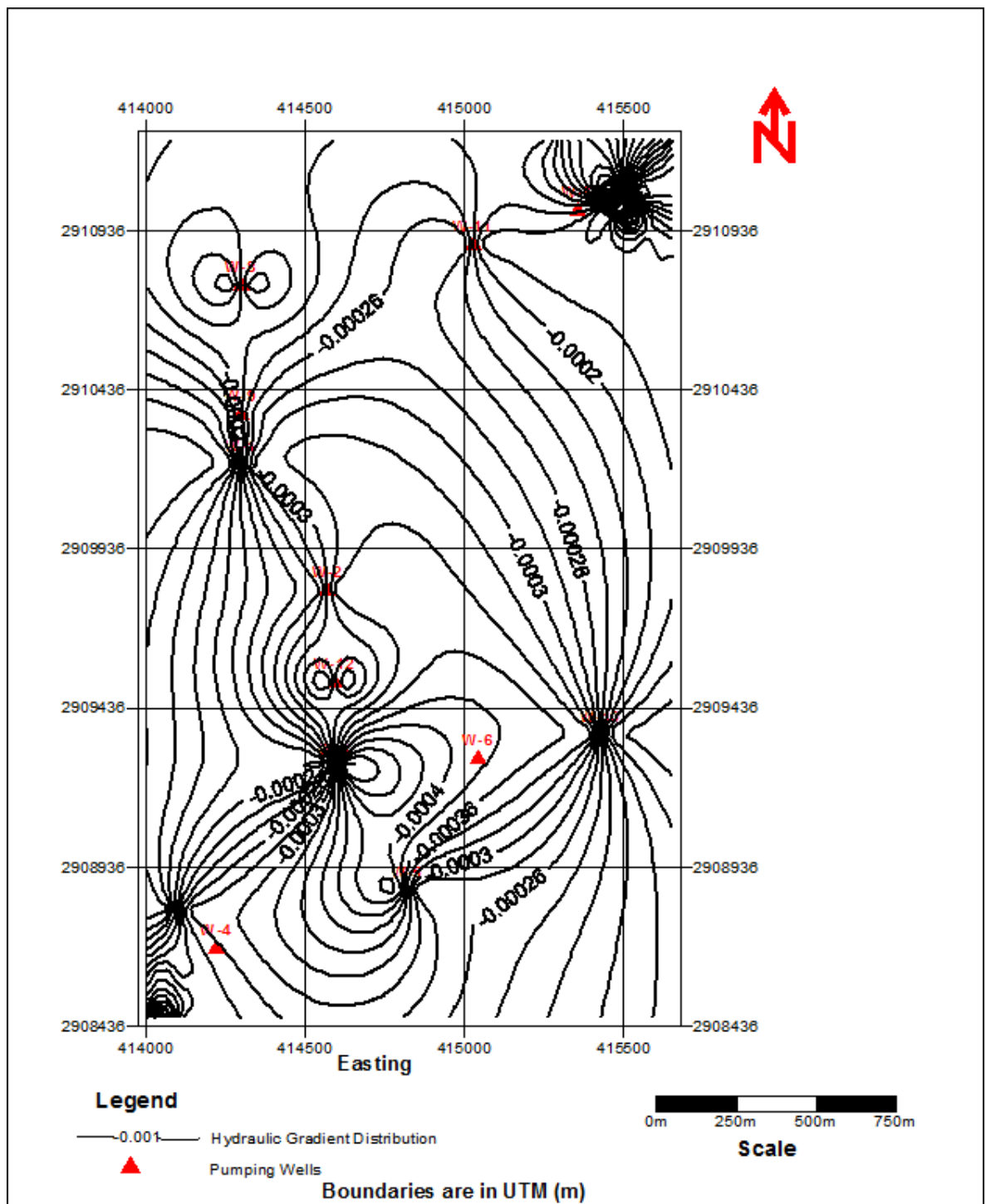


Figure 3.6: Hydraulic gradient distribution in the study area

In the steady-state calibration, all the boundaries of the model were assigned as constant head boundaries. Proper water level data beyond the model boundaries limits were not available to be used as a head gradient inflow to the system. A constant head would be justified because no pumping was taking place in 1967, which was used as the starting period in the model. The boundaries are at least 200 m away from the pumping wells in the modeling domain. Any stress in the model area would not have significant effect on the boundary heads.

In the transient state calibration, variable head boundaries were assigned to the boundaries of the model. Since the research objective is to simulate the effects of pumping on the aquifer system over a long period of time, the choice of variable head boundary is substantiated because variable head boundary enables time-step drawdown to be measured relative to the applied stresses.

As the study area is devoid of rivers, streams and erosional surface, no no-flow boundaries were assigned to any part of the modeling area.

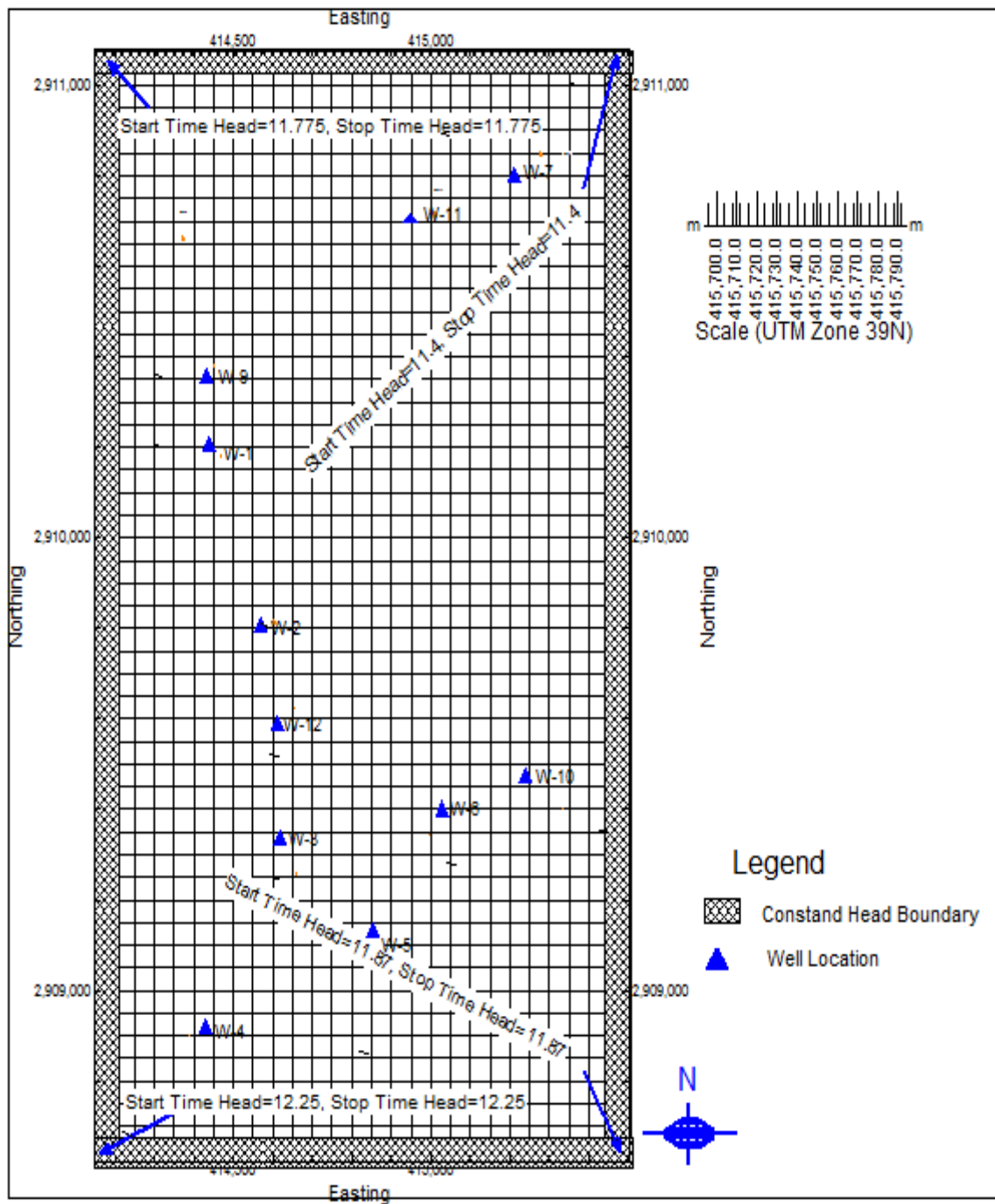


Figure 3.7: Finite difference grid and boundary condition (steady-state)

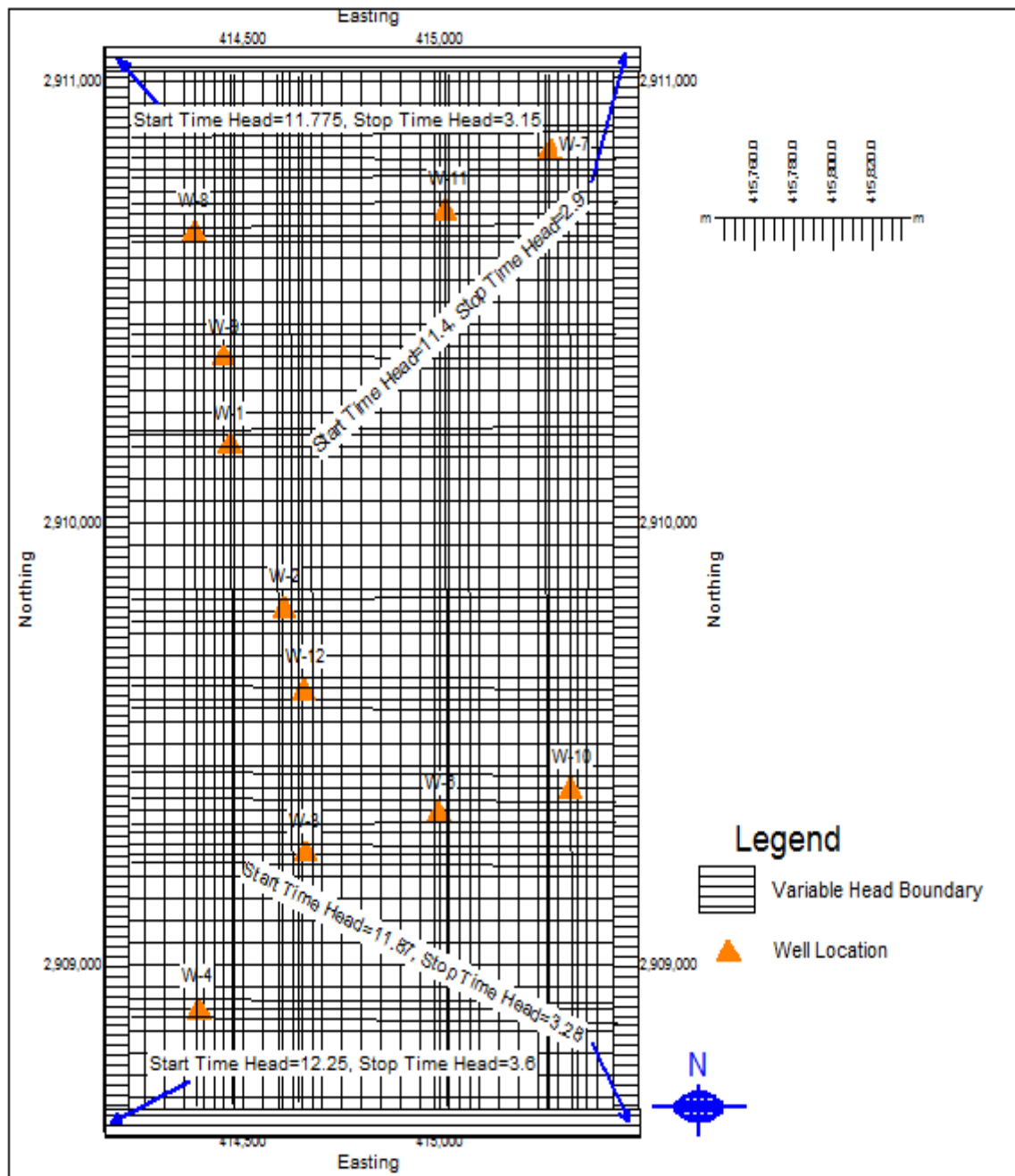


Figure 3.8: Finite difference grid and boundary condition (transient-state)

3.3.5 INITIAL ASSESSMENT OF INPUT PARAMETERS

3.3.5.1 HYDRUALIC PROPERTIES

Steady-state simulation requires identification of horizontal hydraulic conductivity. Visual MODFLOW calculates the transmissivities and vertical leakance terms from the thickness of model layer implicitly given by the top and bottom elevation of the layer.

The aquifer in the study area is unconfined. Hydraulic conductivities were calculated by dividing the available transmissivity values by the thickness of the productive zone of UER aquifer. Transmissivity values were assessed mainly from Italconsult (1969) and GDC (1980) for UER aquifer. Regional measured values of transmissivity and storage coefficient of the aquifer as given by Italconsult (1969) and GDC (1980) are in the range of 7,000 – 10,000 m²/d and 1.3×10^{-5} – 1.6×10^{-8} , respectively.

Development of a full three-dimensional simulation model requires values of vertical conductivity for the aquifer layer. The vertical conductivity was assumed to be one tenth of the horizontal conductivity. This assumption was based on previous hydrogeologic investigations.

In the three-dimensional governing equation (3.1), specific yield (Ss) was used as an input to the model for a confined aquifer. It is equal to the volume of water released from storage within a unit volume of porous material per unit decline in head. The values of the specific storage were obtained after dividing the storativity values by the aquifer productive thickness and assigning to each cell.

The zonings of hydraulic conductivity (K) in the model area are shown in Figure 3.9. The distribution of K values reflects heterogeneity of UER aquifer in the study area.

The horizontal K values range between 50 and 350 m/day, while the specific yield, S_y , values range between 0.04 and 0.07. The variation in hydraulic conductivity values is consistent with regional values used in previous works shown in Figure 2.9, although the K values of the study area fall in the upper range. The vertical K values were taken as one-tenth of the horizontal K values.

3.3.6.2 WELL ABSTRACTIONS

The present study relies mainly on the detailed well abstraction data from KFUPM Maintenance Department and KFUPM Research Institute (Appendix A). Historical water abstraction by GDC (1980) shows that year 1967 was relatively stable in terms of water abstractions. Therefore, the base year for steady-state simulation was taken as 1967 and all calculations were made from that year.

Since 1967, there has been a total of twelve pumping wells at KFUPM. At every point in time since 1967, a well is added either to meet an increased water demand or as a replacement for a pre-existing well that is not functioning. Well No. 1 is the only well that has survived since 1967 till present. The history of the pumping wells at KFUPM was taken into consideration in the transient-state calibration. The pumping capacity of the wells ranges between 2180 m³/day and 5451m³/day. All the pumping data (Appendix A) for each well were provided by KFUPM Maintenance Department except for pumping data for Well No. 8. It was therefore excluded in the modeling.

The design of the pumping wells in KFUPM is shown in Figure 2.10. All the wells were installed with Grundfos Submersible Pump except Well Nos. 6 and 7, which were installed with Peerless Turbine Enclosed Shaft.

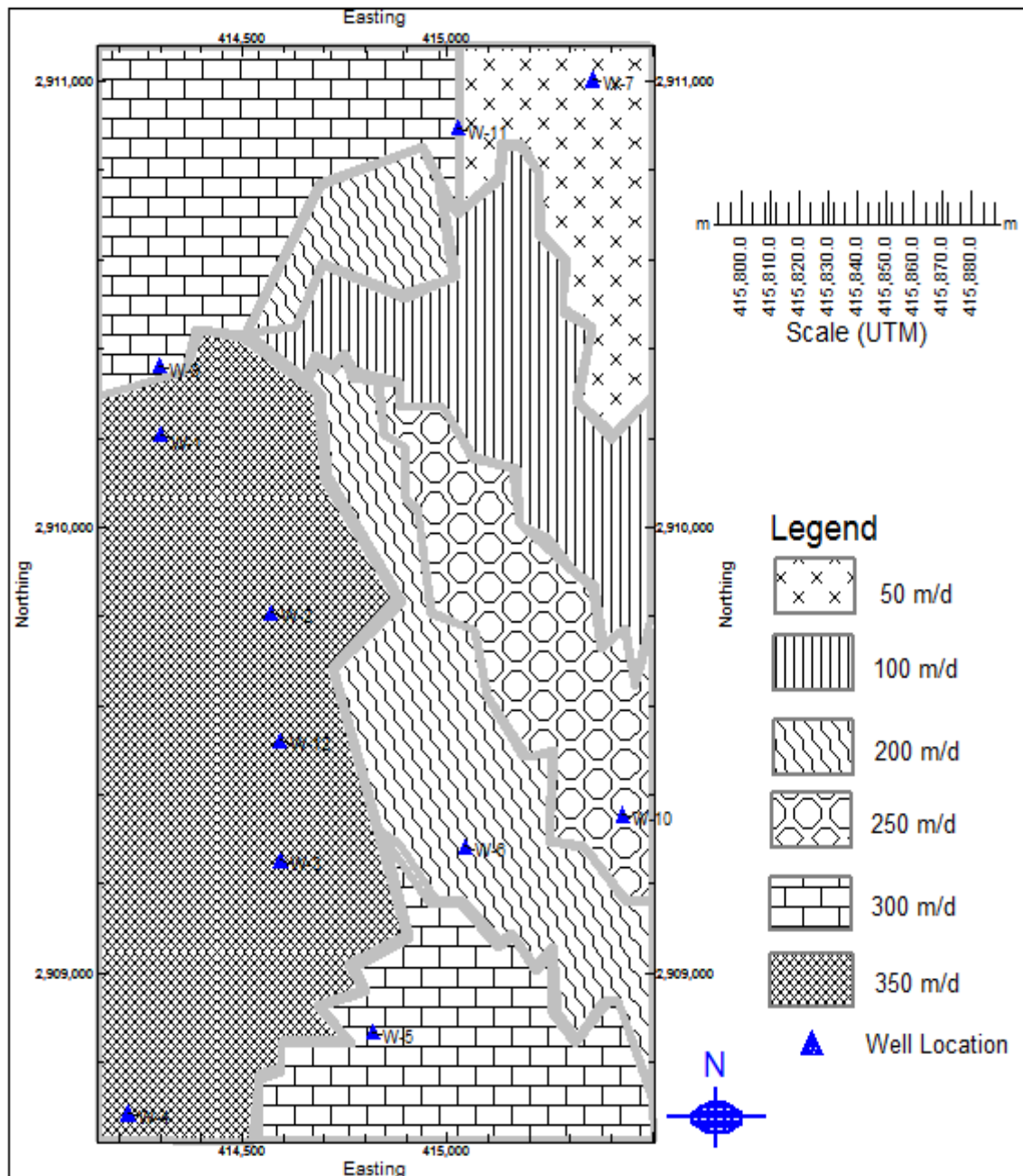


Figure 3.9: Hydraulic conductivity (K) distribution (m/d) in the study area. The values of K in the study area fall within the upper range of regional K values

3.4 MODEL CALIBRATION

Many uncertainties exist in the initial parameter assessment due to minor inconsistencies in the data provided. Therefore, to overcome the uncertainties about the accuracy of the initially assessed aquifer parameter, it is necessary to make thorough and critical comparisons between the simulated and observed field values of hydraulic head distributions. The differences between observed and computed heads provide useful clues from which it is possible to identify the reasons for uncertainties. Identification of such variations and adjustment of aquifer parameters until the simulated heads match the observed values within the acceptable range of accuracy is known as calibration. Model calibration can be carried out either manually or by using automated methods. Automated calibration procedures use inverse methods. Initially the present study was started by using PEST (Parameter Estimation Package). Due to limitations of the number of zones of calibration, the present local study could not be calibrated successfully using the automated option. Satisfactory results could not be obtained even after hundreds of simulation runs due to the complex nature of the UER aquifer system. Therefore, this study adopted a manual approach described in the following section.

3.4.1 STEADY-STATE CALIBRATION

Steady-state conditions exist in the aquifer system prior to the beginning of any development scheme. It is a mean, trend free, stable condition represented by an average groundwater surface with the inflows balancing the outflows. In reality, no such hydrogeologic system exists. Therefore, in the present study, the model was calibrated against the earliest available data which is dated prior to the major developmental activities in the area.

Different accuracy criteria can be used to compare the simulated and measured data during the calibration procedures. Some of the most important criteria that are used to check the calibrated model are Root Mean Square error (RMS) and the Mean Absolute error. Another way of checking the amount of residual error is to compare the total simulated inflows and outflows as computed by water balance. The most frequently used model calibration is adjustment of the model data to obtain a reasonable match between observed data (calibration targets) and model calculation.

Since early piezometric head of UER aquifer was based on many extrapolations, some observation wells in the model area were selected to compare with the computed results. Extrapolation of the observation data back to year 1967 was made based on the present trends of hydraulic heads. This was used in simulating the piezometric head in 1967 (Figure 3.10). This run lasted 1 day.

Statistical analyses were performed by visual MODFLOW after manual trial-and-error adjustment of the selected input parameters, which was based on the best knowledge of the hydrogeology of the area. It involves regression analysis and the calibration of Root Mean Squared Error (RMS) and Mean Absolute Error (MAE). The results of comparison between the calculated and observed head at steady-state (Figure 3.11) gave residual mean of 0.043 m, absolute residual mean of 0.055 m, root mean square of 0.066 m and 95% confidence interval. Maximum residual was noticed in OBS No. 5 and minimum residual was recorded by OBS No. 8. These figures confirmed that there is a very small discrepancy between the calculated and the observed heads.

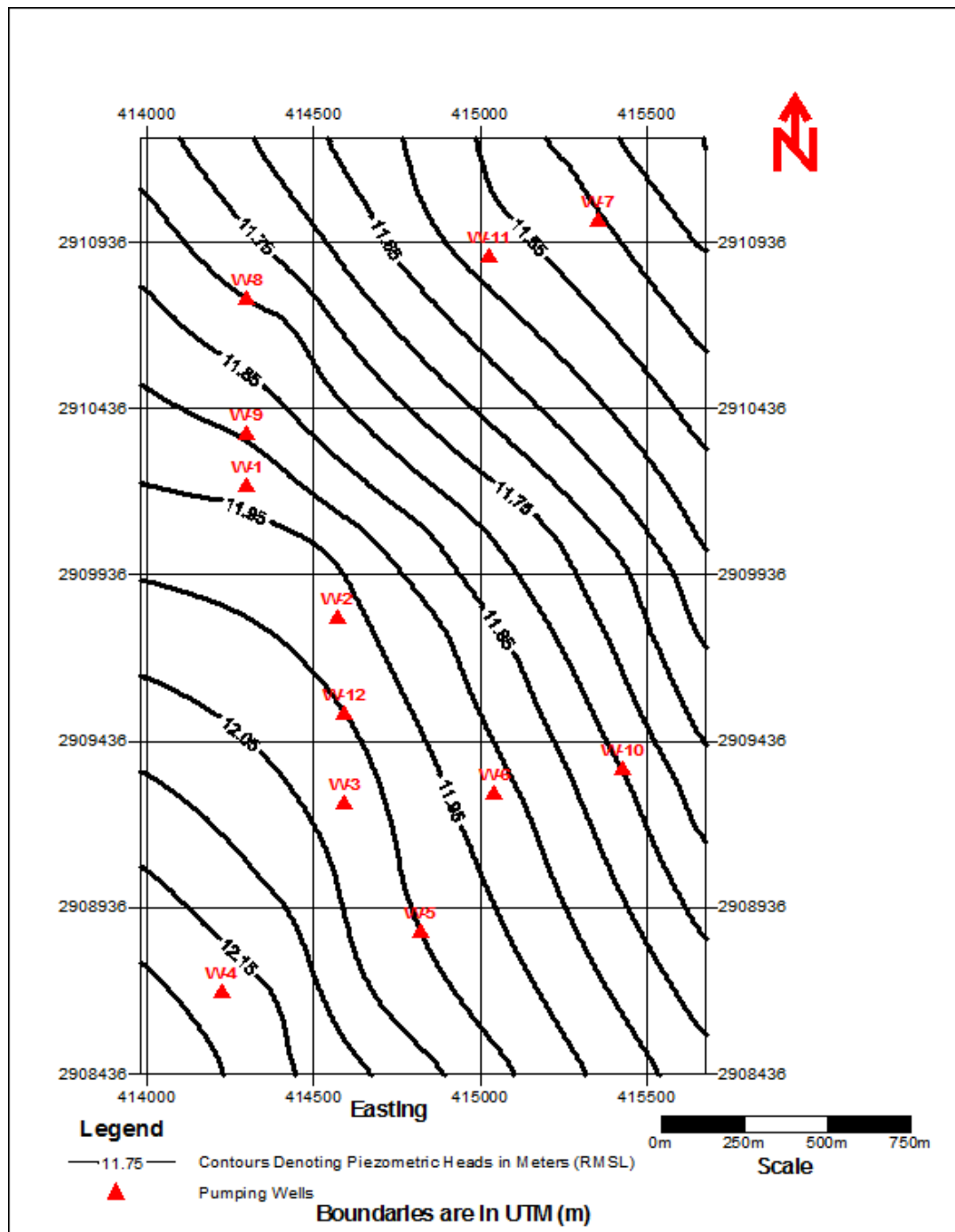


Figure 3.10: Simulated head in UER of the study area (1967 steady-state)

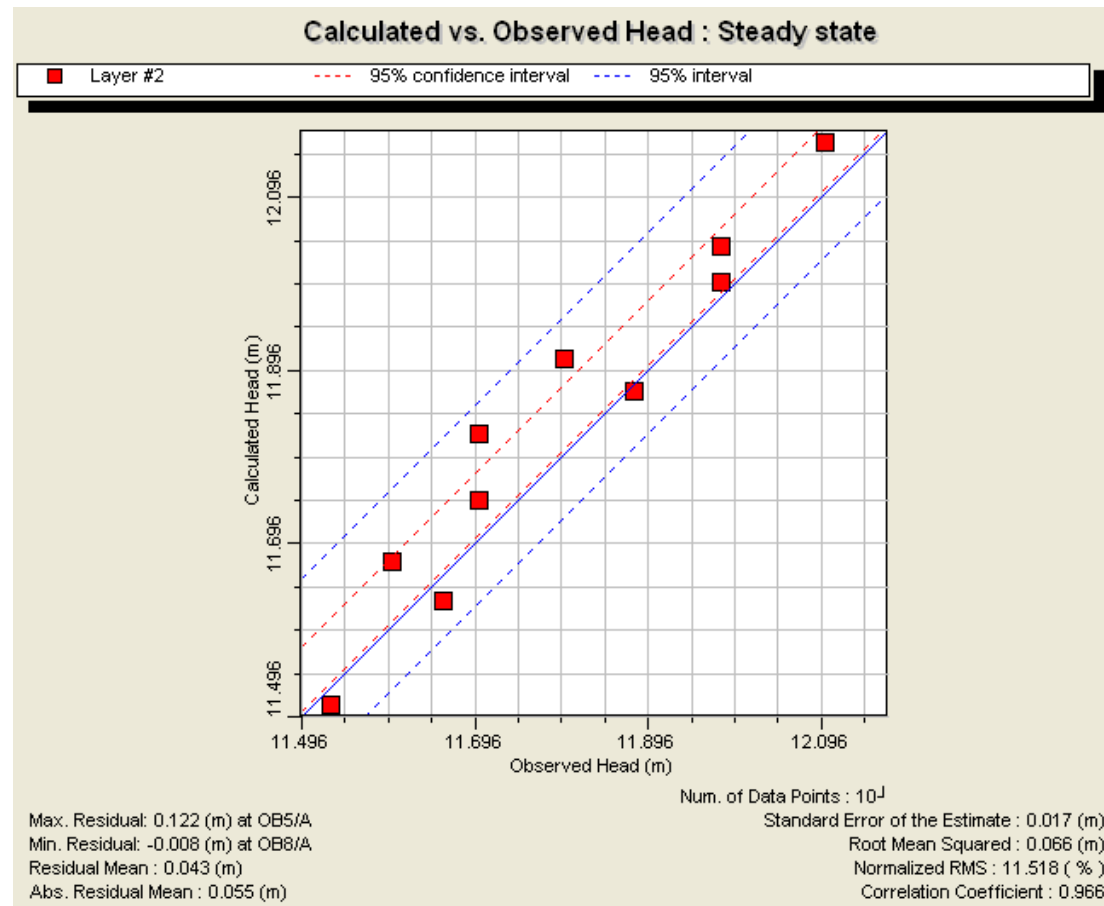


Figure 3.11: Calculated versus observed heads in UER of the study area (1967 Steady-state calibration)

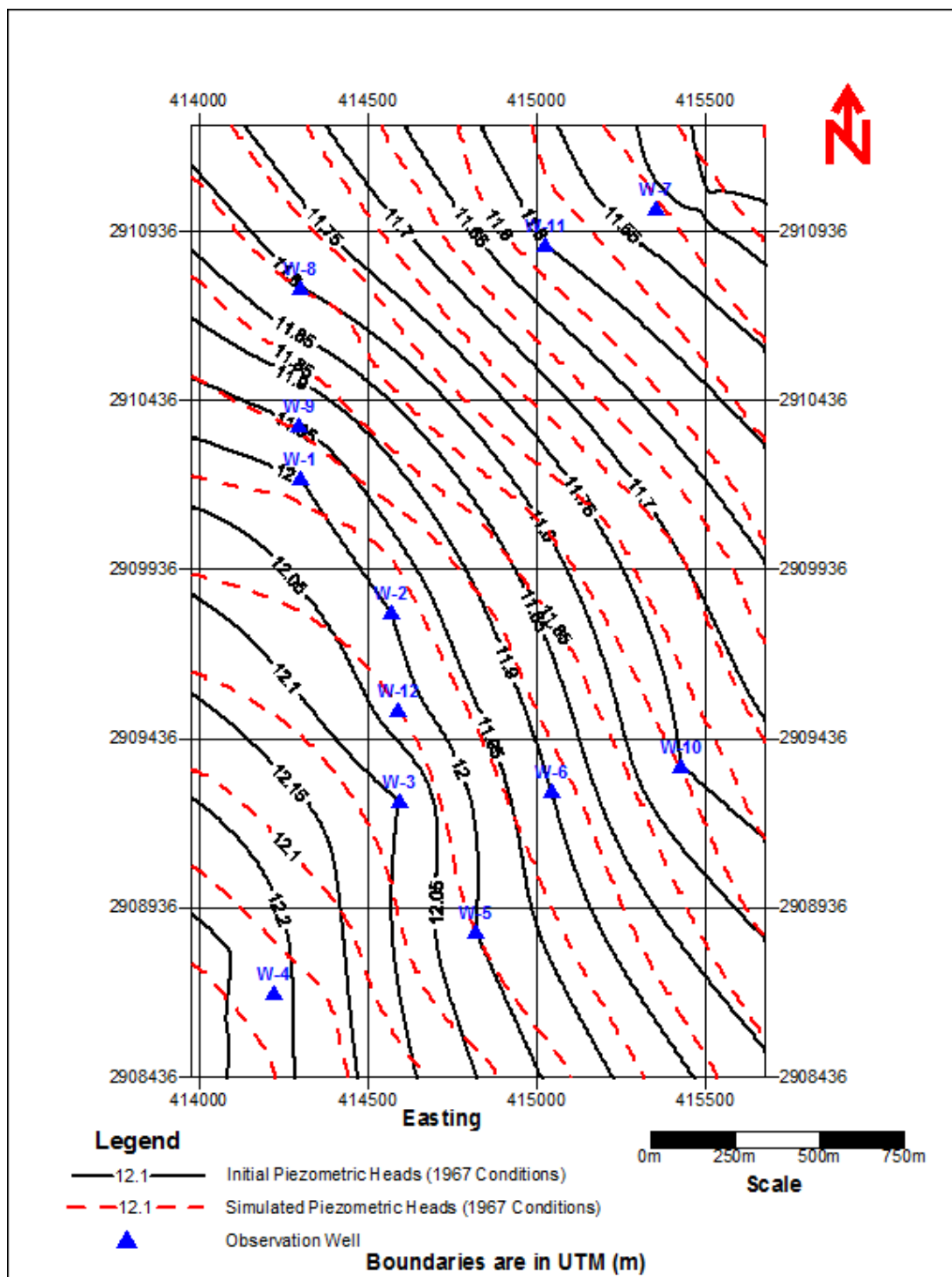


Figure 3.12: Comparison between observed and calculated heads in UER of the study area

Further confirmation of the steady-state calibration was achieved by comparing the 1967 initial piezometric head (Figure 3.4) with the 1967 simulated piezometric head (Figure 3.10)

Both contour maps were superimposed and the resultant contour map is shown in Figure 3.12. Figure 3.12 shows a near perfect match between the observed and the calculated heads. This further confirms the validity of the steady-state calibration.

3.4.1.1 GROUNDWATER FLOW DIRECTION

The orientation of the contour maps of both the observed and the calculated heads in UER of the study area and Figure 3.5 clearly indicate that the groundwater flow direction in the study area is from the southwest to the northeast. Two-dimensional views of Column No. 20 (Figure 3.13) and Row No. 10 (Figure 3.14) of the model also serve as substantiations to the groundwater flow direction in the study area, i.e., from the southwest to the northeast. This flow direction is valid as previous studies by Italconsult (1969), GDC (1977) and GTZ (2006) of UER aquifer in the Eastern Province have also indicated flow in west - east direction towards the Arabian Gulf.

3.4.1.2 STEADY-STATE WATER BUDGET

A steady-state water balance of the aquifer showed that about 16,149 m³/day of water enters the UER in the study area from the southwestern boundary. The water that leaves the study area via the northeastern boundary was about 10,072 m³/day. The total well discharge was about 6,541 m³/day during the steady-state. Vertical leakage into the aquifer and vertical leakage out of the aquifer were calculated as zero by MODFLOW.

Table 3.1 provides a clearer summary of the steady-state water budget.

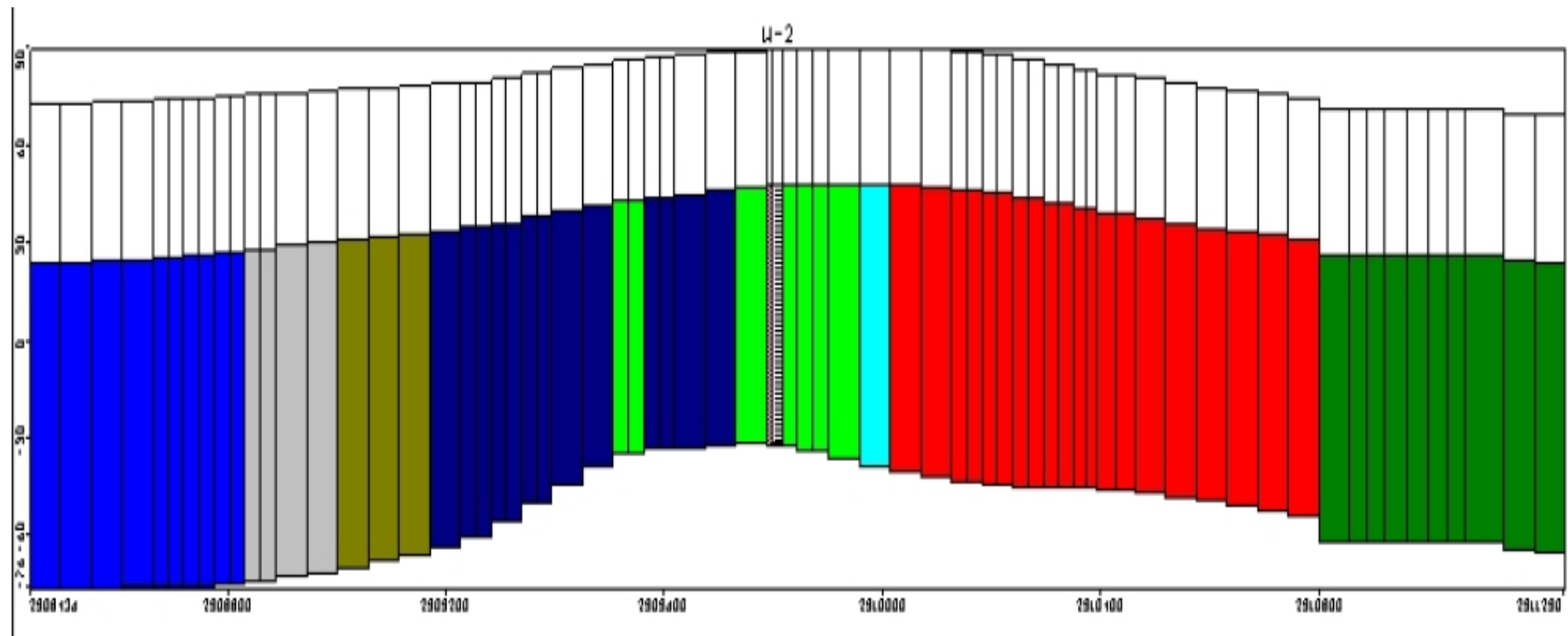


Figure 3.13: 2-D view of Column No. 20 of the model

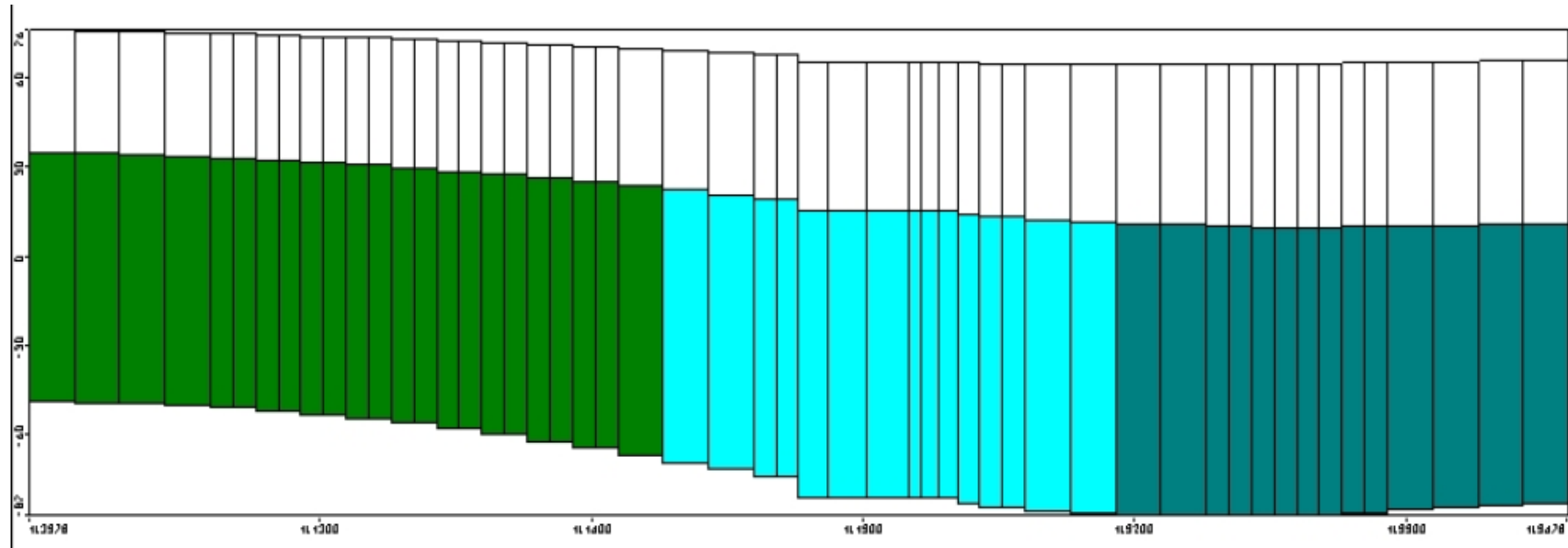


Figure 3.14: 2-D view of Row No. 10 of the model

Table 3.1: Volumetric budget during steady state

	Flow Rate in m ³ /day
Constant Head Boundary Flows; inflow (Southwest)	16149
Constant Head Boundary Flows; outflow (Northeast)	-9609
Discharge from Wells	-6541
Vertical Leakage into the Aquifer	0
Vertical Leakage out of the Aquifer	0
Balance	-1
Percentage Error	0

3.4.2 TRANSIENT-STATE CALIBRATION

Based on the established patterns of the aquifer parameters obtained during steady-state calibration, the model was subjected to transient calibration for a period of 45 years, i.e., between the years 1967 and 2010 (inclusive of both years).

Well abstraction data were obtained mainly from KFUPM Maintenance Department (Appendix A). Since most workers at the KFUPM Maintenance Departments are technicians with no hydrogeologic background, expert information about the history of the wells was sought from KFUPM Research Institute.

Stress period duration was for one year, i.e., 365 days. Therefore, the total simulation period for transient calibration was 16,060 days. The simulation period was divided into 45 stress periods. During each stress period, all boundary conditions were kept constant, while external stresses, mainly groundwater abstraction, were varied according to the history of the pumping wells at KFUPM.

Starting conditions were those obtained from the final run of the steady-state calibration. Boundary conditions specified for the steady-state were changed from constant head to variable head to consider changes in stress with time. At this stage of calibration, values of hydraulic conductivity and specific storage of the aquifer were maintained as they were in the steady-state calibration. Assessment of reliability of the computed parameter distribution was obtained through relevant water balance checks, in terms of changes and final values.

The final run of the transient calibration resulted in the prediction of potentiometric surface in the study area at the end of the year 2010 (Figure 3.15). An average drawdown of 8.5 m was recorded between 1967 and year 2010. Higher drawdowns

were recorded and cones of depressions formed in the areas where the wells are located than the other areas. Volumetric budget at the end of the transient stage simulation is presented in Table 3.2.

3.4.3 VERIFICATION OF THE MODEL

The eleven available observation wells in the study area were used for comparison and verification of simulated water levels. Corresponding model cell locations were obtained by superimposing the finite difference grid over the location map of the observation wells. Simulated heads obtained at the observation wells are almost in accordance with the observed potentiometric heads, for which a detailed discussion will be made in the following section.

3.4.3.1 HISTORICAL WATER LEVELS AND MODEL RESULTS

Hydrographs showing comparisons between simulated and observed heads are shown in Figure 3.16A through Figure 3.16K. All the wells were observation wells located within the model domain. The observation data used were limited for 1 to 4 stress periods. There was a good match in terms of trends and values. There was a near perfect match between the simulated and the observed heads in Well No. 2 (Cell No. 35-18), Well No. 3 (Cell No. 50-19), Well No. 4 (Cell No. 63-8), Well No. 5 (Cell No. 60-27), Well No. 9 (Cell No. 19-12) and Well No. 10 (Cell No. 49-44). Other observation wells maintained a very good match between the simulated and the observed heads. Maximum divergence of the simulated and observed head occurred at Well No. 12 (Cell No. 42-16), but it is still a good match.

Table 3.2: Volumetric budget at the end of the transient state

	Flow Rate in m ³ /day
Storage	464
Variable Head Boundary Flows; inflow (Southwest)	39171
Variable Head Boundary Flows; outflow (Northeast)	-1496
Discharge from Wells	-38143
Vertical Leakage into the Aquifer	0
Vertical Leakage out of the Aquifer	0
Balance	-4
Percentage Error	0

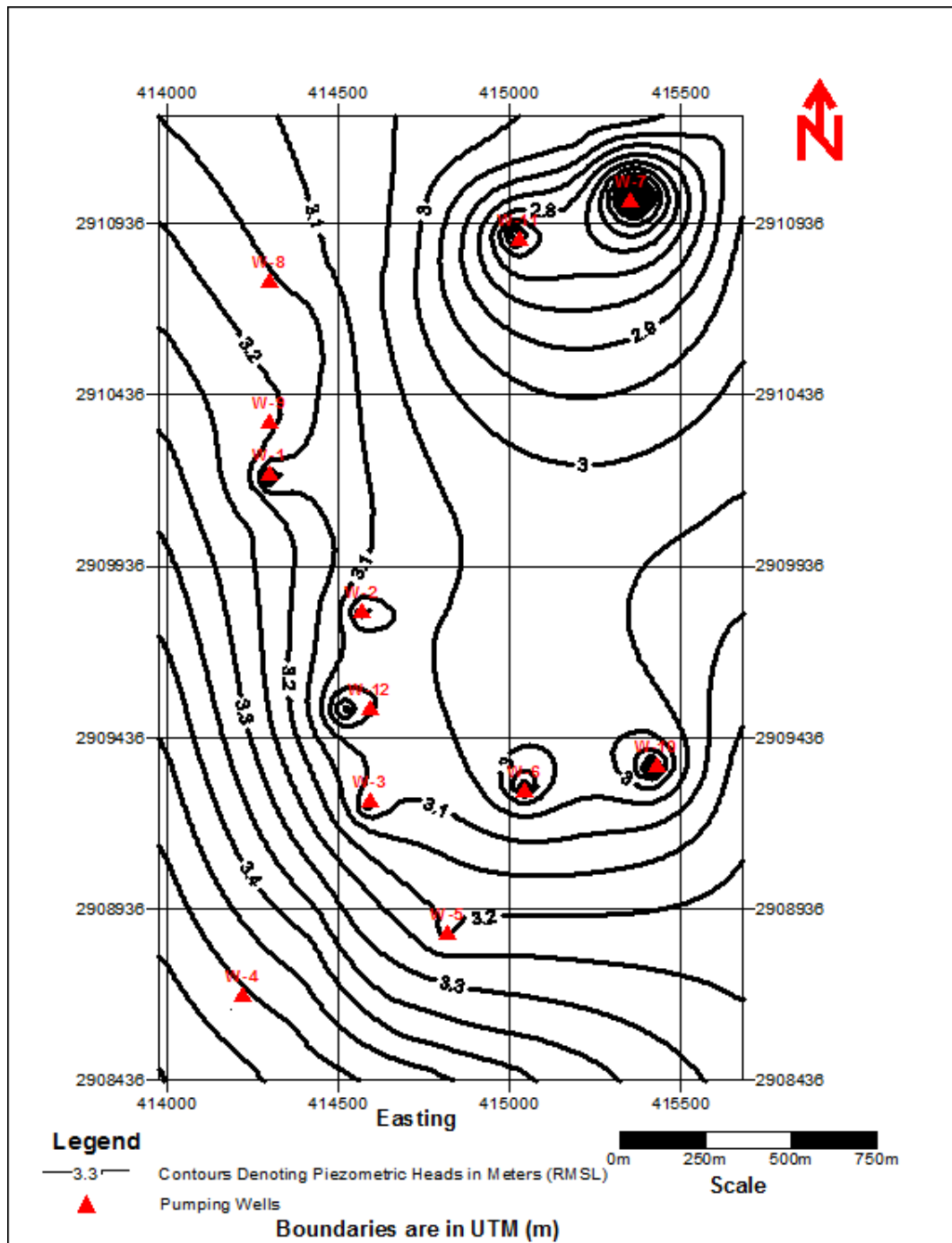


Figure 3.15: Potentiometric surface contour map at the end of year 2010 (transient state simulation)

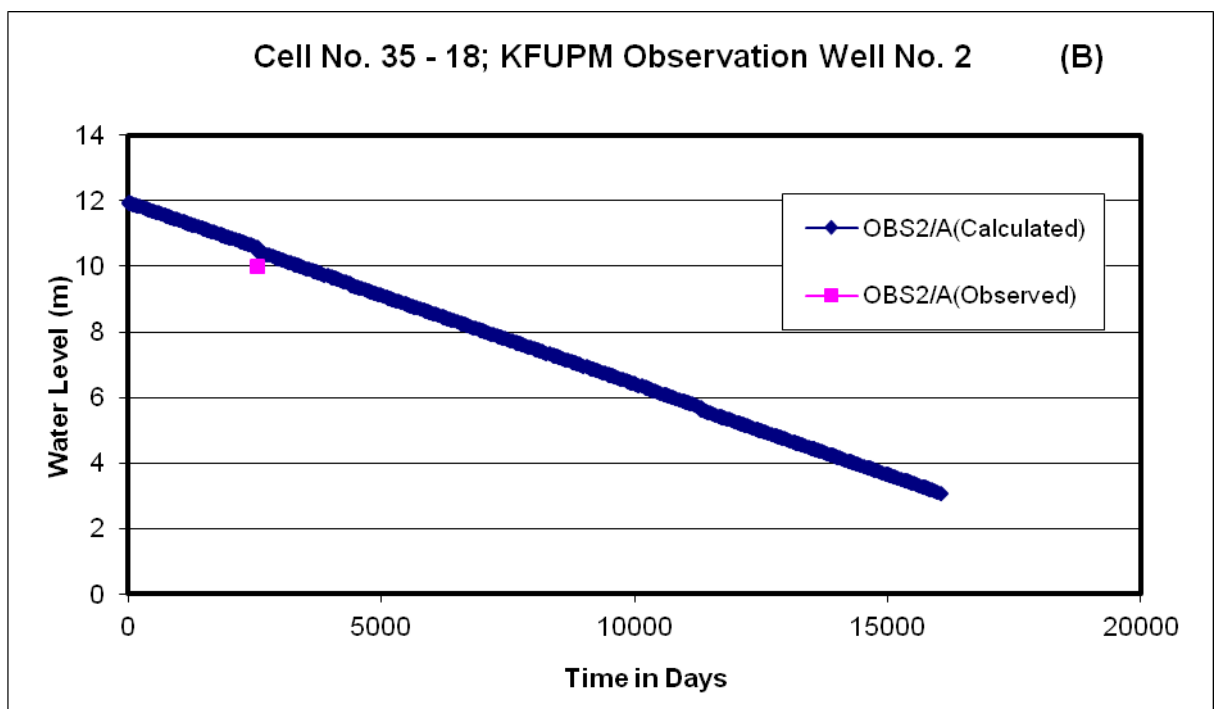
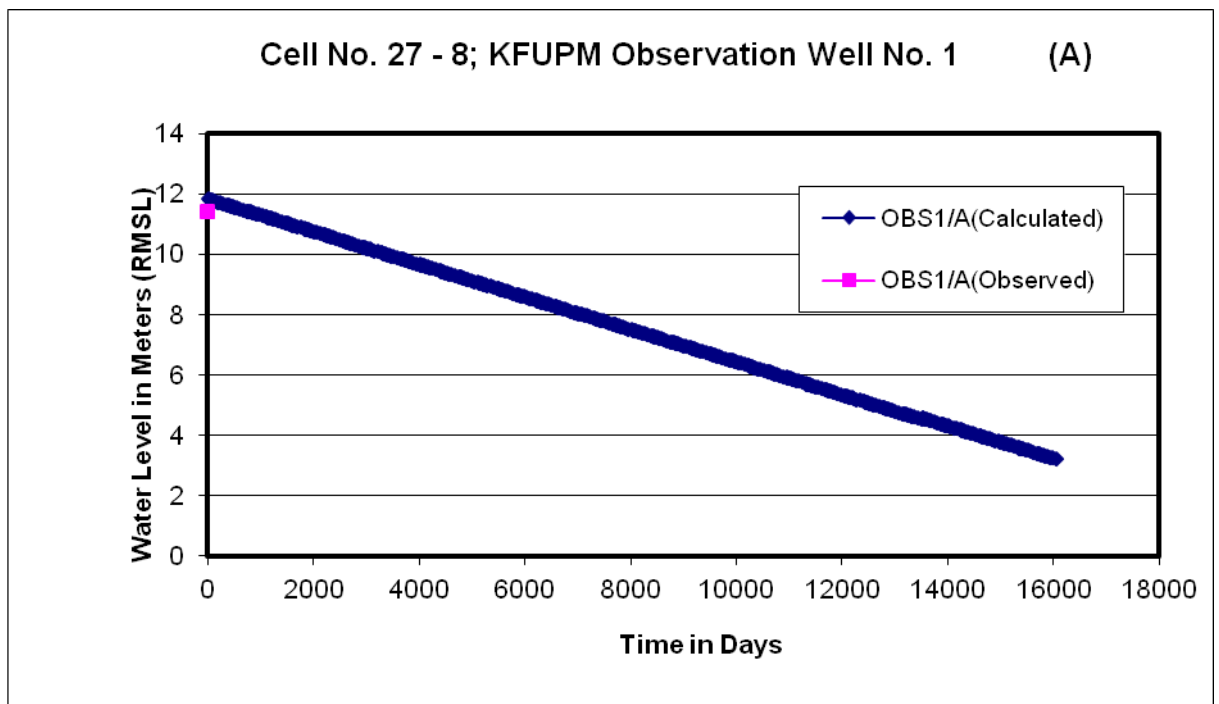


Figure 3.16 (A & B): Hydrographs showing comparison between simulated and observed heads

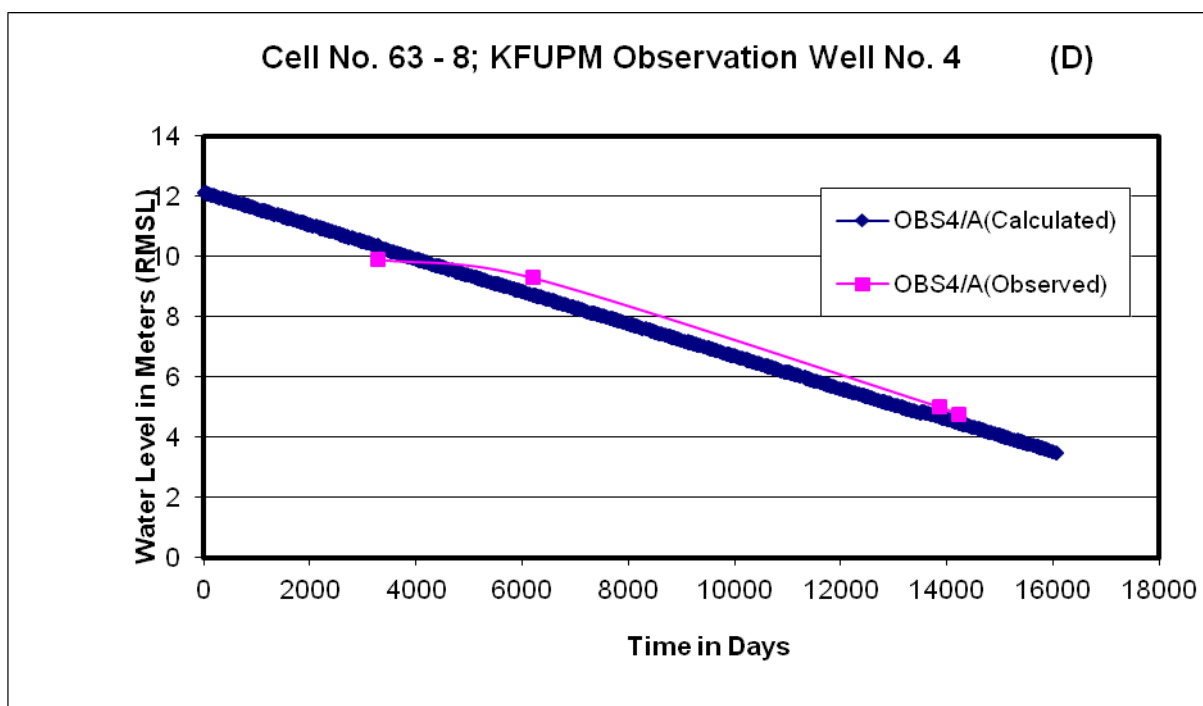
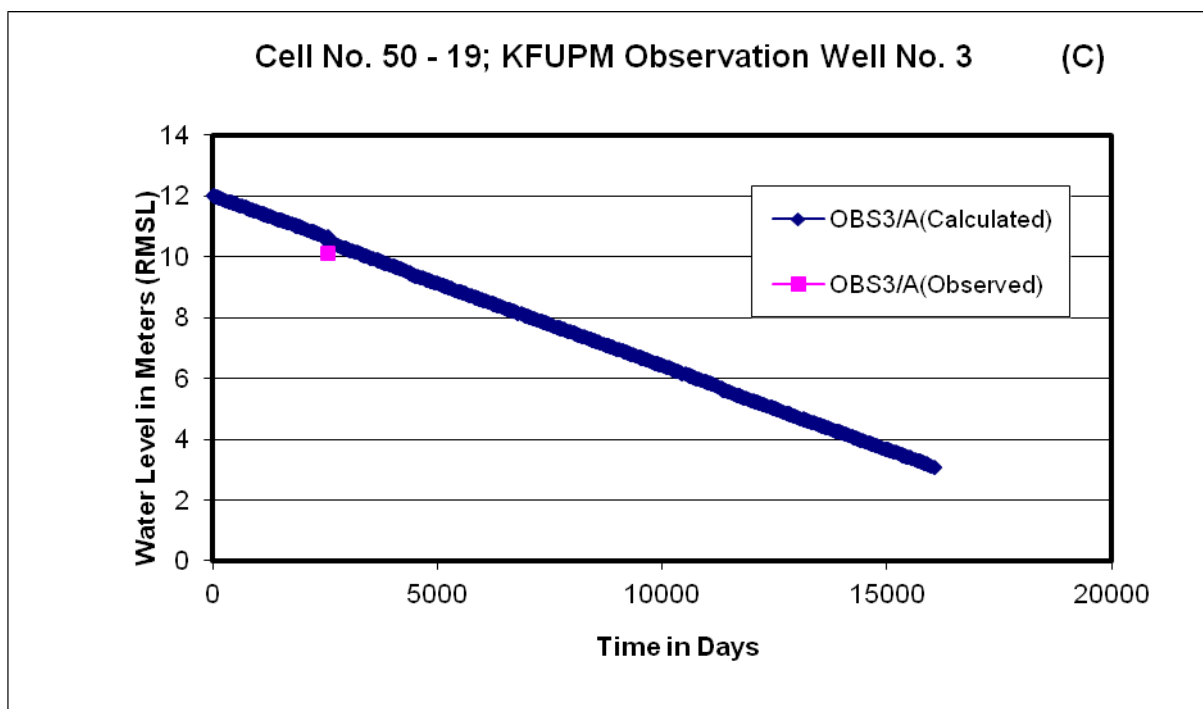


Figure 3.16 (C & D): Hydrographs showing comparison between simulated and observed heads

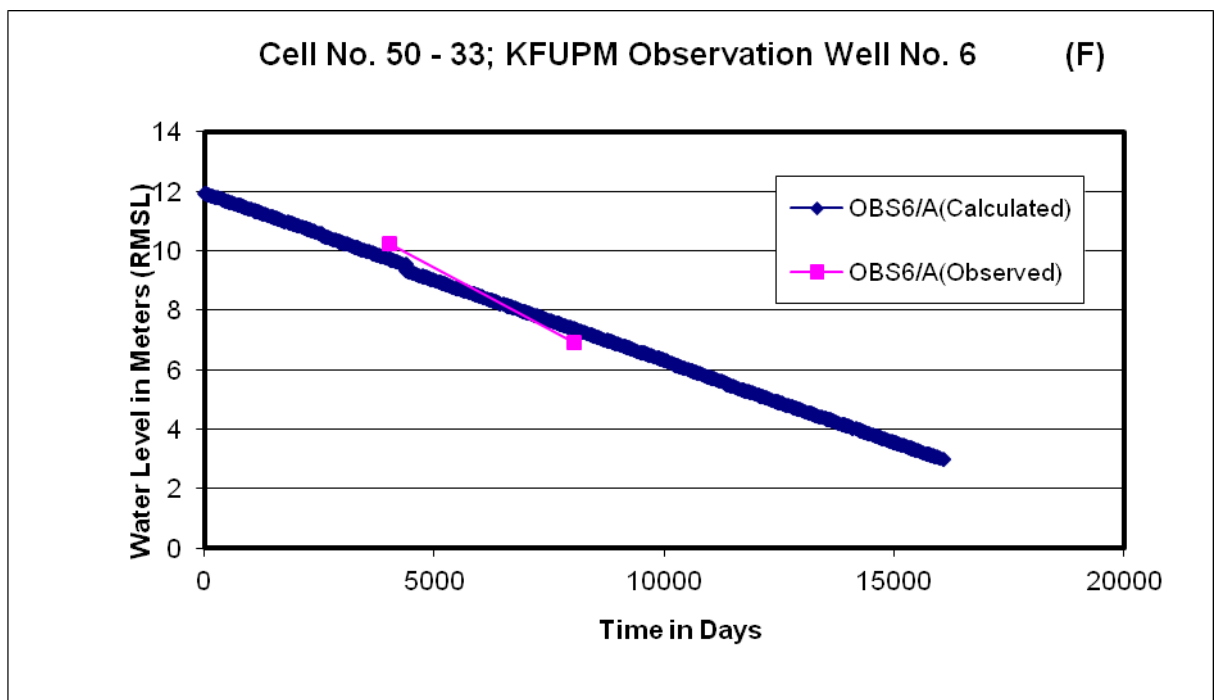
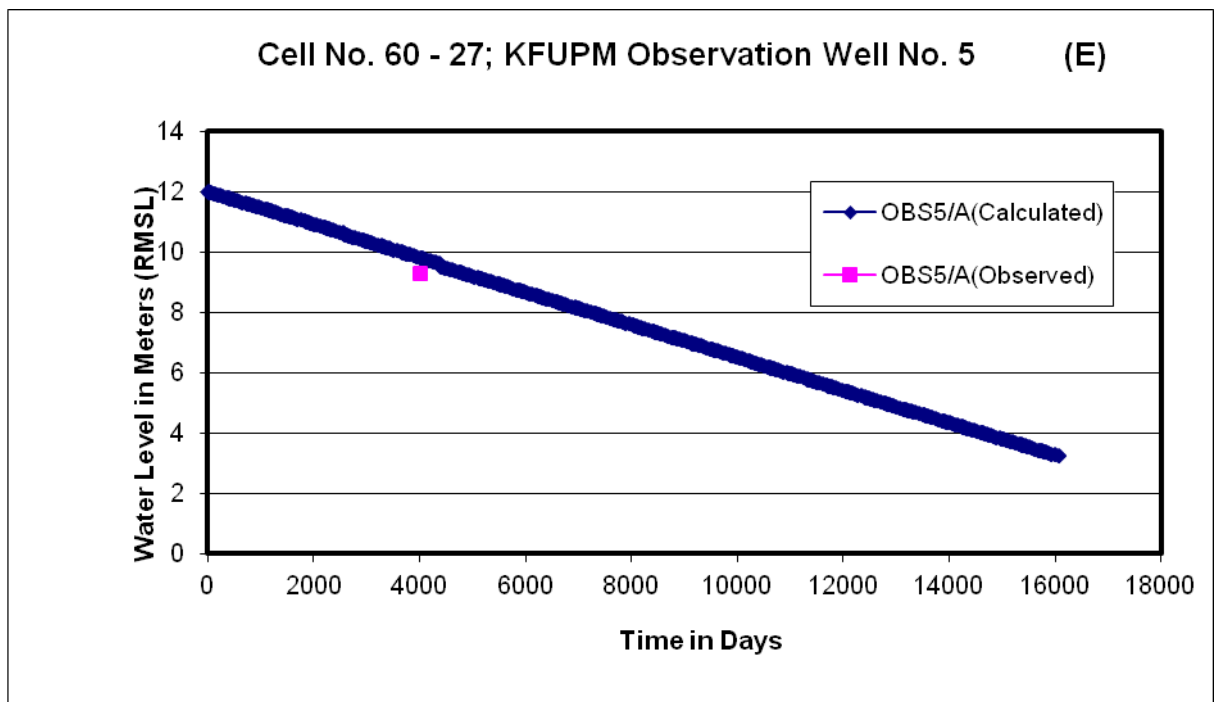


Figure 3.16 (E & F): Hydrographs showing comparison between simulated and observed heads

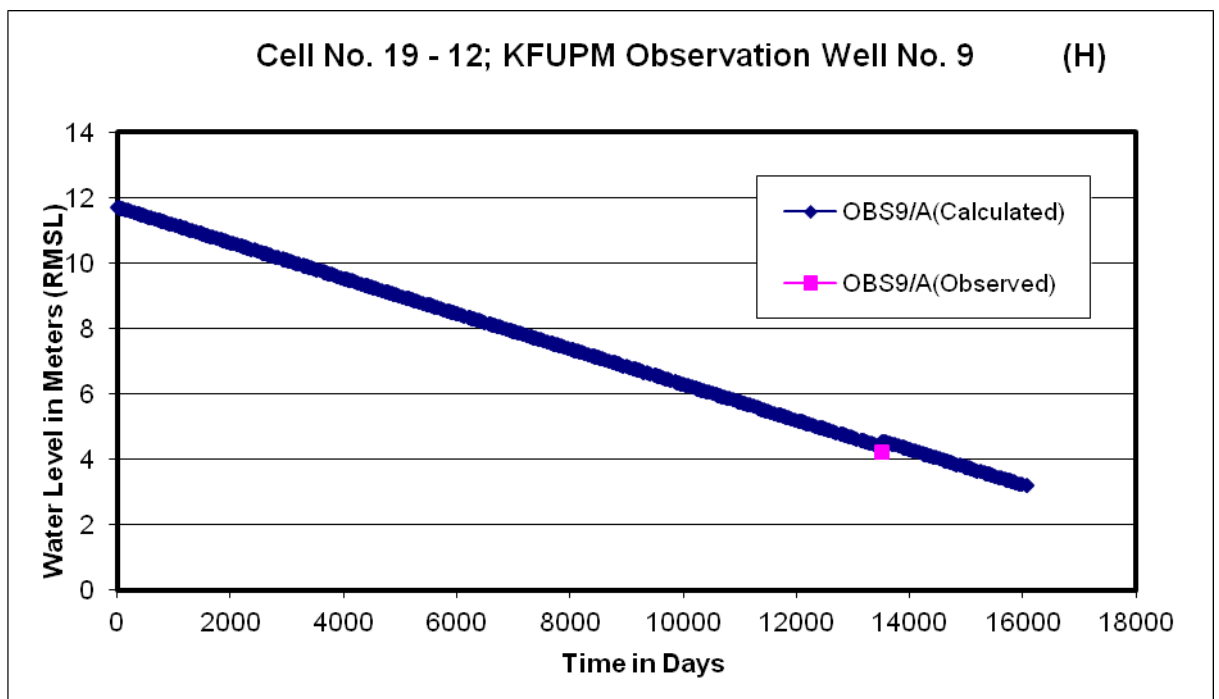
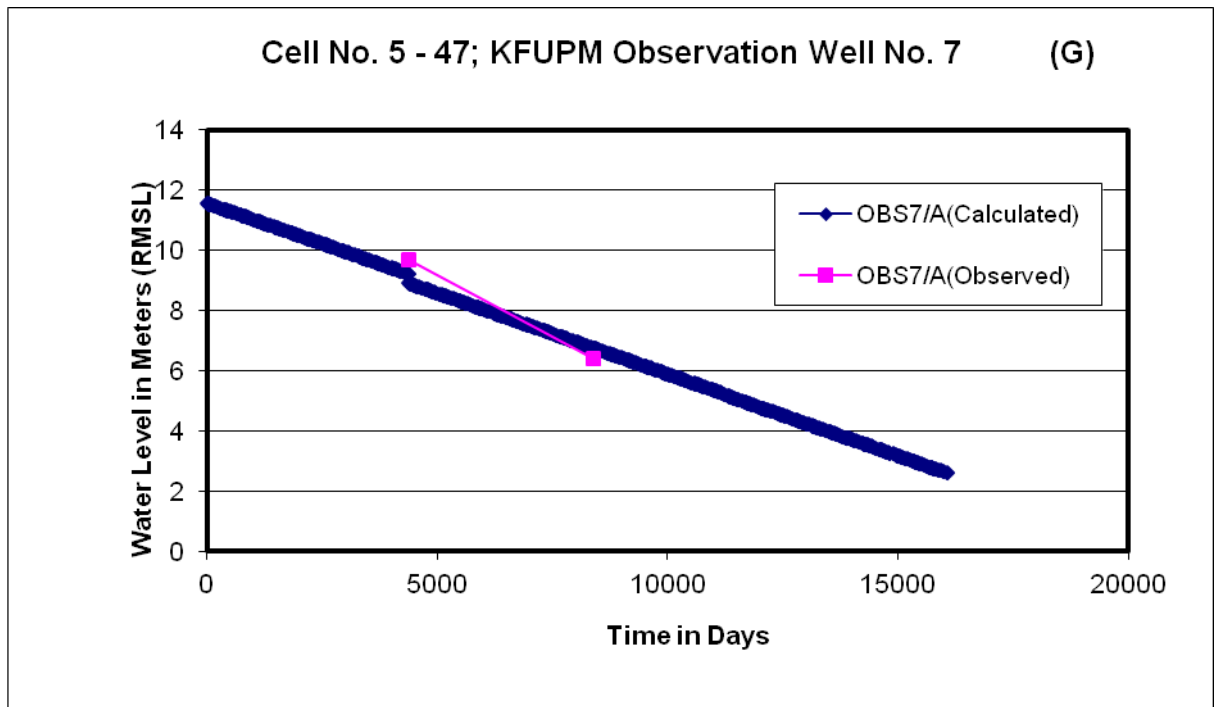


Figure 3.16 (G & H):Hydrographs showing comparison between simulated and observed heads

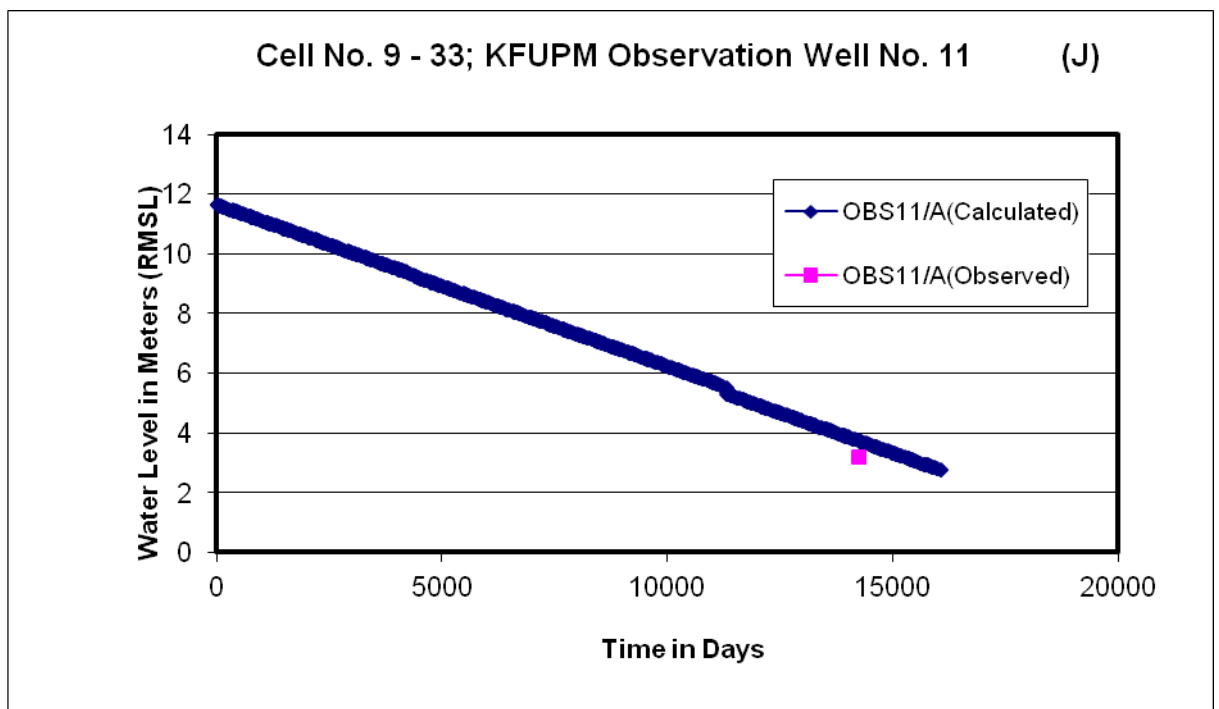
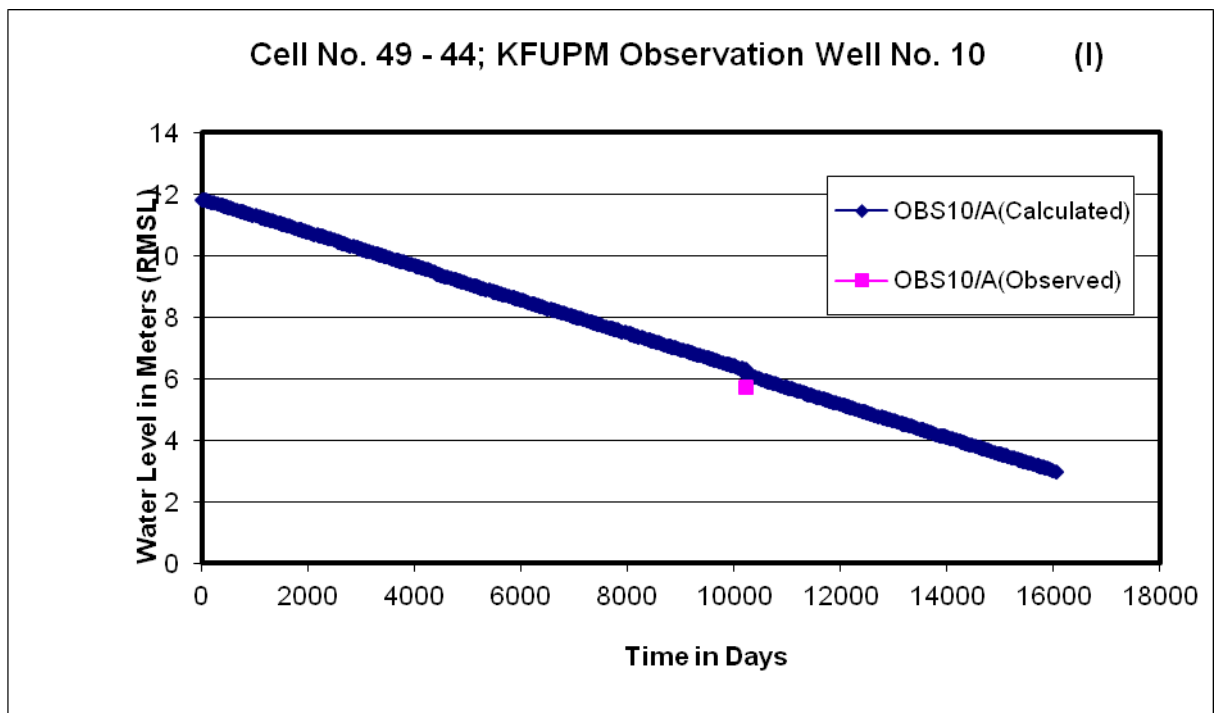


Figure 3.16 (I & J): Hydrographs showing comparison between simulated and observed heads

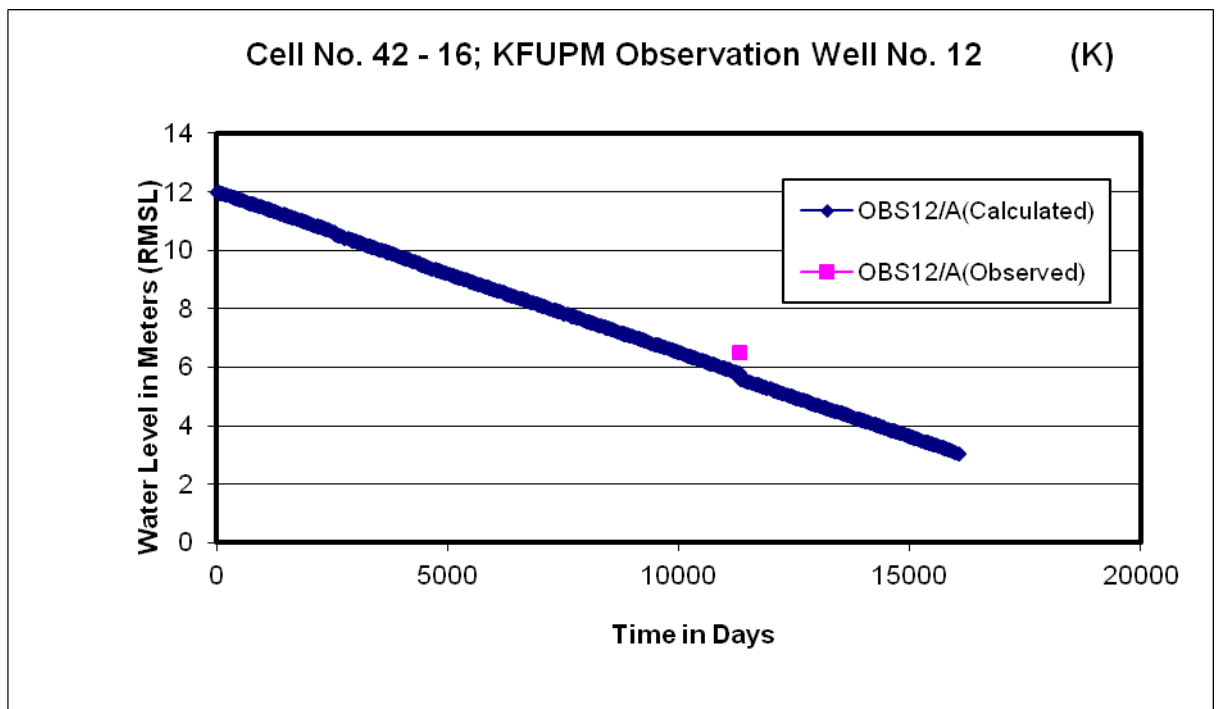


Figure 3.16 K: Hydrographs showing comparison between simulated and observed heads

Based on these results, it can be concluded that the model is capable of representing the flow system and is ready to be utilized as a predictive tool for future aquifer management.

CHAPTER 4

ALTERNATIVE DEVELOPMENT SCHEMES

4.1 INTRODUCTION

A successfully calibrated and verified simulation model can be used for formulating various alternative water development schemes (Abderrahman and Rasheeduddin, 1994; Abderrahman et al. 2007; KFUPM, 2009). The schemes can be compared in terms of their feasibility for efficient utilization of the available groundwater resources. The selected development schemes when implemented must meet the future water demand at a minimum cost, and be commensurate with legal, organizational, political and environmental considerations (Flack, 1981).

A planning horizon of 20 years (2010 - 2030) was selected for the three alternative scenarios. The duration of the planning period is less than the length of the period for which the model was calibrated and validated (i.e., 45 years). Starting conditions in each case were those obtained during transient simulation at the end of 2010. Figure 3.15 shown in the previous chapter illustrates the potentiometric surface of the UER in the study area at the end of 2010.

In order to obtain estimation of abstraction rates for the planning period (2011-2030), a review of similar past studies was made. Abderrahman et al. (2007) formulated three alternative pumping scenarios based on reduction in and addition of certain

percentages of pumping. The same method of formulation of alternative pumping scenarios as Abderrahman et al. (2007) was used by Abu-El-Sha'r & Hatamleh (2007) to estimate future abstraction rates. In both studies, no mention was made of considerations leading to the formulation of the alternative pumping schemes, and so, such approach is considered anecdotal in that it lacks rigorous scientific analysis. However, in this study, real data on KFUPM population was used and trend of population growth of the people living on campus at KFUPM as well as KFUPM future developmental plans and water need was taken into consideration in the formulation of the alternative pumping schemes.

Population data of people living at KFUPM campus were obtained from KFUPM Faculty Housing Department and Student Housing Unit (Appendix B). The population data were provided from year 2003 to year 2010. Statistical analysis of the total population revealed an 8.3% growth rate. This result was used in forecasting what the KFUPM on-campus population would be between the year 2011 and 2030. The results are shown in Table 4.1 and Figure 4.1.

Population for each year from 2011 and 2030 (inclusive of both years) was used in the alternative development schemes to calculate per capita water use for all individuals living on campus. This information was used to estimate the water consumption of all the population living on campus for the three alternative development schemes.

Information on water use for irrigation at KFUPM was collected from the Agricultural Unit of the Faculty Housing Department. Together with water use for other purposes, water use for irrigation was estimated at 32,192 m³/day. When this is added to daily water consumption of all the people living on campus, it would give the total water consumption at KFUPM per day.

Table 4.1: KFUPM on-campus population trend estimate between 2011 and 2030

POPULATION TREND				
Year	Population of Faculty (including families) on Campus	Population of Students on Campus	Total Population on Campus	Population Trend
2003	4051	4297	8348	8352
2004	4136	4379	8515	8426
2005	4248	4506	8754	8588
2006	4113	4627	8740	8765
2007	4119	4821	8940	9075
2008	4082	4951	9033	9253
2009	4211	4971	9182	9283
2010	4535	5175	9710	9577
2011	4587	5284	9871	9680
2012				9858
2013				10035
2014				10212
2015				10389
2016				10566
2017				10743
2018				10920
2019				11097
2020				11275
2021				11452
2022				11629
2023				11806
2024				11983
2025				12160
2026				12337
2027				12514
2028				12692
2029				12869
2030				13046

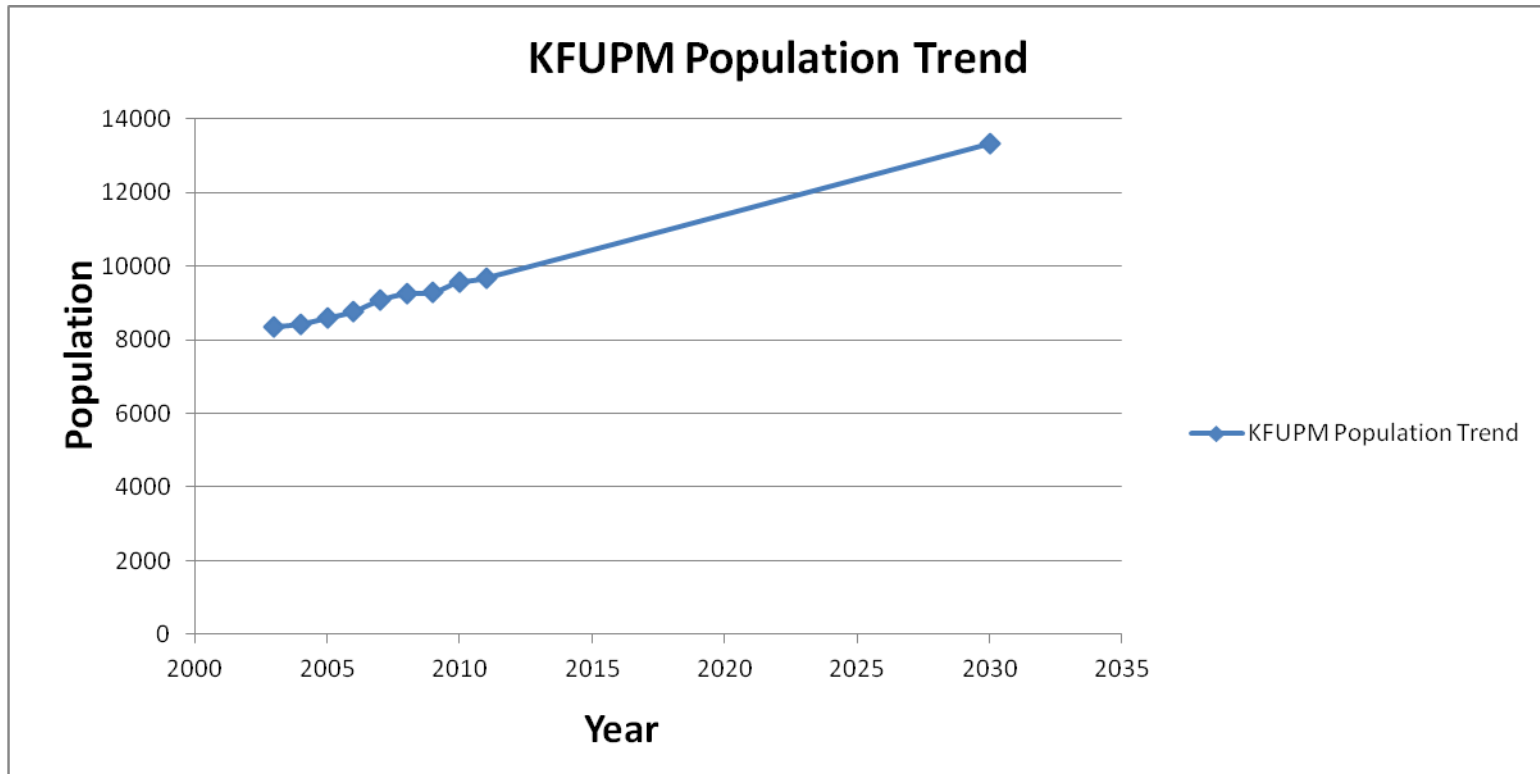


Figure 4.1: Estimated trend of KFUPM population between 2011 and 2030

Emphatically, careful measures were taken in the estimation of total water consumption at KFUPM. Desalinated water that is delivered to KFUPM on a daily basis was considered, and was totally excluded in all calculations.

An estimate of water consumption per day for a grown up individual is provided in Table 4.2. This information was aggregated from various sources including United States Environmental Protection Agency (USEPA) and World Health Organisation (WHO).

From Table 4.2, water consumption per day for an individual range between 226.75 and 348.51 liters which gives an average of 287.63 liters per day. Drinking water was not included in this estimate because the common misconception that everyone should drink 2 liters of water per day is not supported by scientific research. Various reviews of different scientific literature on the topic could not find any solid scientific evidence that recommended drinking eight glasses of water per day. Drinking water was therefore excluded in the calculation.

Based on the aforementioned, water consumption per day of 300 liters was considered as normal for an individual in this work. This value was taken as the basis in the estimation of water consumption for an individual in the three alternative development schemes.

4.2 ALTERNATIVE SCHEME I

In this alternative, a double of the normal water consumption per day for an individual was assumed as the water consumption per capita per day; that is, 600 liters (0.6 m³). This value was multiplied with the total population to obtain the total water use for domestic purpose per day for each year according to the population trend.

Table 4.2: Estimated water use per day for an individual

Activity	Water Use (liters)
Shower	57 – 134
Brushing teeth (water running)	3.75 – 7.51
Shaving (water running)	38 – 57
Washing dishes by hand	75
Washing dishes in dishwasher	34 – 45
Flushing toilet	19 – 30

For water use for irrigation and other purposes, the base value of 32,192 liters was assumed to be increasing at 0.005% for every year. This equals to 10% increase over 20 years. Irrigation water use per day was added to water use for domestic purposes per day to obtain the total water consumption at KFUPM per day for the 20-year period (i.e., from 2011 to 2030). The resulting value was taken to be the total pumping rate for all the 9 wells (as existing in 2010) at KFUPM (Table 4.3). The total pumping rate for all the wells was divided among the 9 wells to obtain the pumping rate for each well based on the pumping capacity of the wells.

In order to accommodate the excess volume of water outside the capacity of the existing wells, an additional pumping well was introduced in the model for the Alternative Scheme I. This well was located in Cell No. 9 – 11.

Figure 4.2 shows the potentiometric surface contour map at the end of year 2030. The potentiometric surface contour map shows that water level in the study area has dropped from the average of 3.2 m (RMSL) obtained at the end of the year 2010 to an average of -2.2 m (RMSL) in year 2030 for Alternative Scheme I. This result is equal to an average drawdown of 5.4 m in the study area over the 20-year planning period. Cones of depression were developed in the areas where the pumping wells were located. Maximum drawdowns were noticed in areas surrounding the wells. There was prevalence of cone of depression in the northwest of the study area. This is due to the proximity of Well No. 7 to Well No. 11.

Table 4.3: Total water consumption for Alternative Scheme I

WATER CONSUMPTION TREND FOR ALTERNATIVE I				
Year	Population Trend	Water for Domestic Use (m ³ /day)	Water for Irrigation and other Purposes (m ³ /day)	Total Water Consumption (m ³ /day)
2011	9680	5808.024	32192	38000
2012	9857	5914.53	32353	38267
2013	10034	6020.745	32515	38535
2014	10211	6126.96	32677	38804
2015	10388	6233.175	32841	39074
2016	10566	6339.681	33005	39345
2017	10743	6445.896	33170	39616
2018	10920	6552.111	33336	39888
2019	11097	6658.326	33502	40161
2020	11274	6764.832	33670	40435
2021	11451	6871.047	33838	40709
2022	11629	6977.262	34007	40985
2023	11806	7083.477	34178	41261
2024	11983	7189.983	34348	41538
2025	12160	7296.198	34520	41816
2026	12337	7402.413	34693	42095
2027	12514	7508.628	34866	42375
2028	12691	7615.134	35041	42656
2029	12869	7721.349	35216	42937
2030	13046	7827.564	35392	43219

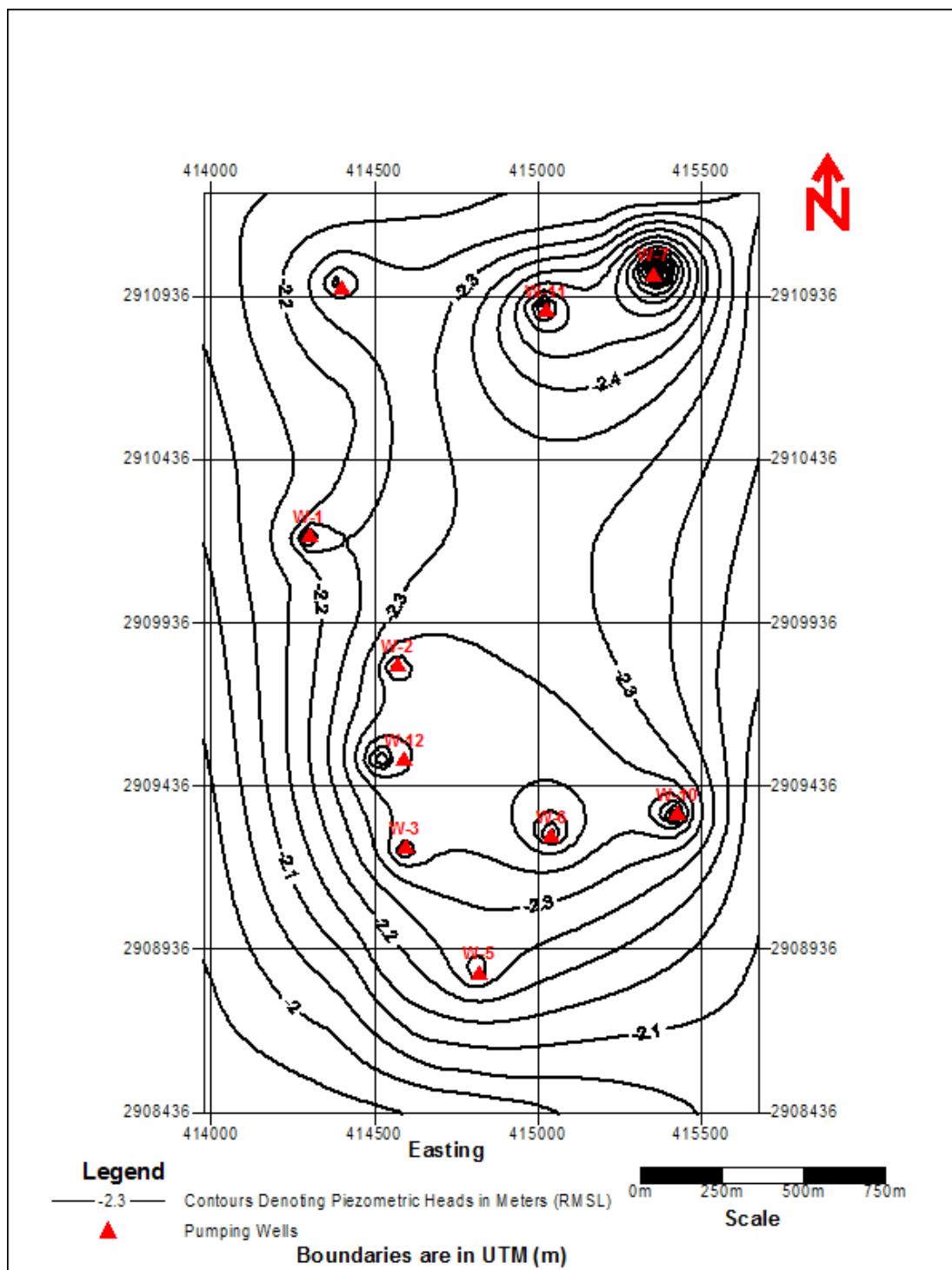


Figure 4.2: Potentiometric surface contour map at the end of 2030 (Alternative I)

4.3 ALTERNATIVE SCHEME II

In this alternative, conservatory measures were adopted. Water consumption per capita per day was kept at the normal rate of 300 liters (0.3 m^3). This was multiplied with the population trend to obtain the domestic water use for each year. Water use for irrigation and other purposes were assumed to be decreasing at the rate of 0.1% per year, which is equivalent to 20% decrease over the 20-year planning period (2011-2030). This theorem was used in evaluating the total water consumption per day, which is the sum of domestic water use and irrigation water use. This is presented in detail in Table 4.4.

Table 9 shows that the total water consumption in KFUPM between the year 2011 and year 2030 decreases from 35096 to 33181 m^3/day for the Alternative Scheme II. These values were assumed to be the total pumping rate for all the wells in KFUPM and were divided among the wells based on the capacity of each well. Since there was no excess volume of water, no new well was added in this alternative scheme.

Figure 27 shows the potentiometric surface contour map at the end of the year 2030. The potentiometric surface contour map shows that water level in the study area has dropped from the average of 3.2 m (RMSL) obtained at the end of the year 2010 to an average of 0.2 m (RMSL) in year 2030 for Alternative Scheme II. This result is the same as an average drawdown of 3 m in the study area over the 20-year planning period. Cones of depression were developed in the areas where the observation wells were located. Maximum cone of depression and drawdowns were noticed in wells at the northwest of the study area. Cones of depression also occurred prevalently around Well No. 7 and Well No. 11. This can be attributed to the proximity of their positioning.

Table 4.4: Total water consumption for Alternative Scheme II

WATER CONSUMPTION TREND FOR ALTERNATIVE II				
Year	Population Trend	Water for Domestic Use (m ³ /day)	Water for Irrigation and other Purposes (m ³ /day)	Total Water Consumption (m ³ /day)
2011	9680	2904.17	32192	35096
2012	9857	2957.27	32031	34988
2013	10034	3010.37	31871	34881
2014	10211	3063.48	31712	34775
2015	10388	3116.59	31553	34670
2016	10566	3169.84	31395	34565
2017	10743	3222.95	31238	34461
2018	10920	3276.06	31082	34358
2019	11097	3329.16	30927	34256
2020	11274	3382.42	30772	34154
2021	11451	3435.52	30618	34054
2022	11629	3488.63	30465	33954
2023	11806	3541.74	30313	33854
2024	11983	3594.99	30161	33756
2025	12160	3648.1	30010	33658
2026	12337	3701.21	29860	33561
2027	12514	3754.31	29711	33465
2028	12691	3807.57	29562	33370
2029	12869	3860.67	29415	33275
2030	13046	3913.78	29268	33181

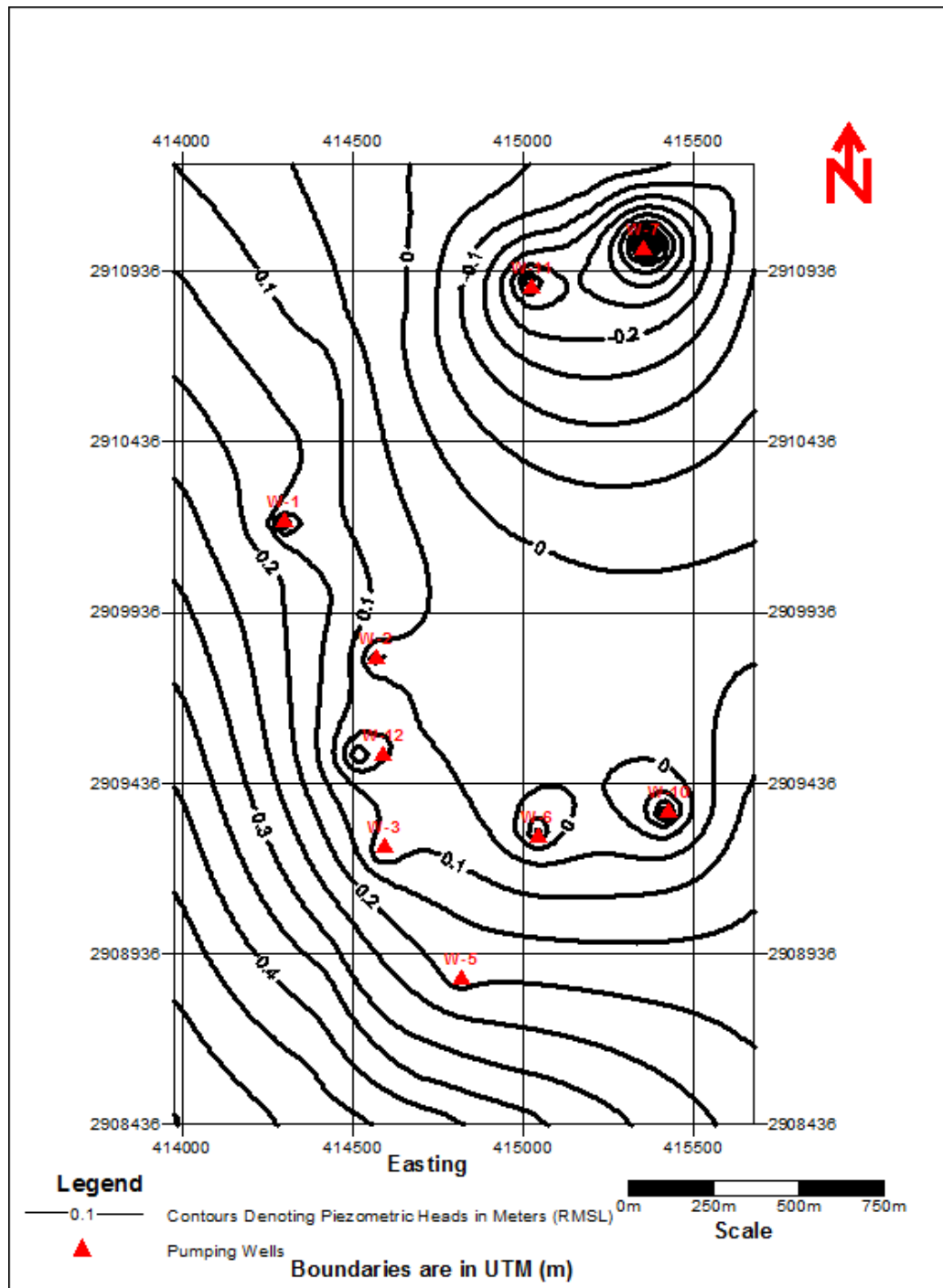


Figure 4.3: Potentiometric surface contour map at the end of 2030
(Alternative II)

4.4 ALTERNATIVE SCHEME III

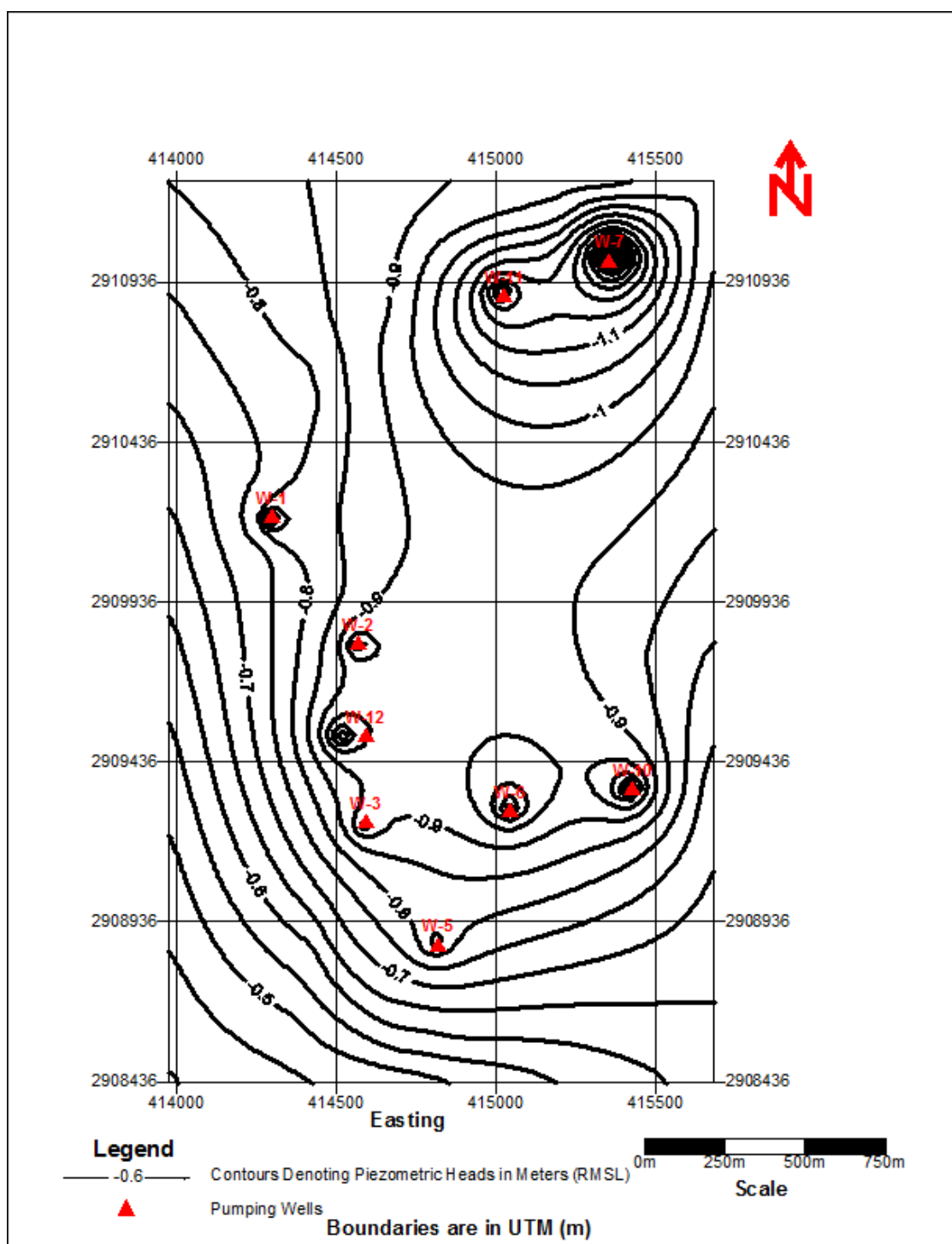
In this alternative, a scenario similar to what currently exists at KFUPM was adopted. Water consumption per capita per day was assumed to be 450 liters (0.45 m^3). This was multiplied with the population trend to obtain the domestic water use for each year. Water use for irrigation and other purposes was assumed to be constant. Both the domestic water use and the water use for irrigation were added to obtain the total water consumption for the each corresponding year.

Table 4.5 shows that the total water consumption at KFUPM between the year 2011 and year 2030 ranges between 36548 and 38063 m^3/day for Alternative Scheme III. These values were assumed to be the total pumping rate for all the wells at KFUPM and were divided among the wells based on the pumping capacity of each well. Since there was no excess volume of water, no new well was added in this alternative scheme.

Figure 4.4 shows the potentiometric surface contour map at the end of the year 2030. The potentiometric surface contour map shows that water level in the study area has dropped from the average of 3.2 m (RMSL) obtained at the end of the year 2010 to an average of -0.9 m (RMSL) in the year 2030 for Alternative Scheme III. This result is equal to an average drawdown of 4.1 m in the study area over the 20-year planning period. Cones of depression were developed in the areas where the observation wells were located. Maximum drawdowns were noticed in areas surrounding the wells. There was prevalence of cone of depression in the northwest of the study area. This was caused by closeness in the positioning of Well No. 7 and Well No. 11.

Table 4.5: Total water consumption for Alternative Scheme III

WATER CONSUMPTION TREND FOR ALTERNATIVE III				
Year	Population Trend	Water for Domestic Use (m ³ /day)	Water for Irrigation and other Purposes (m ³ /day)	Total Water Consumption (m ³ /day)
2011	9680	4356	32192	36548
2012	9857	4436	32192	36628
2013	10034	4516	32192	36708
2014	10211	4595	32192	36787
2015	10388	4675	32192	36867
2016	10566	4755	32192	36947
2017	10743	4834	32192	37026
2018	10920	4914	32192	37106
2019	11097	4994	32192	37186
2020	11274	5074	32192	37266
2021	11451	5153	32192	37345
2022	11629	5233	32192	37425
2023	11806	5313	32192	37505
2024	11983	5392	32192	37584
2025	12160	5472	32192	37664
2026	12337	5552	32192	37744
2027	12514	5631	32192	37823
2028	12691	5711	32192	37903
2029	12869	5791	32192	37983
2030	13046	5871	32192	38063



**Figure 4.4: Potentiometric surface contour map at the end of 2030
(Alternative III)**

4.5 COMPARATIVE ASSESSMENT OF DROP IN WATER LEVEL OF THE THREE ALTERNATIVE SCHEMES

Hydrographs showing assessments of water level of the Alternative Development Schemes are shown in Figure 4.5A through Figure 4.5K. All the wells were observation wells located within the model domain. Each well was positioned close to a pumping well. The observation data used were limited for only 1 stress period. There was a good match in terms of trends and values between the observed and the calculated heads.

For all the observation wells, Alternative Scheme I recorded the highest drop in water level among the three alternative development schemes. It recorded an average drop in water level of -2.2 m (RMSL). It recorded maximum drop in water level of -2.6 m (RMSL) in Observation Well Nos. 7 (Cell No. 5 – 47) and 11 (Cell No. 9 – 33). It recorded minimum drop in water level of -2.1 m (RMSL) in Observation Well No. 5 (Cell No. 60 – 27).

The second highest drop in water level among the Alternative Development Schemes was recorded by the Alternative Scheme III. It recorded an average drop in water level of -0.9 m (RMSL). Like the Alternative Scheme I, it also recorded maximum drop in water level in Observation Well Nos. 7 and 11, and minimum drop in water level in Observation Well No. 5. The maximum and minimum drop in water levels are -1.3 (RMSL) and -0.5 (RMSL), respectively.

Alternative Scheme III recorded the lowest drop in water level among the three Alternative Development Schemes. It recorded an average of 0.2 m (RMSL). For all the observation wells, it did not record a drop in water level below the sea level,

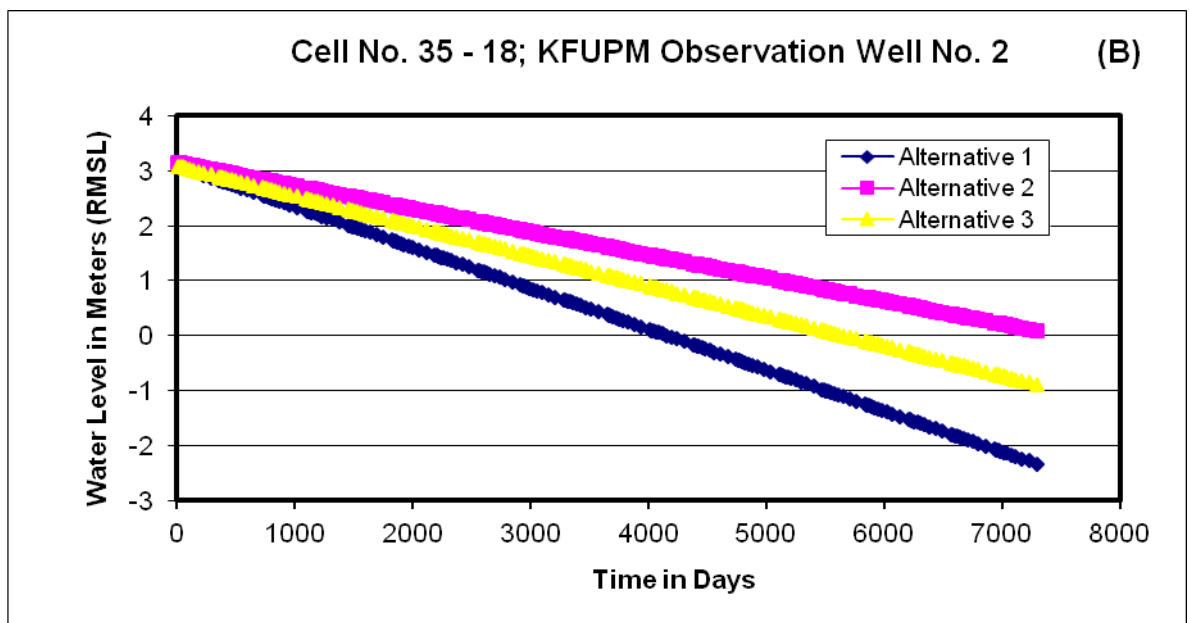
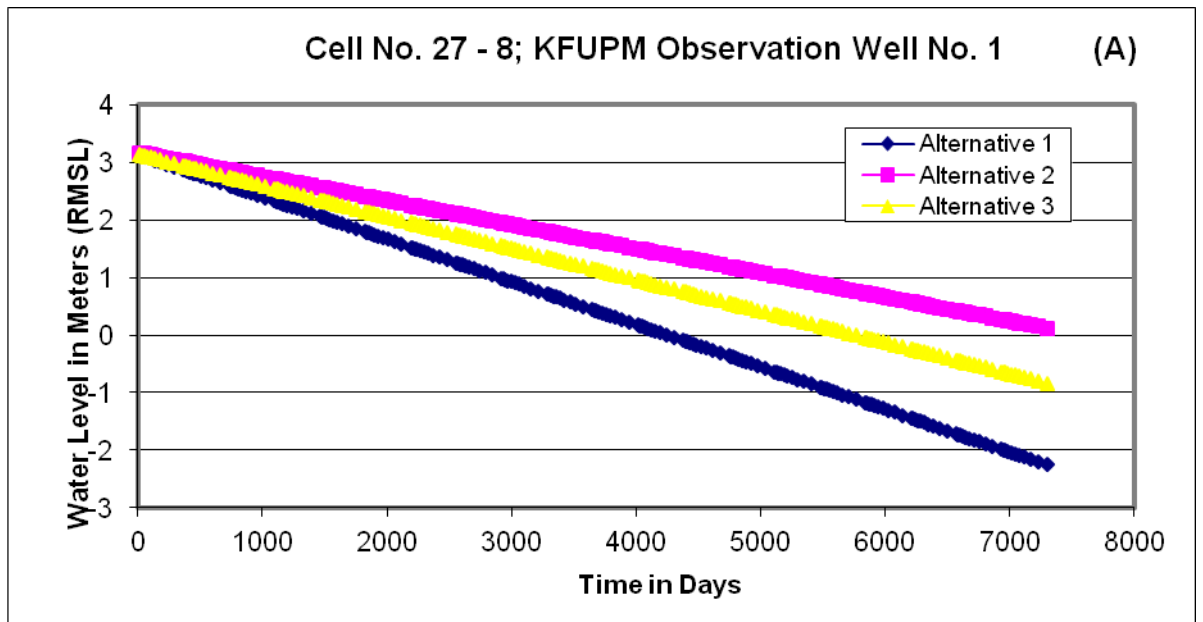


Figure 4.5 (A – B): Hydrograph showing comparing drop in water level

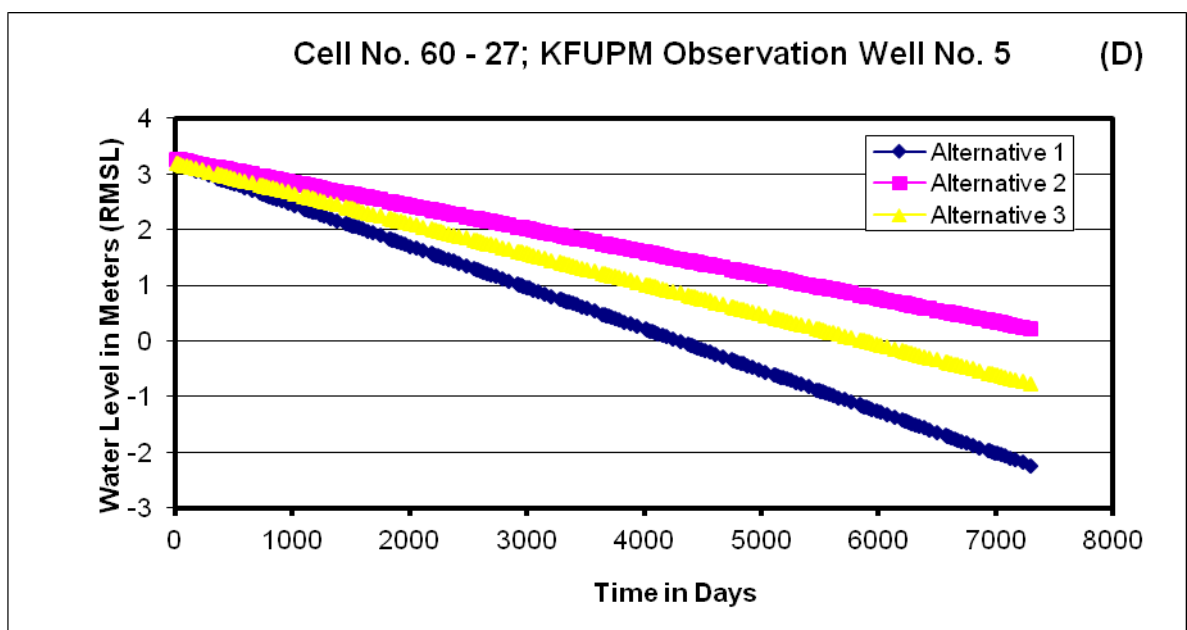
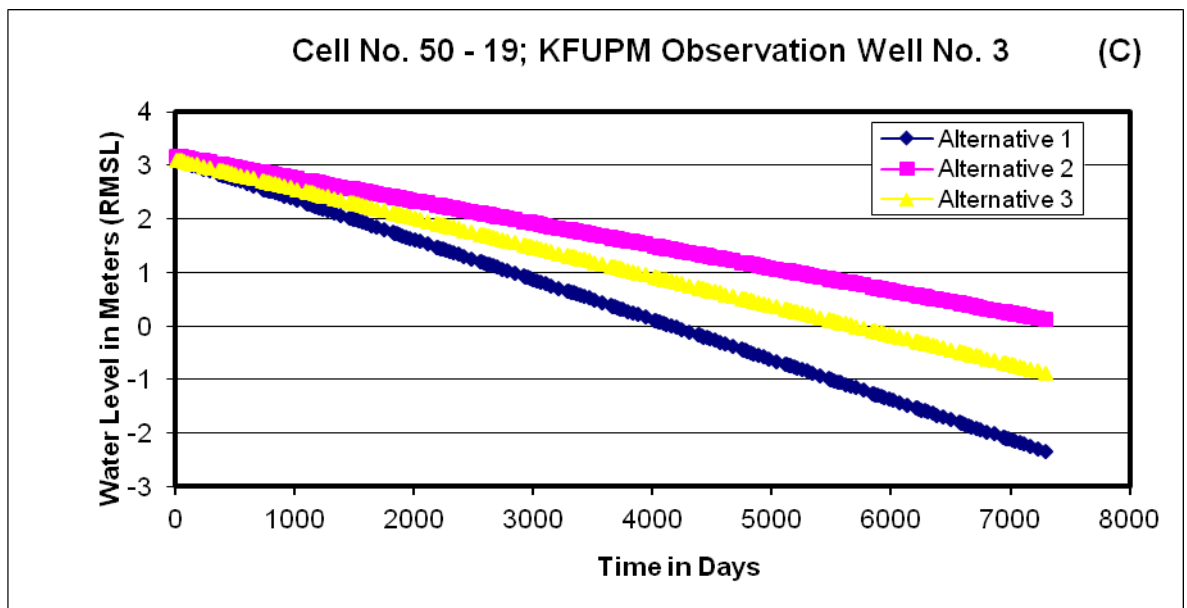


Figure 4.5 (C – D): Hydrograph showing comparing drop in water level

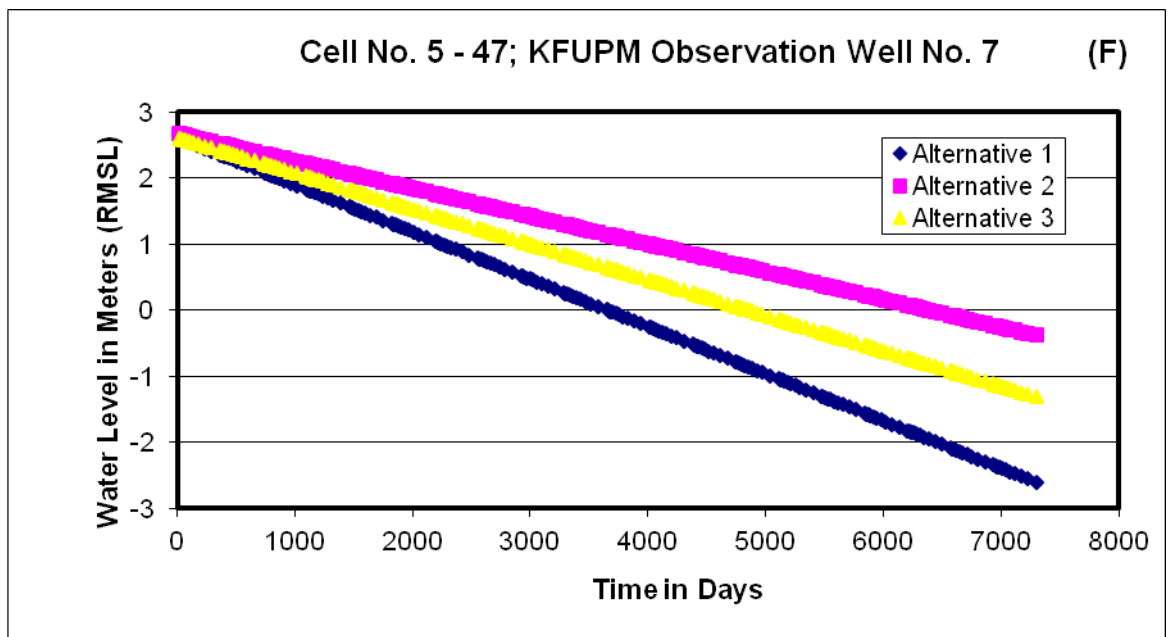
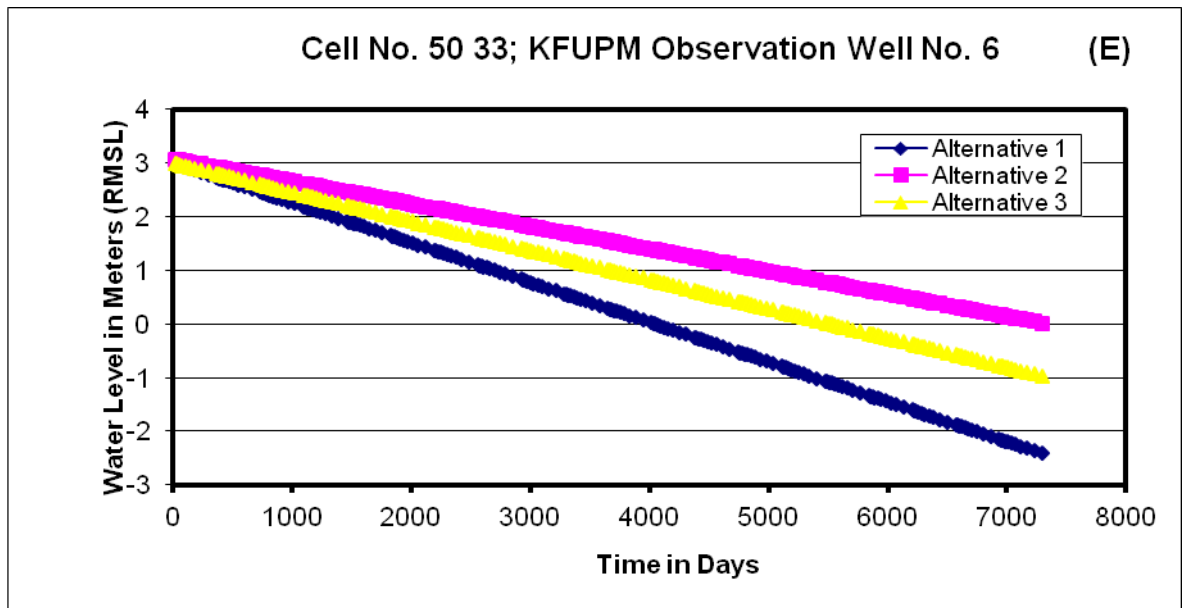


Figure 4.5 (E – F): Hydrograph showing comparing drop in water level

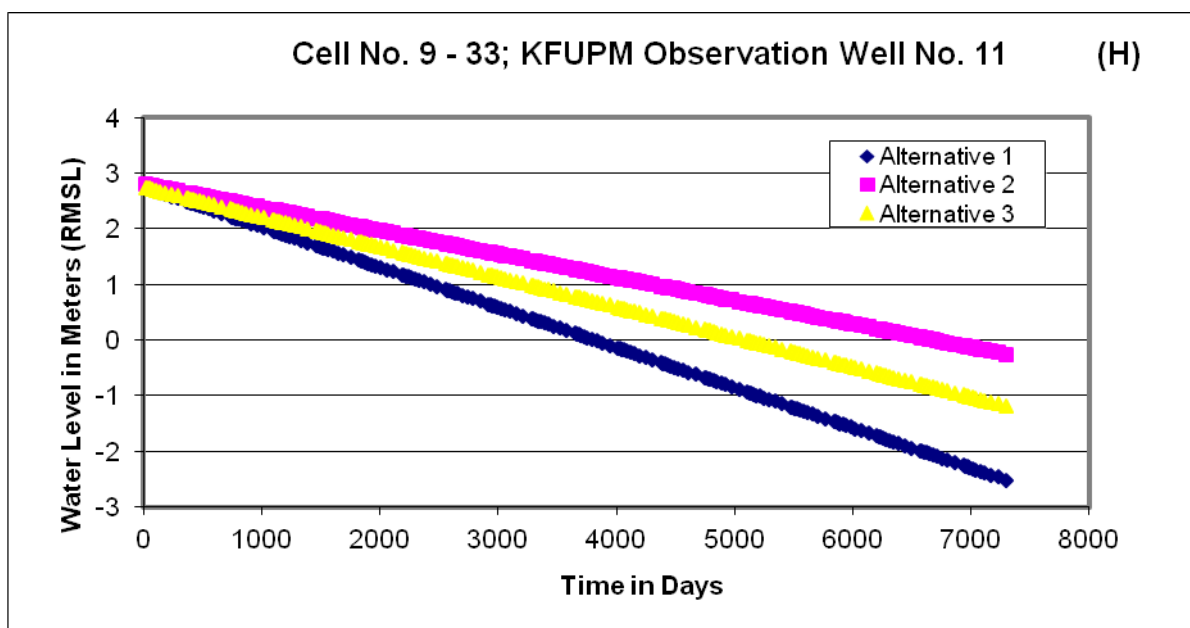
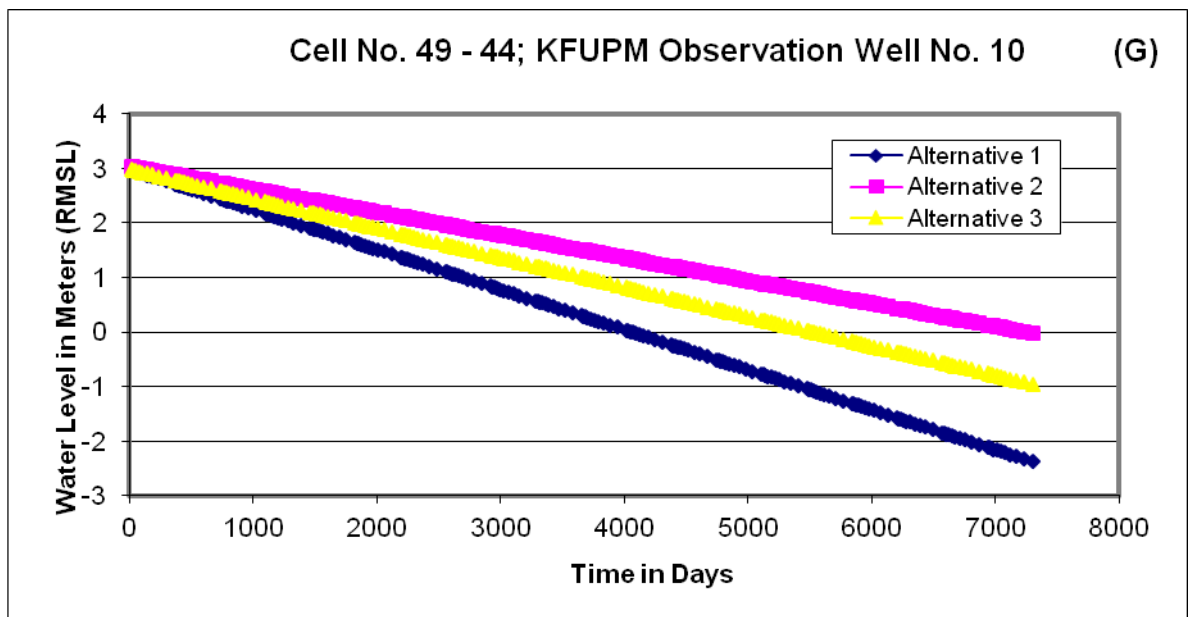


Figure 4.5 (G – H): Hydrograph showing comparing drop in water level

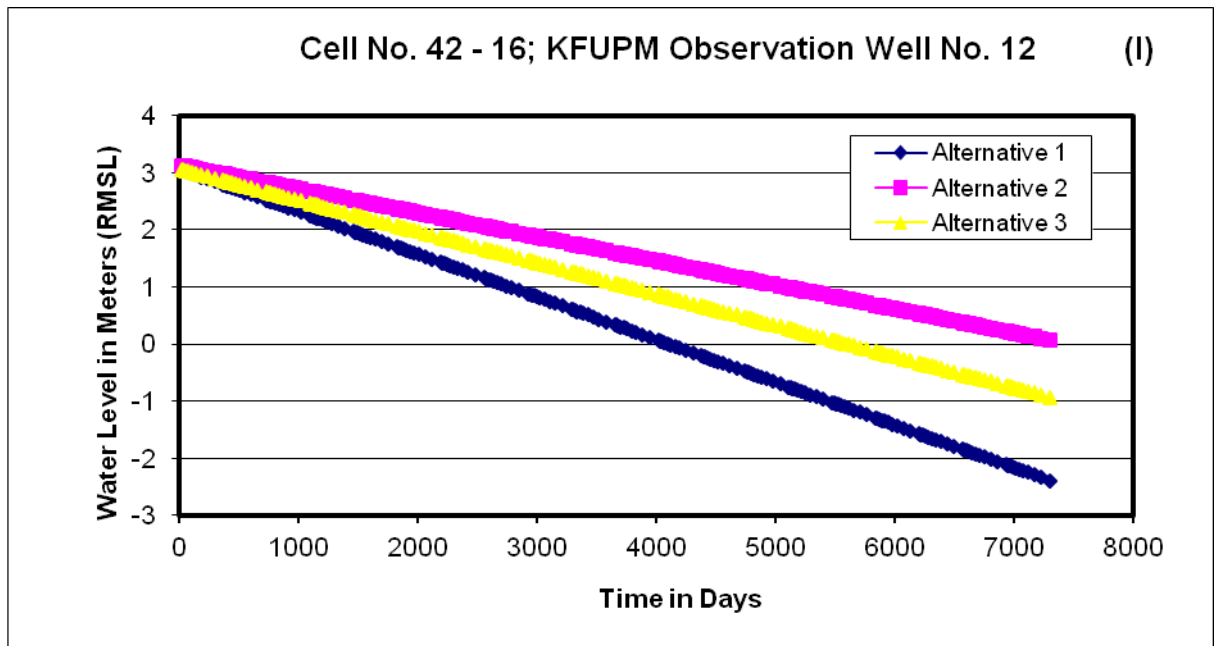


Figure 4.5 (I): Hydrograph showing comparative assessment of drop in water level

except in Observation Well Nos. 7 and 11 in which maximum drop in water level of 0.3 m (RMSL) were recorded.

For all the three Alternative Development Schemes, the trends of drop in water level indicate that the heads will not stabilize by the end of year 2030. The heads will continue to drop beyond that time. However, Alternative II still presents the best scenario.

CHAPTER 5

DEVELOPMENT OF SOLUTE TRANSPORT MODEL

5.1 INTRODUCTION

In several aquifers, the groundwater system consists of saturated porous medium containing miscible fluids of variable solute concentrations. The salty groundwater tends to remain separated from the overlaying relatively fresh groundwater. However, the zone of dispersion, which is also known as the interface, forms between these two fluids. This interface has been found to vary in thickness. The interface is not static but responsive to recharge and discharge mechanisms. Thus when it is desired to pump relatively fresh groundwater, the well should be installed and operated so that a minimum of salty groundwater mixing occurs either within the well or within the aquifer itself.

When a well which is a partially penetrating relatively fresh groundwater starts pumping, it disturbs the equilibrium between the relatively fresh groundwater and salty groundwater in the aquifer (Figure 5.1). The interface starts moving towards the bottom of the well leading to mixing of the salty groundwater with the fresh groundwater. This phenomenon is known as salty groundwater upconing. It is the process through which groundwater salinity is increased.

In this work, the conceptual model used in the flow model was maintained for the solute transport model.

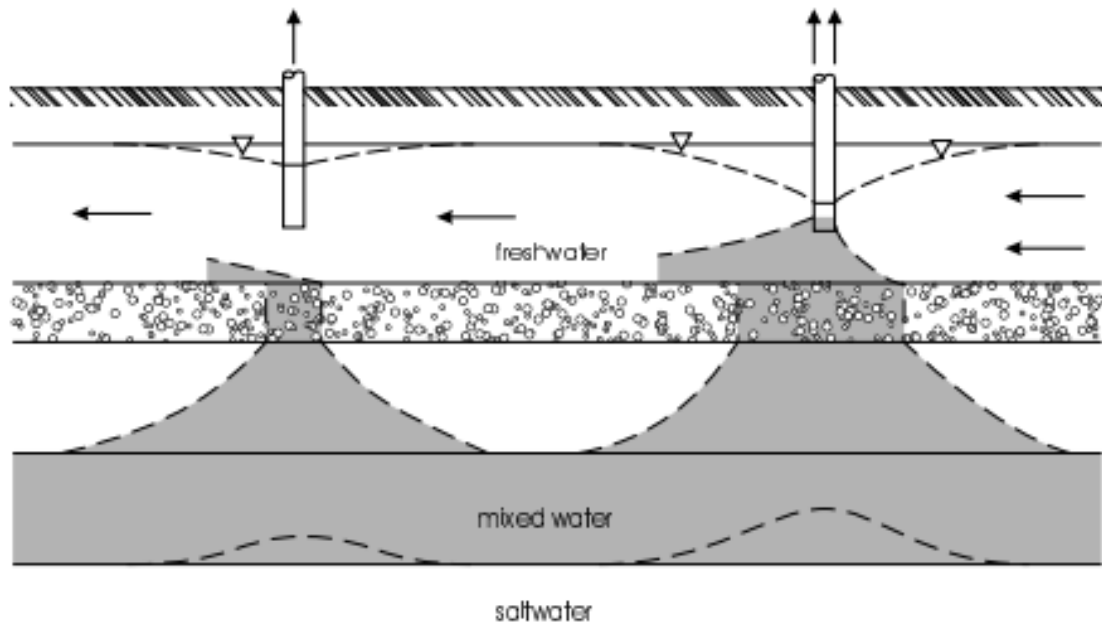


Figure 5.1: Upconing in homogenous and isotropic aquifer

This initiative is valid since we are dealing with a single aquifer within relatively small area. The depth of the productive zone of the aquifer in this model is moderate. This nullifies the need to divide the aquifer into two or more layers for the solute transport model.

5.2 MODELING TECHNIQUE

The main objective of the solute transport model is to simulate the hydrologic behavior of the total dissolved solids (TDS) in terms of space and time in UER aquifer in the study area under long-term increase in groundwater pumping. The model was used as a tool to interpret and define the relationships between changes in the hydrologic stresses, mainly groundwater pumping and TDS.

A solute transport model for the study area has been formulated and developed to simulate the future levels of TDS. The present study uses MODFLOW and MT3D (modular three-dimensional, 3-D, transport model referred to as MT3D) software codes. MODFLOW simulates groundwater flow, and MT3D simulates the transport and resulting salinity distribution. MT3DMS can be used to simulate changes in concentrations of miscible contaminants in groundwater considering advection, dispersion, diffusion, and some basic chemical reactions, with various types of boundary conditions and external sources or sinks (Zheng and Wang, 1999). The chemical reactions included in the model are equilibrium-controlled or rate-limited linear or nonlinear sorption and first-order irreversible or reversible kinetic reactions. It should be noted that the basic chemical reaction package included in MT3DMS is intended for single-species systems. MT3DMS can accommodate very general spatial discretization schemes and transport boundary conditions, including: (a) confined, unconfined, or variably confined/unconfined aquifer layers; (b) inclined model layers

and variable cell thickness within the same layer; (c) specified concentration or mass flux boundaries; and (d) the solute transport effects of external hydraulic sources and sinks such as wells, drains, rivers, areal recharge, and evapotranspiration. The MT3D transport model uses a mixed Eulerian-Lagrangian approach to solve the three-dimensional advection-reaction transport equation. The model can be used to simulate changes in concentration of single species of miscible contaminants in groundwater considering advection, dispersion and some simple chemical reactions. The transport model was prepared upon completion of the inputs for the flow model.

5.2.1 MODEL FORMULATION

The modeled region for the solute transport model was similar to that of the groundwater flow model. It covers an area of 2814 x 1691 m². The whole area was discretized into a non-uniform mesh of comprising 50 rows and 34 columns in the steady-state, and 69 rows and 52 columns in the transient-state, with a grid spacing of approximately 65 m in cells where pumping wells are absent and approximately 33 m in cells surrounding the pumping wells.

All boundaries of the model were assigned as constant concentration boundaries in the steady-state. The constant concentration boundary condition acts as a contaminant source providing solute mass to the model domain in the form of a known concentration to allow for adjustment of TDS at the boundary of the system. In the transient-state, the boundaries of the model were assigned variable concentration boundaries to allow for variations in concentration with pumping and with time.

5.2.2 PREPARATION OF INPUT PARAMETERS

Initial concentration of total dissolved solids (TDS) for UER aquifer in the study area was obtained from results of past studies and is shown in Figure 5.2. Steady-state and transient-state pumping rates were the same as the values used in the groundwater flow simulation model. Calibrated hydraulic conductivities from the flow simulation model were used. Transverse to longitudinal dispersivity ratio of 0.1 was used.

5.2.3 STEADY-STATE SOLUTE TRANSPORT SIMULATION

The year 1967 was considered as pseudo-steady state conditions. The model was calibrated against the TDS values of year 1967. Hydraulic conductivities and pumping rates of year 1967 were used from the groundwater flow model. Figure 5.3 shows the simulated values of TDS in 1967. The simulated concentration values range from 2,450 to 3,120 mg/L. The average TDS value was 2,850 mg/L.

5.2.3.1 STEADY-STATE SOLUTE TRANSPORT CALIBRATION

During the calibration of the solute transport model, mainly dispersivity coefficients and initial TDS concentration in the bottom Layer 2 (UER aquifer) were modified and adjusted until acceptable values of TDS were obtained. The simulated TDS contour map was superimposed on the initial (measured) TDS contour map as shown in Figure 5.4. The differences between the measured and simulated TDS values were very minimal. This confirms the accuracy of the model.

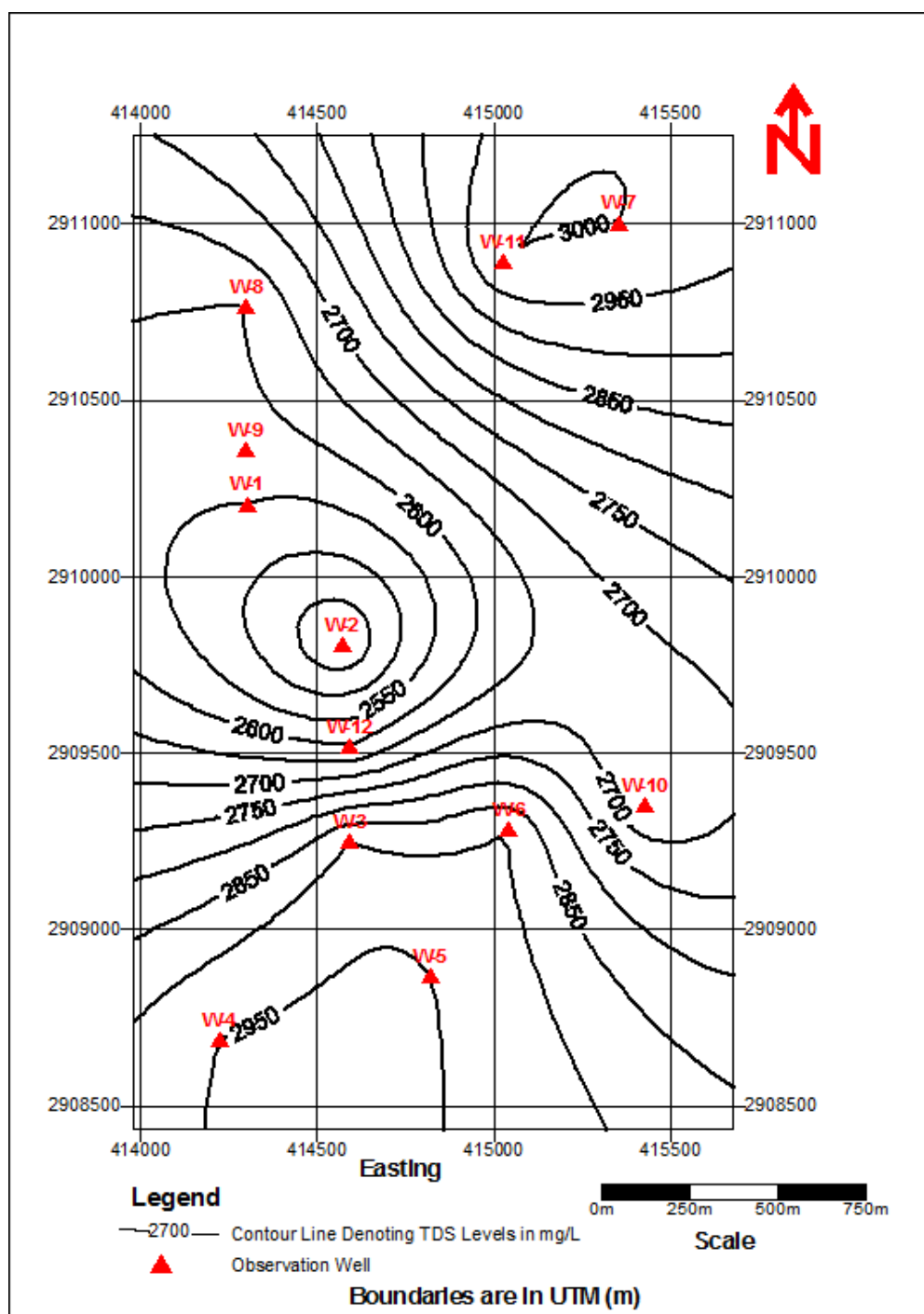


Figure 5.2: Initial TDS contour map (1967 steady-state condition)

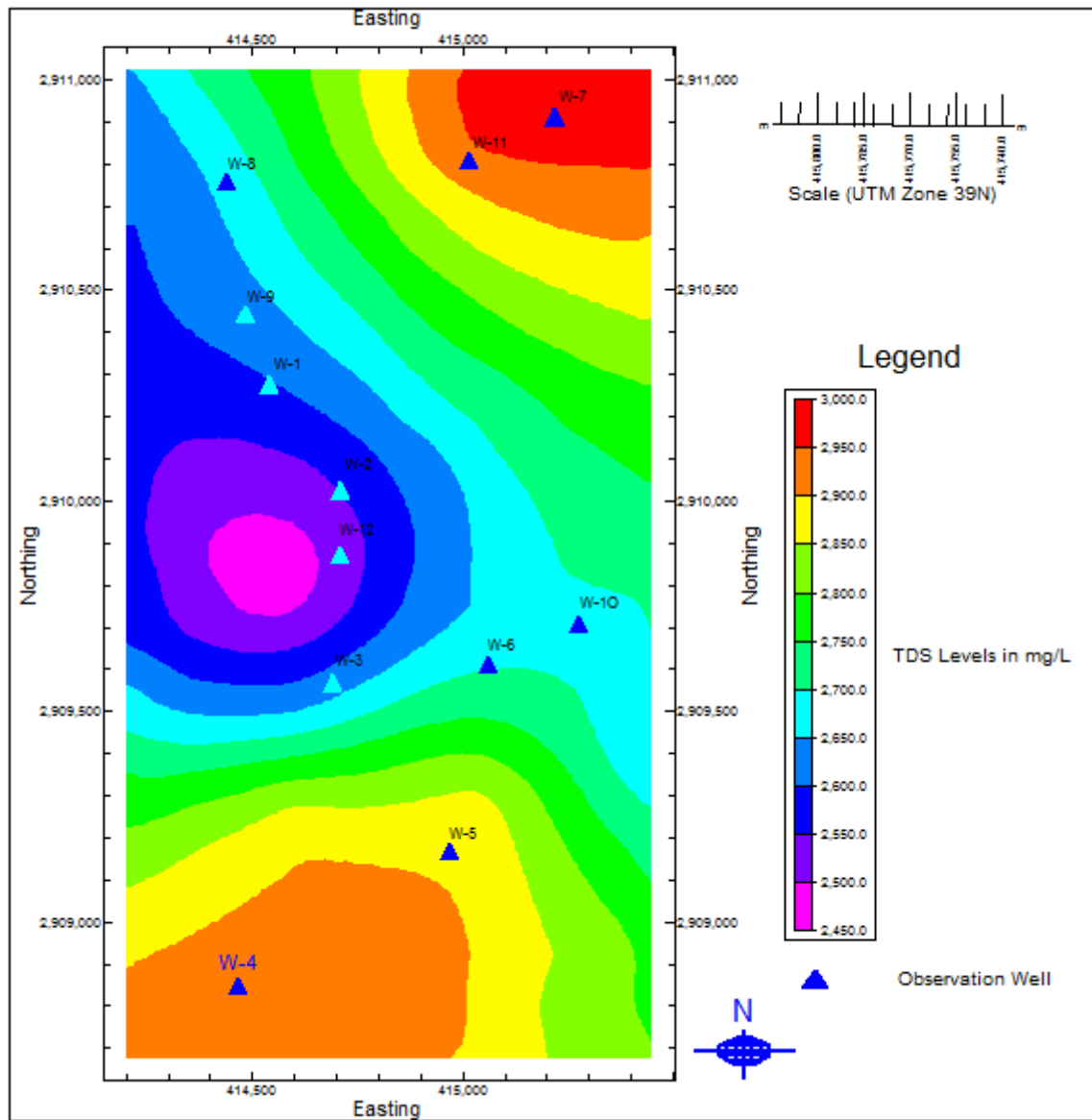


Figure 5.3: Simulated TDS contour map for year 1967 (steady-state)

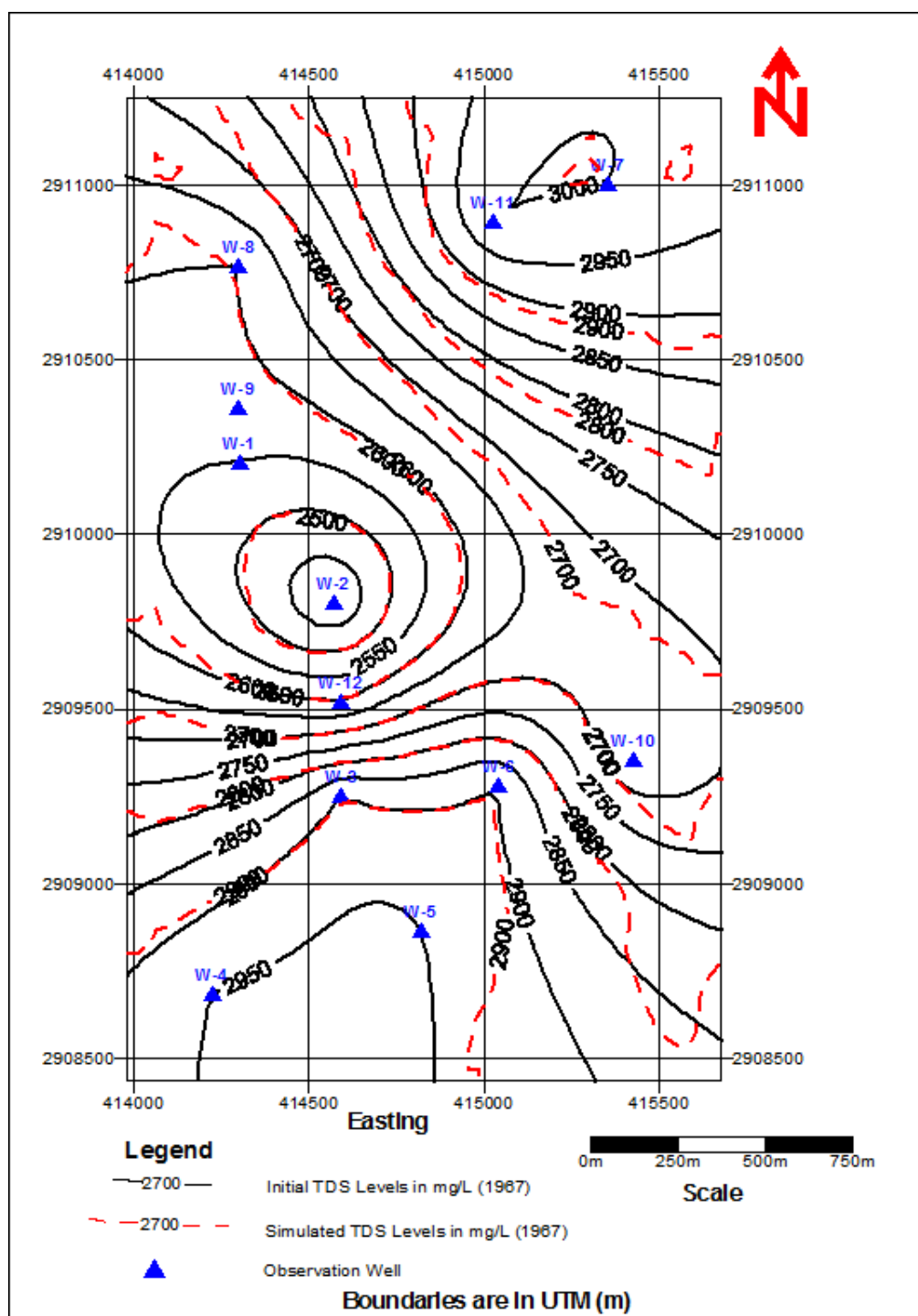


Figure 5.4: Comparison between measured and simulated TDS (steady-state)

5.2.4 TRANSIENT-STATE SOLUTE TRANSPORT SIMULATION

The transient calibration of the solute transport model was performed using the calibrated parameters, such as dispersivity coefficients and initial TDS values during the steady-state simulation. The model was calibrated for the period from 1967 to 2010. The calibrated longitudinal dispersivity coefficients for Layer 2 (UER aquifer) were ranged from 4 to 25 m; the ratio of horizontal to longitudinal dispersivity was 0.1, and the ratio of vertical to longitudinal dispersivity was 0.005. Pumping rates were the same as the values used in the groundwater flow simulation.

Figure 5.5 shows the simulated TDS values at the end of year 2010. The simulated concentration values range from 3,900 to 4,700 mg/L. Average TDS value was 4,200 mg/L. It is evident from Figure 5.5 that the maximum value of TDS occurred at the southwestern part of the study area. The available TDS values obtained from KFUPM Maintenance Department for the year 1993 to 2003 were used for comparison and verification of the simulated TDS levels. The simulated and measured values showed strong agreement in TDS concentrations, which validates the correctness of the simulated TDS values.

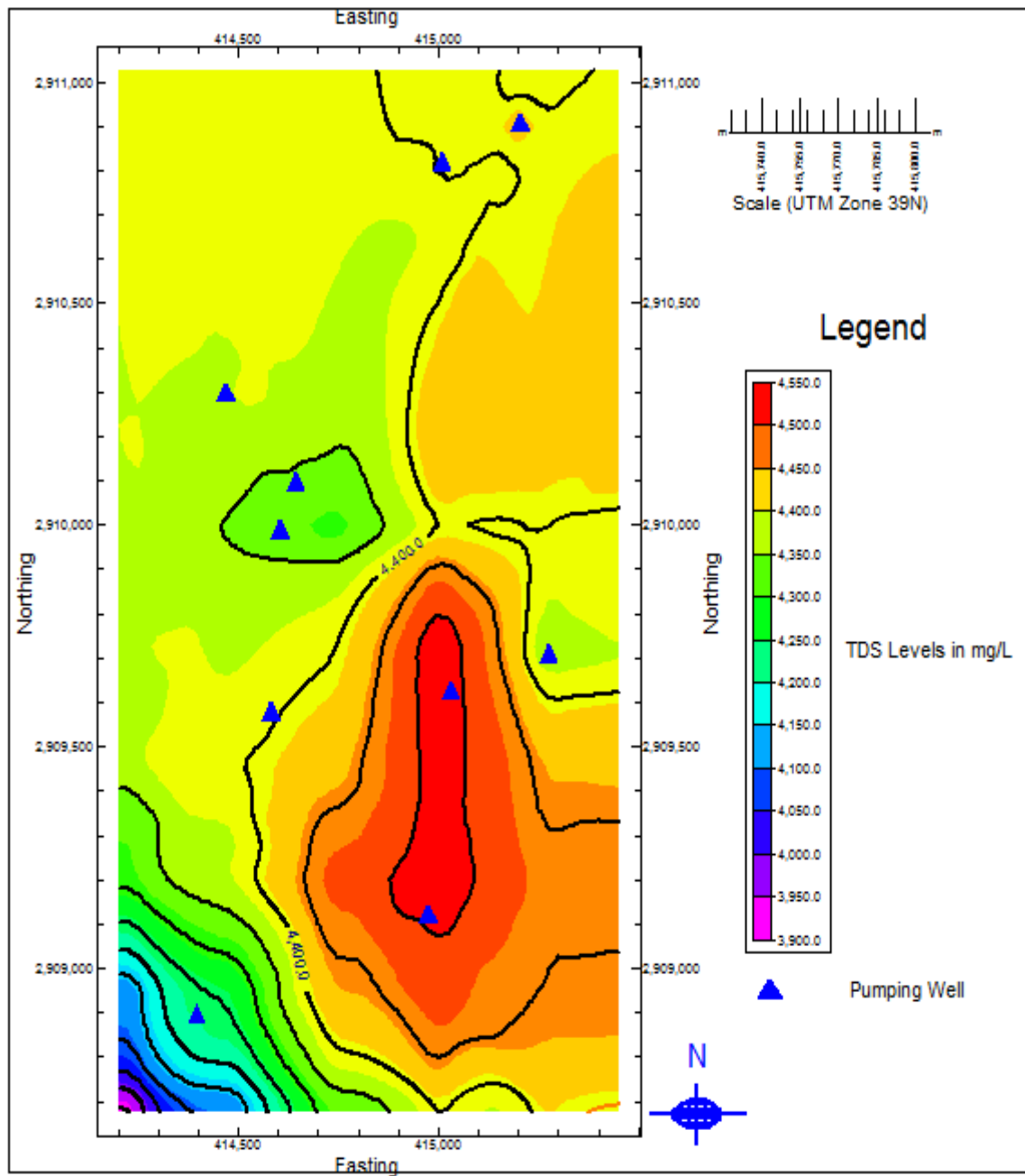


Figure 5.5: Simulated TDS contour map for year 2010

5.3 PREDICTION OF FUTURE CHANGES IN TDS

5.3.1 ALTERNATIVE SCHEME I

The calibrated model was used to predict future TDS distribution in UER aquifer in the study area under long-term increase in groundwater abstraction. A simulation run was made to assess the TDS levels for the period of 20 years (2011-2030) under three different pumping alternatives, which are the same as in the flow model. The well locations and the abstraction rates are similar to the values used in the groundwater flow model. The simulated TDS contour map for year 2030 is shown in Figure 5.6.

The simulation results for UER aquifer indicate that there would be an increase in TDS at the locations of the wells. The TDS concentrations at the end of year 2030 at KFUPM for Alternative Scheme I are expected to range between 5,100 and 5,850 mg/L with an average value of 5,600 mg/L. This represents about 37% increase in the average concentration of TDS since 2010.

5.3.2 ALTERNATIVE SCHEME II

In this alternative, the well locations and the extraction rates are similar to the values used in the groundwater flow model. The simulated TDS contour map for year 2030 is shown in Figure 5.7. The simulation results for UER aquifer indicate that there would be an increase in TDS towards the center of the study area. The TDS concentrations at the end of year 2030 at KFUPM for Alternative Scheme II are expected to range between 4,400 and 5,050 mg/L with an average concentration of 4,550 mg/L. This represents about 8% increase in the average concentration of TDS since 2010.

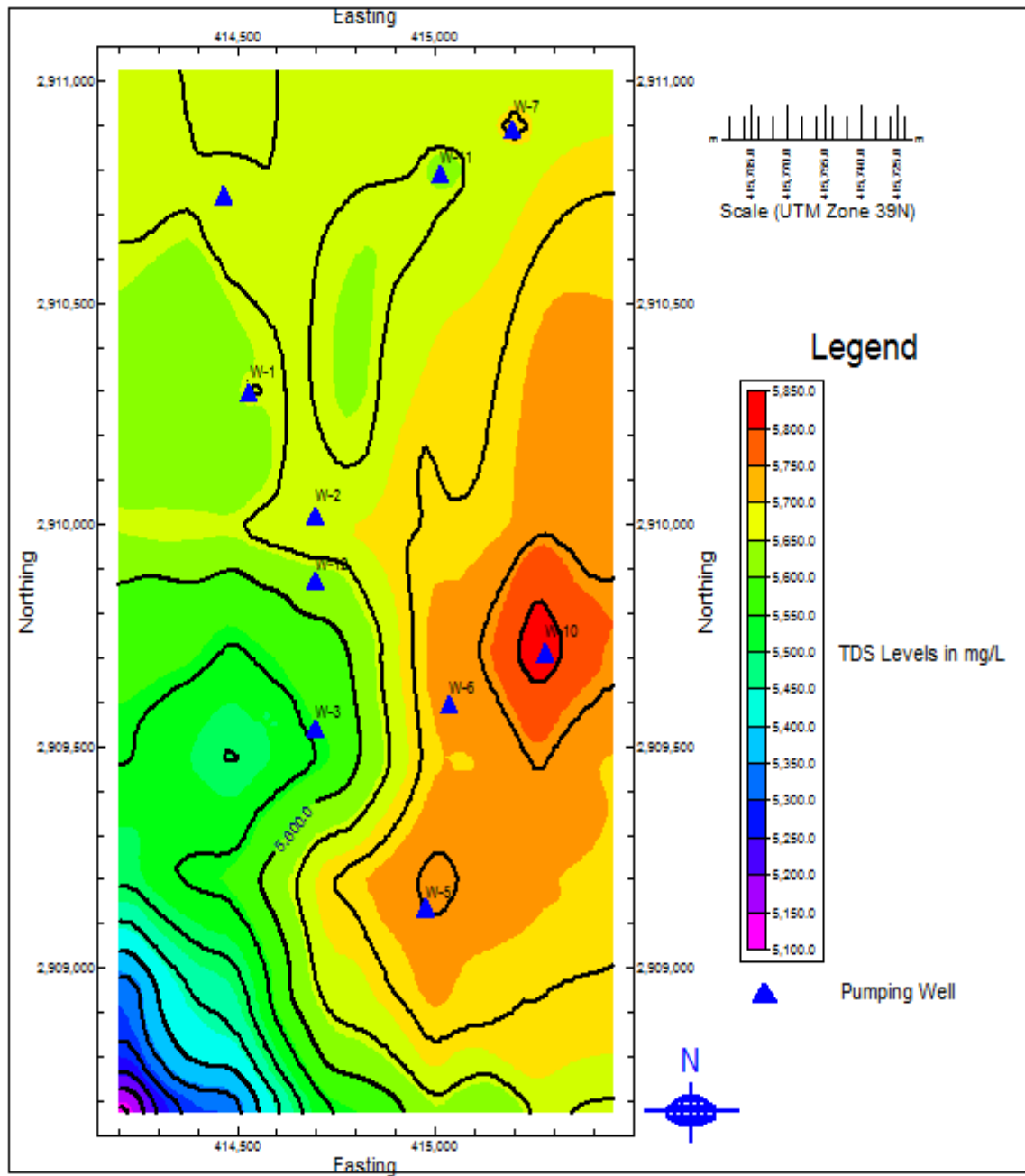


Figure 5.6: Simulated TDS level for year 2030 (Alternative I)

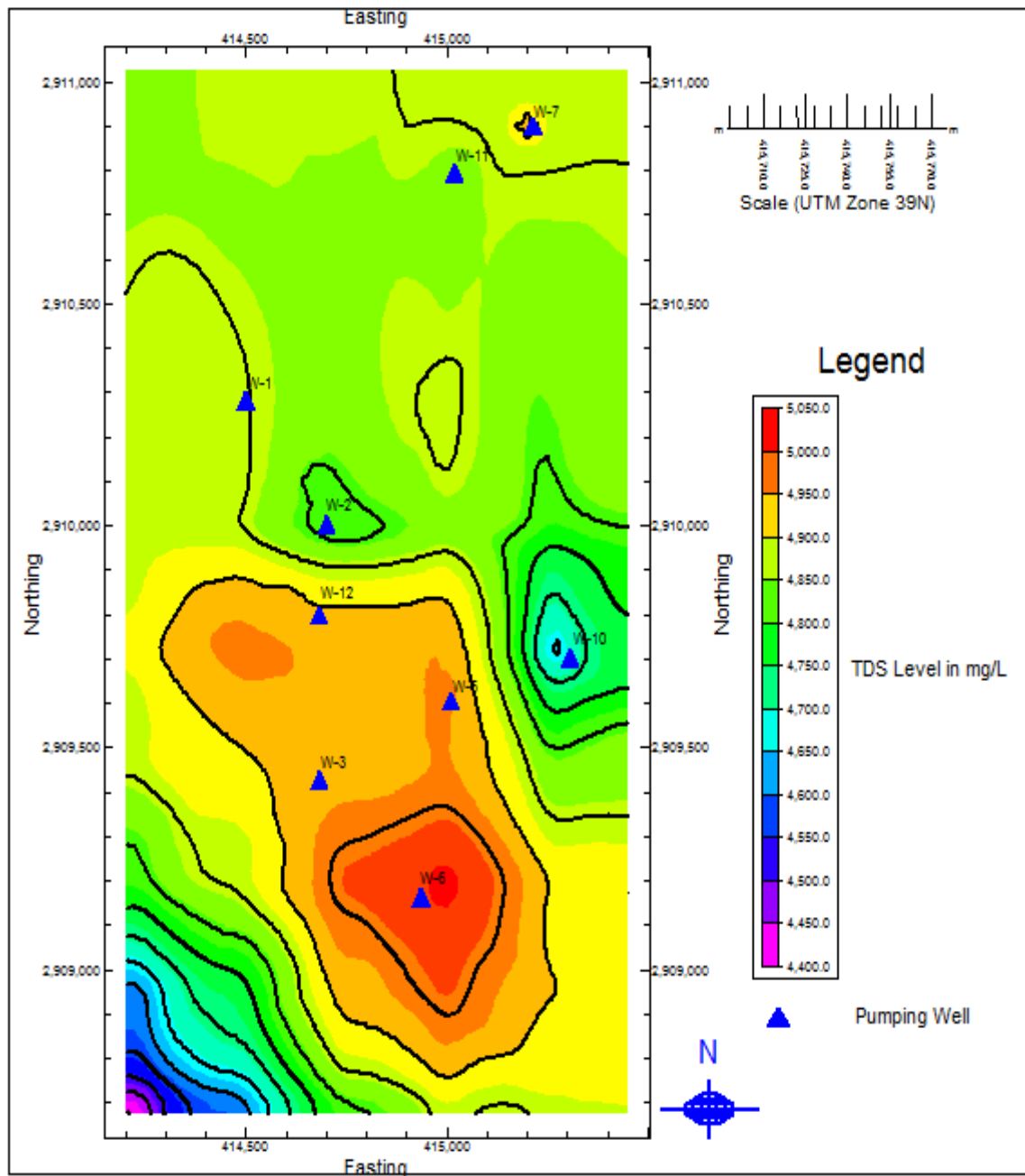


Figure 5.7: Simulated TDS level for year 2030 (Alternative II)

5.3.3 ALTERNATIVE SCHEME III

Like the previous Alternative Development Schemes, the well locations and the extraction rates are similar to the values used in the groundwater flow model. The simulated TDS contour map for the year 2030 is shown in Figure 5.8. The simulation results for UER aquifer indicate that there would be an increase in TDS at the center of the study area and around the wells. The TDS concentrations at the end of year 2030 at KFUPM for Alternative Scheme III are expected to range between 4,950 and 5,550 mg/L with an average value of 5,300 mg/L. This represents about 27% increase in the average value of TDS since 2010.

5.4 COMPARATIVE ASSESSMENT OF TDS LEVEL OF THE THREE ALTERNATIVE DEVELOPMENT SCHEMES

For the purpose of clarity, maximum TDS concentrations for each alternative scheme between year 2011 and year 2030 was obtained. This is shown in Table 5.1. The data were used to make a plot of TDS concentration against time and the result is shown in Figure 5.9.

From Figure 5.9, it can be seen that TDS level for each of Alternative increases with time. This is a direct result of groundwater abstraction. Figure 5.9 also reveals that Alternative I, if implemented, would have the highest TDS levels for all the planning period. It is closely followed by the Alternative III. The TDS level for Alternative II increases at a relatively moderate trend. In summary, the TDS levels for Alternative II would be far lower than the TDS levels for the other two Alternatives by the end of year 2030.

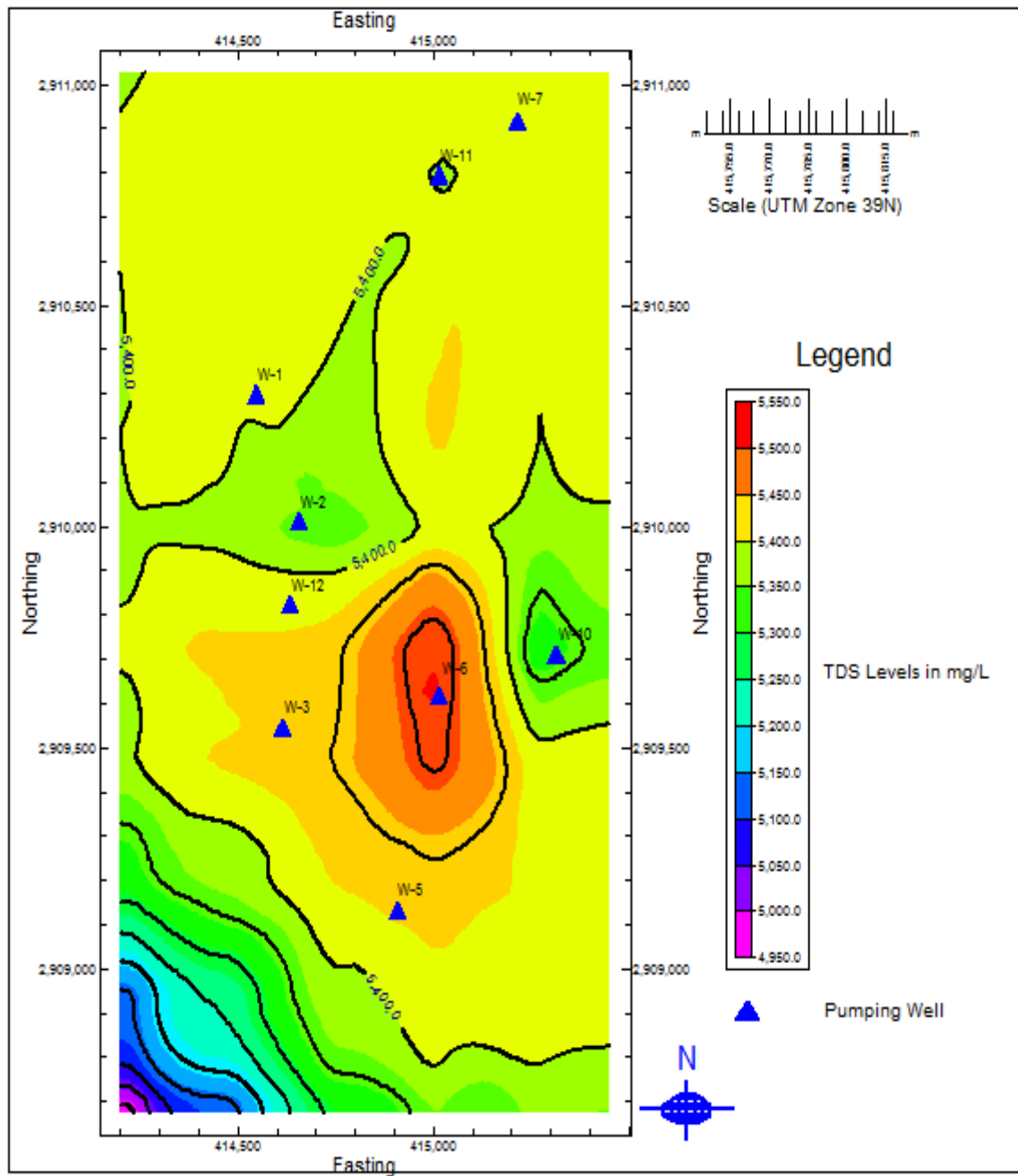


Figure 5.8: Simulated TDS level for the year 2030 (Alternative III)

Table 5.1: Maximum TDS level for the three alternative development schemes for the planning period

TOTAL DISSOLVED SOLIDS (TDS -mg/L) FOR EACH ALTERNATIVE			
Year	Alternative I	Alternative II	Alternative III
1967	2800	2800	2800
1990	3157	3157	3157
2000	3527	3527	3527
2010	4061	4061	4061
2011	4115	4109	4112
2012	4173	4118	4167
2013	4234	4126	4223
2014	4297	4134	4281
2015	4362	4142	4341
2016	4430	4151	4403
2017	4501	4159	4467
2018	4574	4167	4532
2019	4651	4176	4600
2020	4731	4184	4670
2021	4815	4192	4743
2022	4903	4201	4818
2023	4995	4309	4896
2024	5091	4418	4976
2025	5191	4526	5060
2026	5297	4534	5146
2027	5408	4643	5236
2028	5525	4751	5329
2029	5648	4860	5426
2030	5850	5050	5527

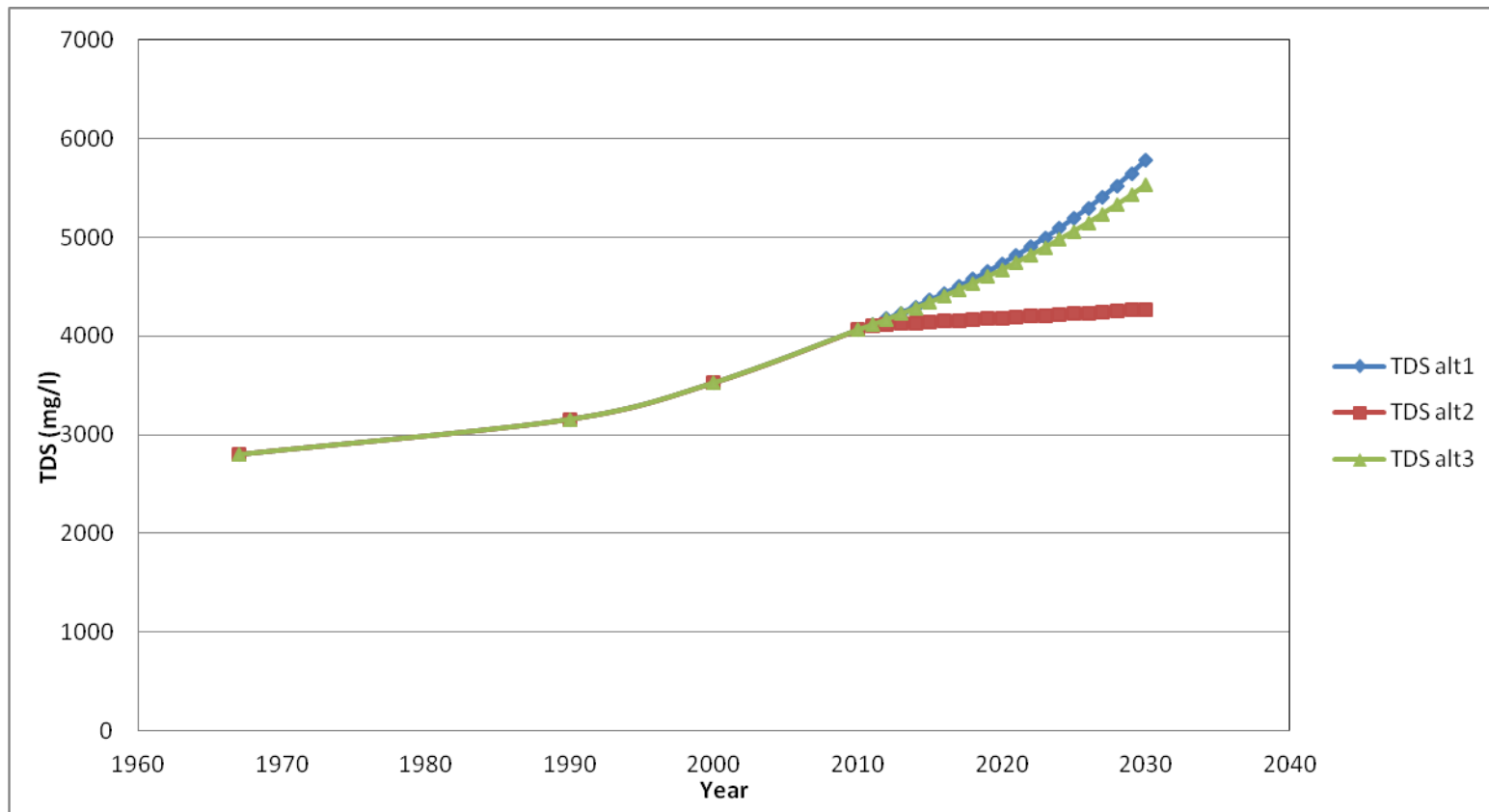


Figure 5.9: TDS versus time graph for the three Alternative Schemes

CHAPTER 6

HYDROCHEMISTRY

6.1 METHODOLOGY

The method applied in the hydrochemical study of the groundwater in the study area involved two major parts: groundwater sampling and laboratory analyses.

6.1.1 GROUNDWATER SAMPLING

Water samples were collected from groundwater wells (Figure 6.1) inside KFUPM campus in January 2012. At the time of the sampling, only eight wells were functioning. Therefore, the sampling and hydrochemical analyses were restricted to the eight wells. The wells were allowed to run for at least five minutes before water samples were collected to ensure that the sampled water is the actual water coming from the ground and not the water stored in the pipes. Each water sample was filled into 250 ml brown bottle, after the bottle was rinsed three times with the water. The bottles were labeled according to their respective well numbers. The bottles were immediately taken to the lab where they were stored in a refrigerator (below 4⁰C). The field sampling was carried out in accordance with the United States Environmental Protection Agency (EPA, 2004) guidelines and strict considerations were given to individual parameter holding time criteria as outlined by American Public Health Association (APHA, 1995).



Figure 6.1: Sampling of KFUPM Well 12

6.1.2 LABORATORY ANALYSES

6.1.2.1 SAMPLE PREPARATION

Eight groundwater samples were taken to the lab at KFUPM Research Institute to analyse for selected parameters. Samples for total and fecal coliforms were immediately sent to microbiology lab for subsequent analysis. Preparations including sterilizing of sample bottles and media preparations were made in advance. Samples for other parameters were stored in cold room at 4°C till the time of the analysis. Samples were later homogenized and filtered through 0.45 µm membrane filter.

6.1.2.2 GEOCHEMICAL ANALYSES

Critical parameters like EC, pH, TDS and volatile solids were measured immediately on receipt of samples, before the samples were stored in the refrigerator. Analysis was conducted on the filtered samples for all other physico-chemical parameters.

For metal analysis, 50 ml of each sample, after filtration, was acidified to pH <2 using 50% HNO₃ and stored in 100 ml clear bottles. According to USEPA guideline, the acidified samples were left for at least 16 hours before metal analysis begun. Metals were analysed using EPA method 200.7, Inductively Coupled Plasma Atomic Emission Spectroscopy (ICP-OES). All QA/QC protocols were observed during the analysis.

Table 6.1 shows the summary of the techniques used for each analysis.

Table 6.1: Methods applied for each parameter in the hydrochemical analyses

Parameter	Units	Method ref	Technique
pH		EPA 150.1	Potentiometric
TDS	mg/L	EPA	Gravimetric
Conductivity	uS/cm	EPA 120.1/9050A	Conductivity cell
Nitrate	mg/L	SM 4500, IC- 3000	Ion Chromatography
Chloride	mg/L	SM 4500, IC- 3000	Ion Chromatography
Sulphate	mg/L	SM 4500, IC- 3000	Ion Chromatography
Fecal Coliform	CFU/100 ml	SM 9221 E	MPN Fermentation
Total coliform	CFU/100 ml	SM 9221 B	MPN Fermentation
Al	mg/L	EPA 200.7	ICP-OES
Ca	mg/L	EPA 200.7	ICP-OES
Cd	mg/L	EPA 200.7	ICP-OES
Cu	mg/L	EPA 200.7	ICP-OES
Co	mg/L	EPA 200.7	ICP-OES
Cr	mg/L	EPA 200.7	ICP-OES
Fe	mg/L	EPA 200.7	ICP-OES
K	mg/L	EPA 200.7	ICP-OES
Mg	mg/L	EPA 200.7	ICP-OES
Mn	mg/L	EPA 200.7	ICP-OES
Na	mg/L	EPA 200.7	ICP-OES
Ni	mg/L	EPA 200.7	ICP-OES
Pb	mg/L	EPA 200.7	ICP-OES
Zn	mg/L	EPA 200.7	ICP-OES

6.2 HYDROCHEMICAL CHARACTERISTICS

6.2.1 PHYSICAL PARAMETERS

Average groundwater temperature was 31°C which was higher than the ambient local air temperature of 19°C at the time of sampling. pH values of the groundwater in the study area range between 6.87 and 7.40, with an average pH of 7.01 (Table 6.2). Albeit the pH values are in the usual range of natural groundwater (Hem, 1985), they are on the lower end of the range.

Electrical Conductivity (EC) ranges between 5440 $\mu\text{S}/\text{cm}$ and 6340 $\mu\text{S}/\text{cm}$, with an average of 5775 $\mu\text{S}/\text{cm}$. Highest EC value is recorded in W-12 located at the west-central part of the study area. The measured Total Dissolved Solids (TDS) values range between 3100 mg/L and 4600 mg/L, with the highest concentration occurring at W-12.

6.2.2 CHEMICAL AND BIOLOGICAL PARAMETERS

Major ions that are normally considered in groundwater quality studies have been analyzed for the groundwater in the study area. Table 6.2 shows the detail of the geochemical analysis results and physical parameters. The samples have also been analyzed for biological parameters in terms of total coliforms and E.Coli. Table 6.3 shows biological analysis results for total coliform and E.Coli.

In the following sections, individual parameters are discussed and the analysis results are presented.

Table 6.2: Results of hydrochemical analyses and physical parameters

Well ID	pH(31°C)	EC ($\mu S cm^{-1}$)	Concentration(mg/L)											CO ³⁻⁻ + HCO ³⁻
			TDS	Ca++	K ⁺	Mg++	Na+	Fe+++	F-	Cl ⁻	Br ⁻	NO ³⁻	SO ⁴⁻⁻	
W-1	6.89	5440	3100	256.80	43.88	134.68	442.88	0.00	0.876	1772	6.122	3.337	862.1	238.7
W-2	7.18	5760	3420	285.10	44.80	143.60	455.18	0.01	0.737	1507	5.243	1.578	803.2	241.9
W-5	6.96	6090	3970	288.53	48.10	163.58	505.85	0.02	0.704	1692	5.742	4.609	893.6	233.9
W-6	6.91	5850	4550	297.35	48.90	181.98	524.25	0.03	0.718	1727	5.627	2.453	911.1	238.2
W-7	7.40	5510	4450	276.70	45.10	147.83	471.80	0.00	0.899	1762	6.083	4.066	873.0	201.4
W-10	6.86	5470	4400	299.18	45.90	152.55	478.88	0.01	0.808	1585	5.637	4.061	935.0	246.6
W-11	7.00	5740	3980	281.98	45.58	151.00	484.33	0.00	0.780	1684	5.429	3.670	830.0	209.2
W-12	6.87	6340	4600	302.03	47.33	157.18	504.03	0.01	0.780	1692	5.712	1.650	868.0	244.5

Table 6.3: Results of the analysis for total coliform and E.Coli

Well Number	Total Coliform (MPN Index/100 ml)	E.Coli
Well 1	1.1×10^4	Absent
Well 2	1.3×10	Absent
Well 5	3.4×10^4	Absent
Well 6	2.9×10^3	Absent
Well 7	2.4×10^4	Absent
Well 10	2.2×10^4	Absent
Well 11	1.8×10^4	Absent
Well 12	1.1×10^2	Absent

6.2.2.1 CALCIUM (Ca²⁺) AND MAGNESIUM (Mg²⁺)

Hem (1985) termed calcium and magnesium dissolved significantly in natural water as alkaline earth metals. They are normally present in natural water in dissociated form as bivalent ions and are mostly responsible for causing hardness in water. Calcium and magnesium in all the analyzed groundwater range between 256.8 mg/L and 302.03 mg/L, and 134.68 mg/L and 181.98 mg/L, respectively. The average concentration of calcium is 286 mg/L, while the average concentration of magnesium is 154.05 mg/L. Figures 6.2 and 6.3 show the distribution of calcium and magnesium, respectively, in the study area. While calcium is uniformly distributed, magnesium has higher concentration at the south of the study area with a gradual decrease in concentration towards the north.

6.2.2.2 SODIUM (Na⁺) AND POTASSIUM (K⁺)

Sodium and potassium are usually the most abundant members of the alkali-metal group in groundwater (Hem, 1985). Higher levels of sodium than potassium can be due to potassium bearing minerals weather more slowly than those containing sodium. Sodium concentration in analyzed groundwater samples ranges between 442.88 mg/L and 524.25 mg/L (Figure 6.4), while concentration of potassium in the analyzed samples ranges between 43.88 mg/L and 48.9 mg/L (Figure 6.5). Potassium is evenly distributed in the study area. Sodium shows higher concentration in the south of the study area than in the north. As the study area is just a few kilometers to the Arabian Gulf, high sodium concentration may be a signal of sea water intrusion.

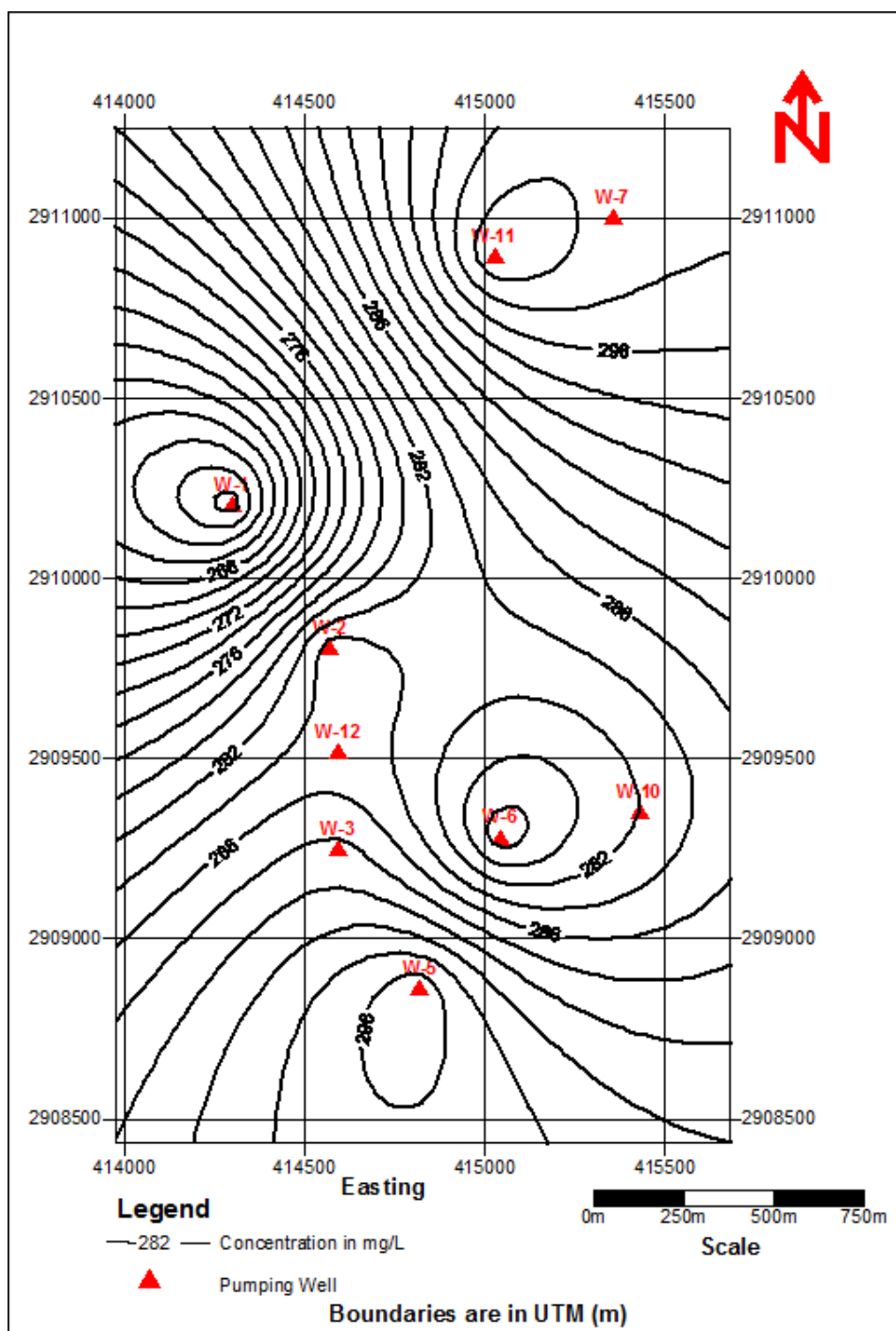


Figure 6.2: Calcium concentration (mg/L) variation in the study area

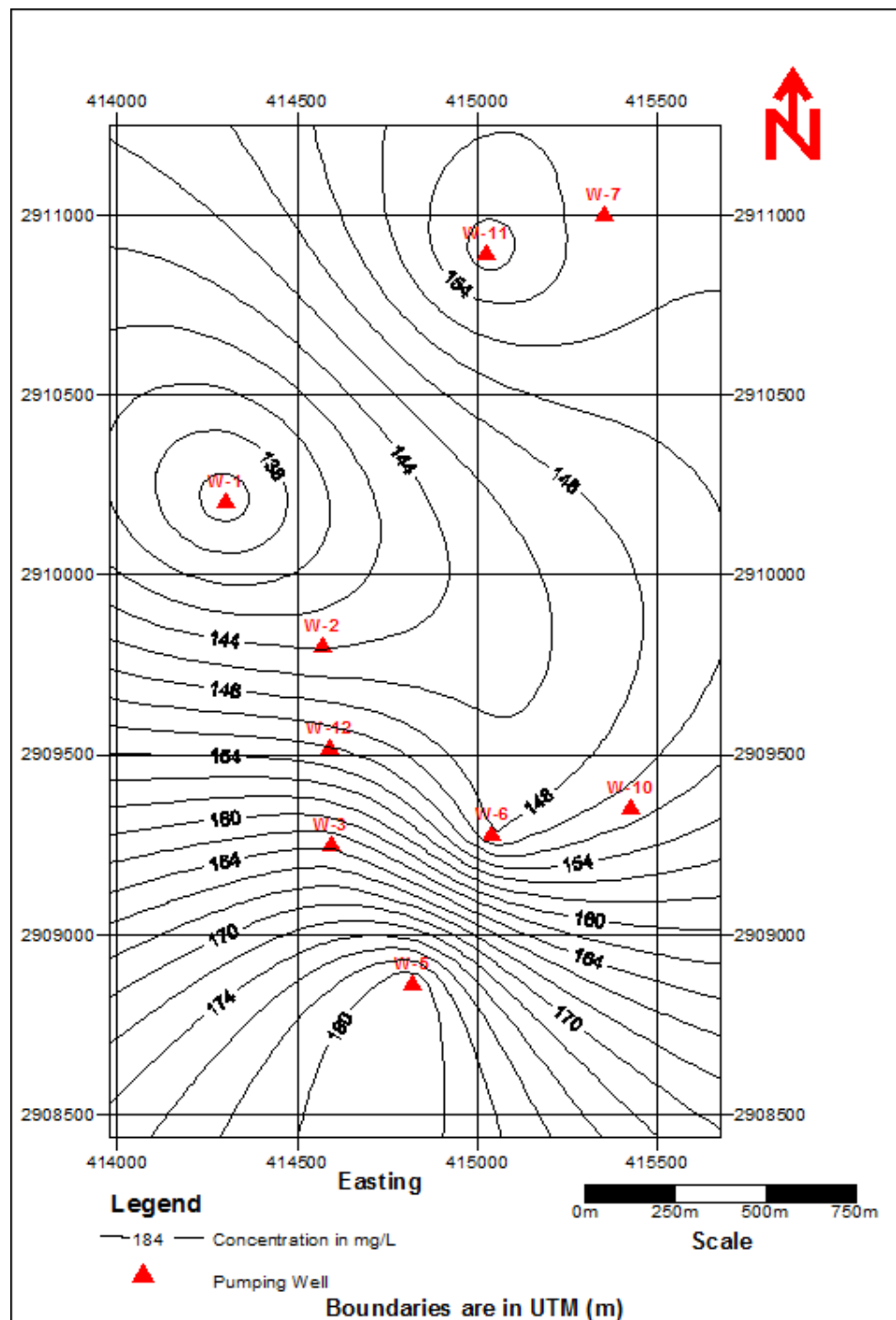


Figure 6.3: Magnesium concentration (mg/L) variation in the study area

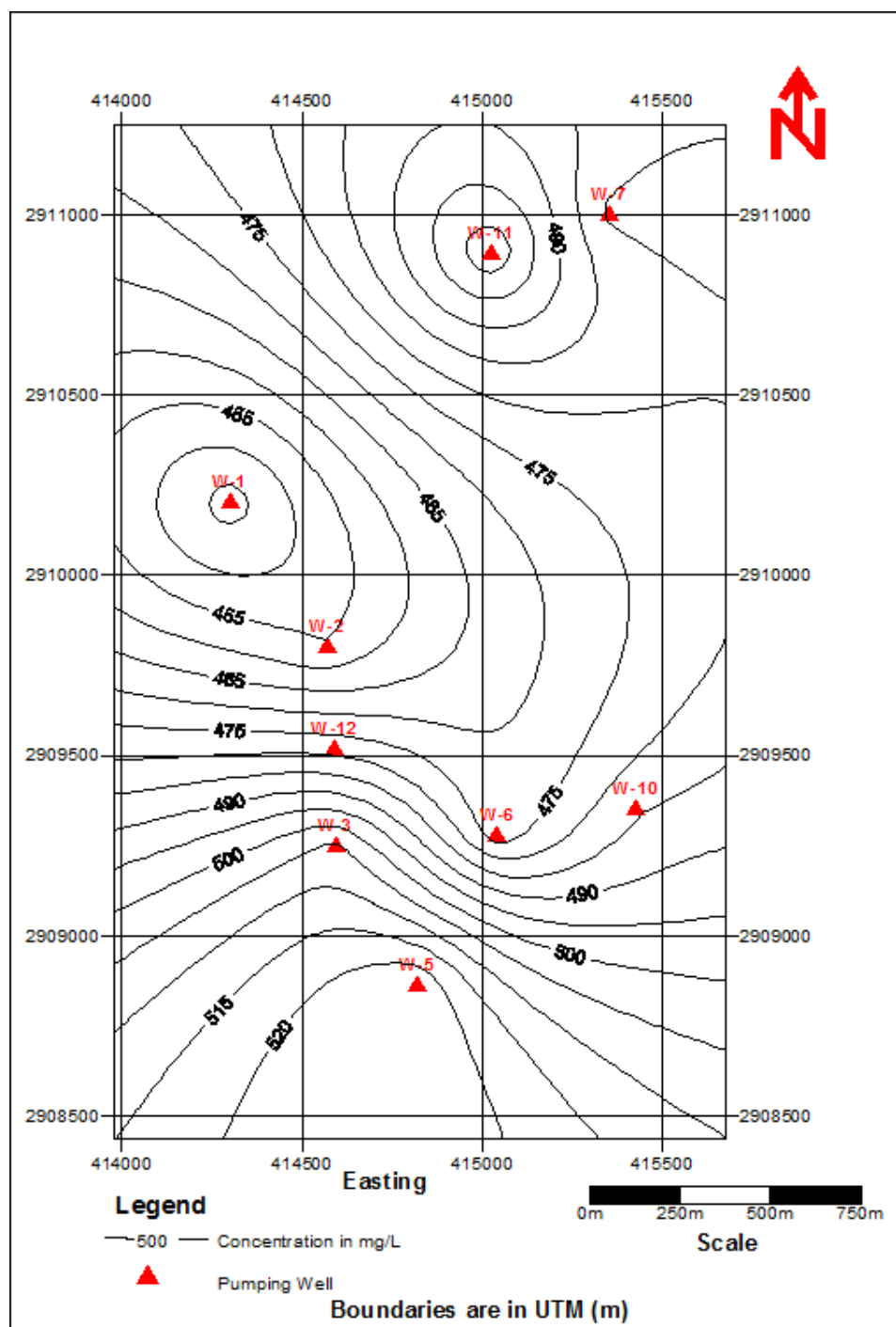


Figure 6.4: Sodium concentration (mg/L) variation in the study area

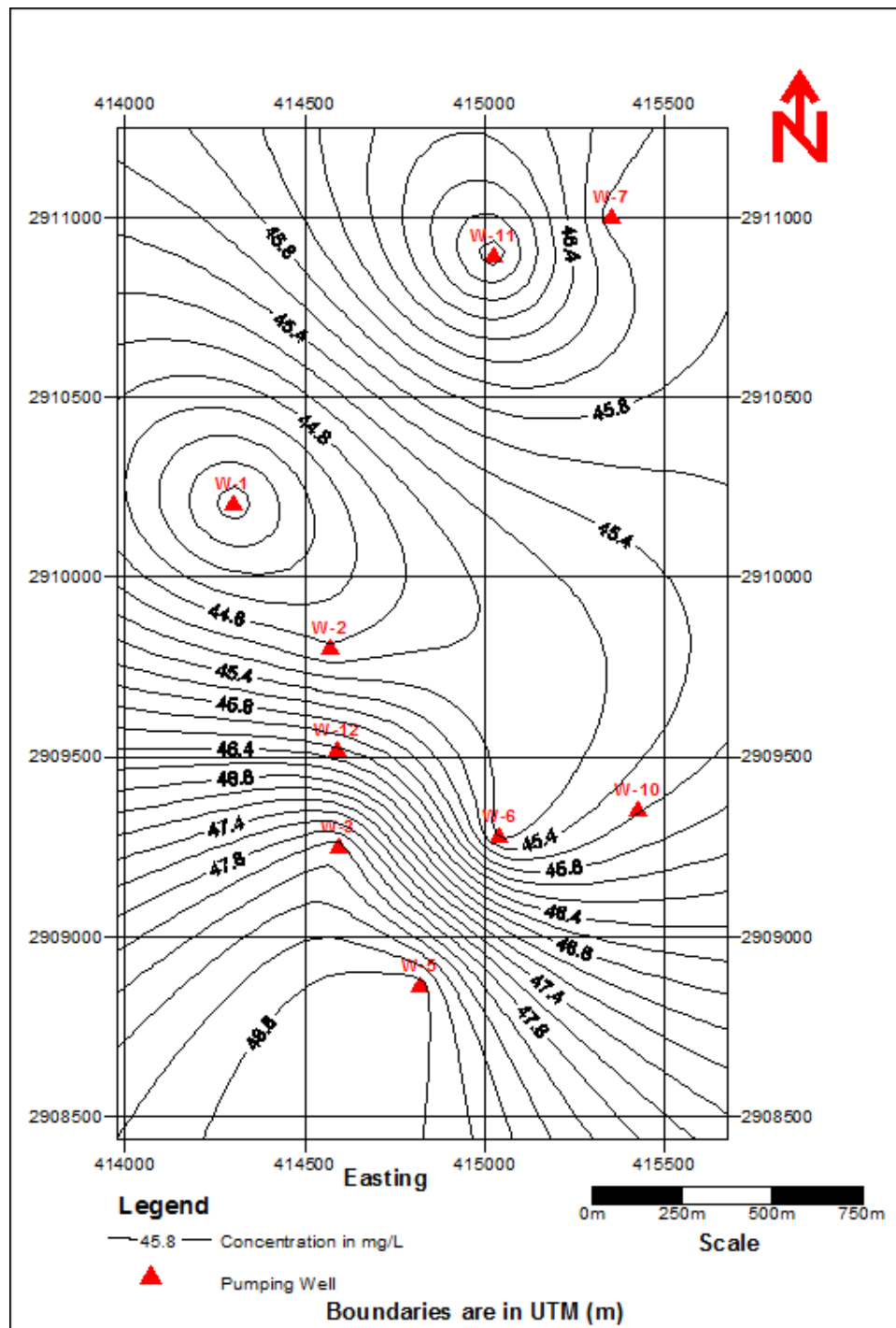


Figure 6.5: Potassium concentration (mg/L) variation in the study area

6.2.2.3 BICARBONATE (HCO_3^-) AND CARBONATE (CO_3^{2-})

Bicarbonate concentration in the analyzed groundwater samples is in the range of 201.4 mg/L and 246.6 mg/L, with an average concentration of 231.8 mg/L. In natural groundwater, bicarbonate and carbonate are usually present because of the weathering of the carbonate minerals and presence of CO_2 , which helps to dissolve the elements (Rainwater and Thatcher, 1960). Concentrations of bicarbonate more than 200 mg/L are not uncommon in groundwater, especially where the aquifer is made of carbonate rocks (as it is in the study area) and CO_2 is present. There is an even distribution of bicarbonate in the study area (Figure 6.6).

6.2.2.4 CHLORIDE (Cl^-)

Chloride concentration in the analyzed groundwater samples ranges between 1507 mg/L and 1772 mg/L, with an average concentration of 1677.6 mg/L (Figure 6.7). Chloride is a primary indicator of salinity in water. In natural groundwater, most chloride comes from evaporates, salty connate water or due to the presence of shale that has lost chloride by leaching as a result of near surface exposure (Hem, 1985). Chloride is also an indicator of septic system pollution (Alhajjar et al., 1990). Thus based on the analyzed data and local geology, it can be said that high chloride concentration may be caused by percolations from septic water and sewage waste. The high chloride concentration is also indicative of sea water intrusion as the study area is just 7 km west of the Arabia Gulf.

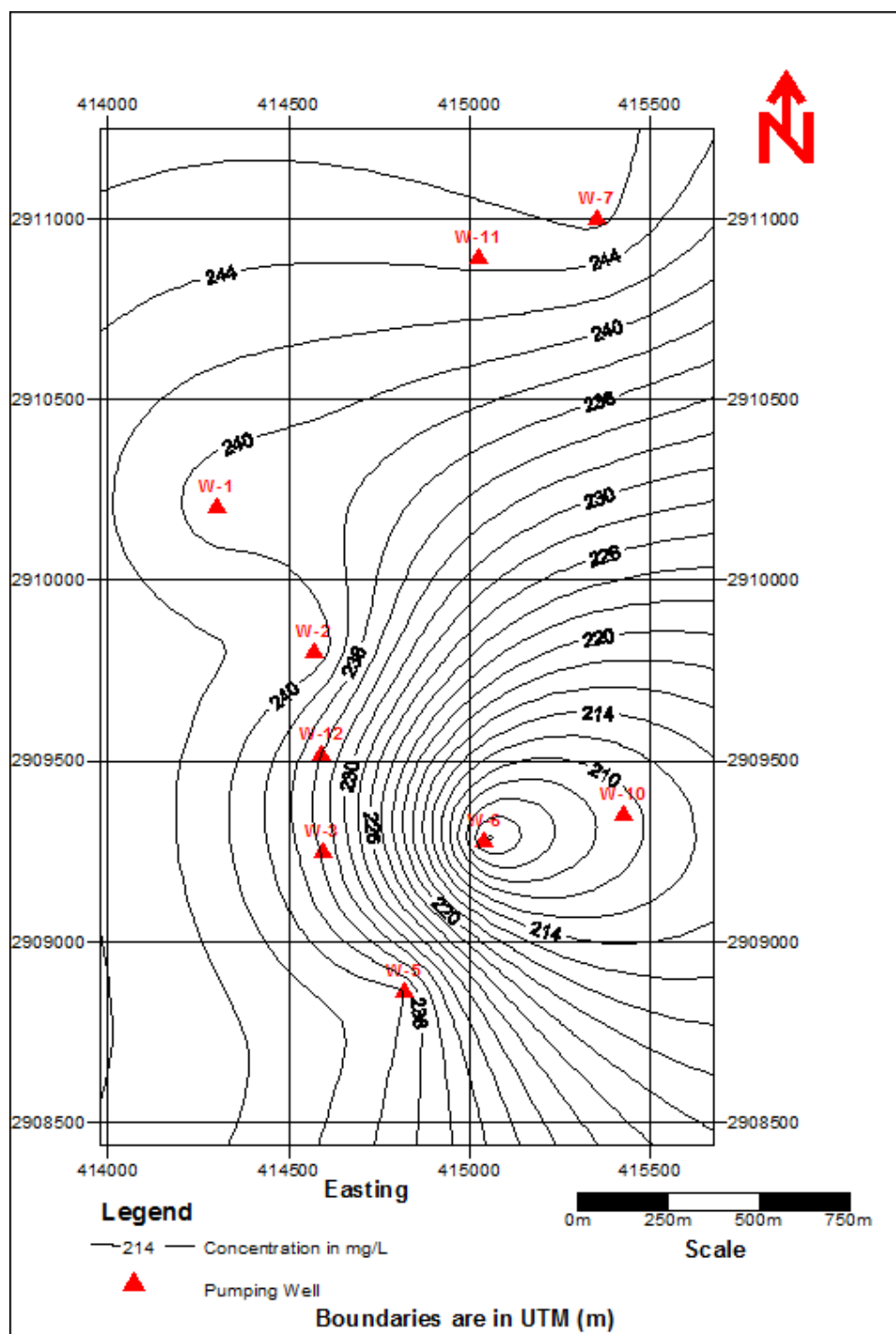


Figure 6.6: Bicarbonate concentration (mg/L) variation in the study area

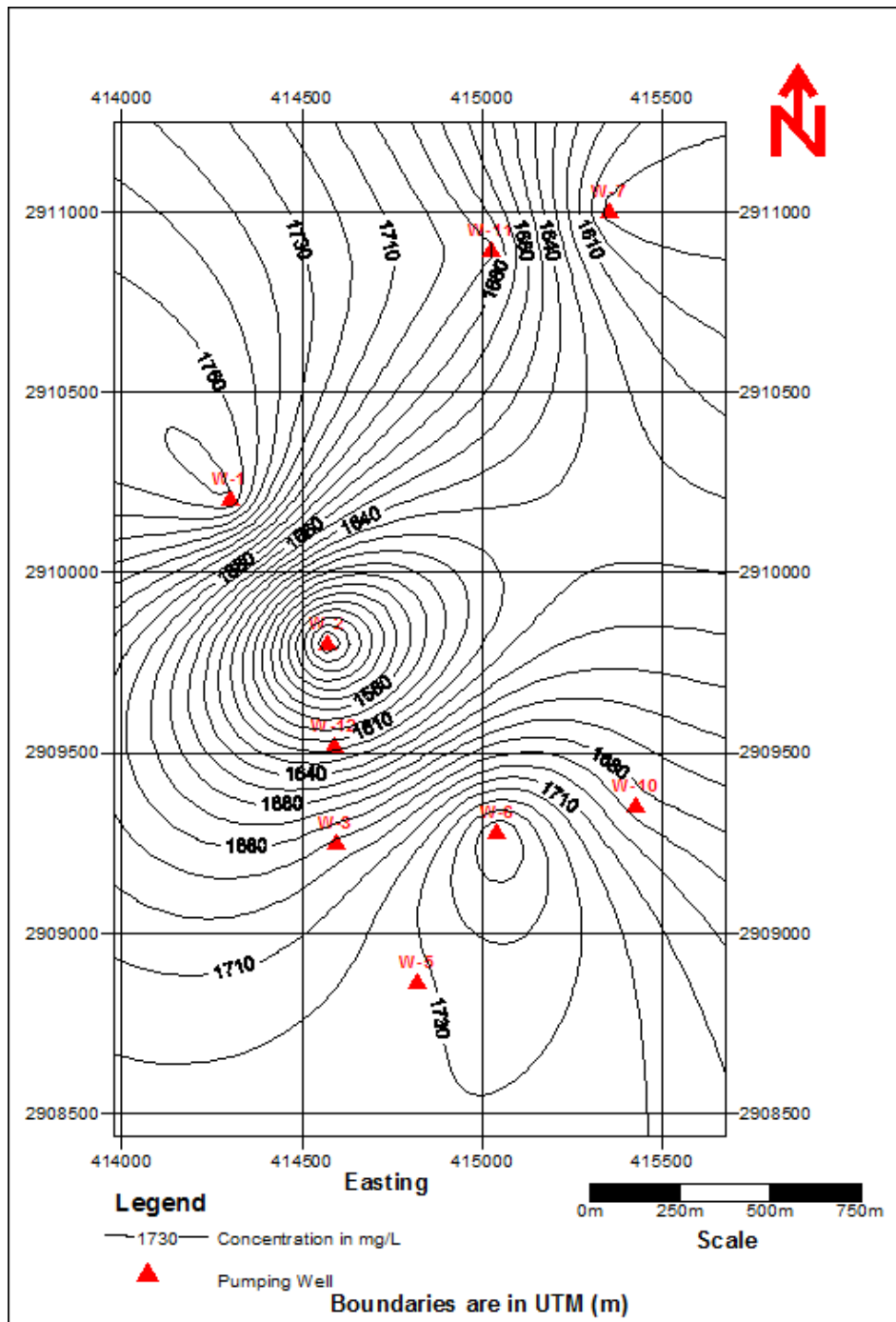


Figure 6.7: Chloride concentration (mg/L) variation in the study area

6.2.2.5 NITRATE (NO_3^-)

Nitrates are the most prevalent form of nitrogen in groundwater (Hem, 1985), and are the most commonly used indicator of contamination of groundwater from septic systems. Nitrate concentration in the groundwater samples ranges between 1.578 mg/L and 4.609 mg/L, with an average concentration of 3.178 mg/L. Figure 6.8 shows the distribution of nitrate in the study area. There is slightly higher concentration in areas to the south and central part of the study area, where faculty housing and academic buildings are located than other areas. Generally, the presence of nitrate in the groundwater of the study area is not unexpected due to the locally unconfined nature of Umm Er Radhuma aquifer, which is the source of groundwater in the study area. Therefore, the presence of nitrate in the groundwater indicates a possible contamination of the aquifer from sewage leaks.

6.2.2.6 SULPHATE (SO_4^{2-})

Sulphate concentration in the analyzed groundwater sample ranges between 803.2 mg/L and 935 mg/L, with an average concentration of 872 mg/L. The origin of most sulphate compounds in groundwater is the oxidation of sulphite ores (Hem, 1985), the presence of shales (Mathess, 1982), or leakage of industrial wastes. Sulphate concentration in excess of 205 mg/L will have a bitter taste and can produce laxative effect (Matthess, 1982). There is uniform distribution of sulphate in the study area (Figure 6.9).

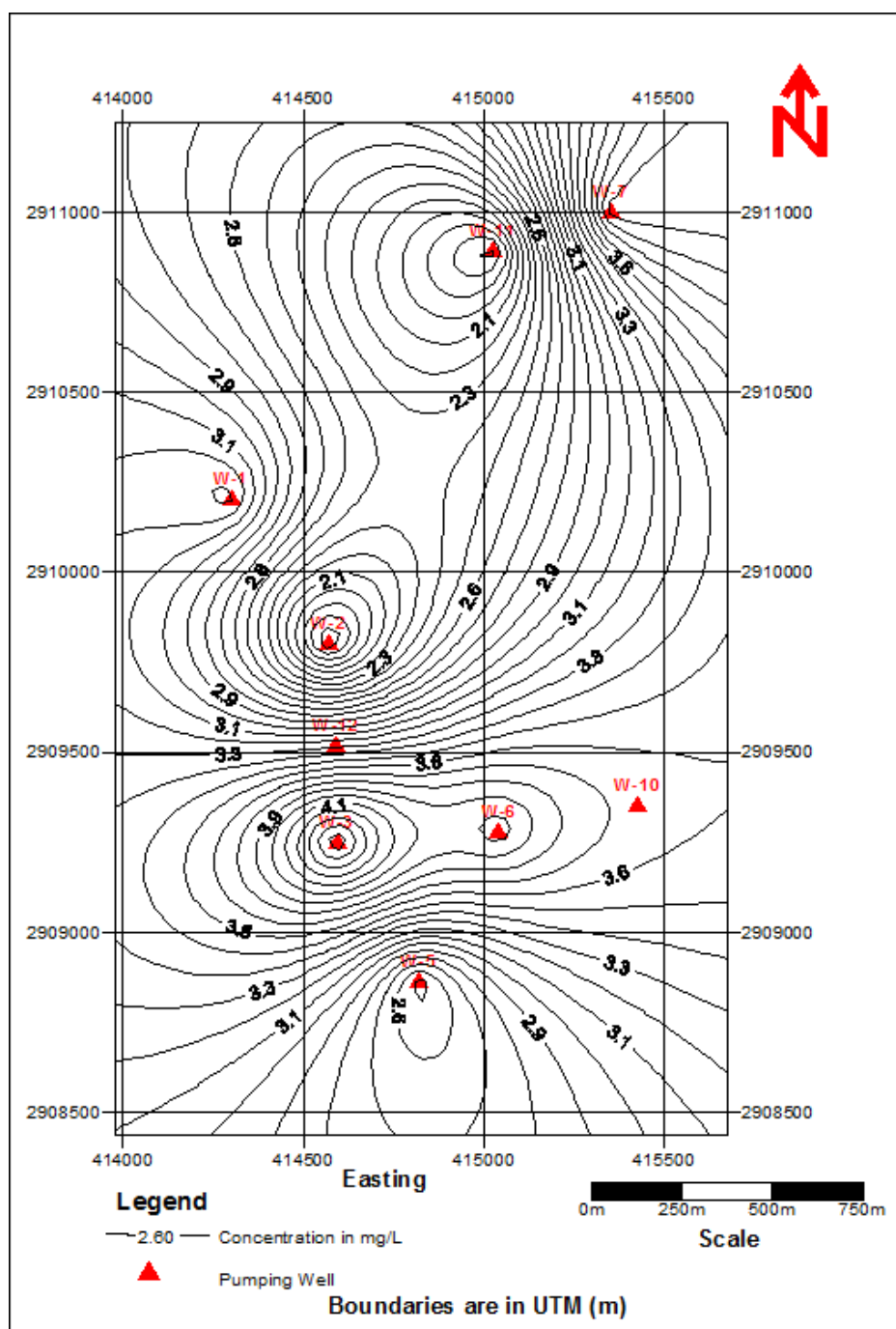


Figure 6.8: Nitrate concentration (mg/L) variation in the study area

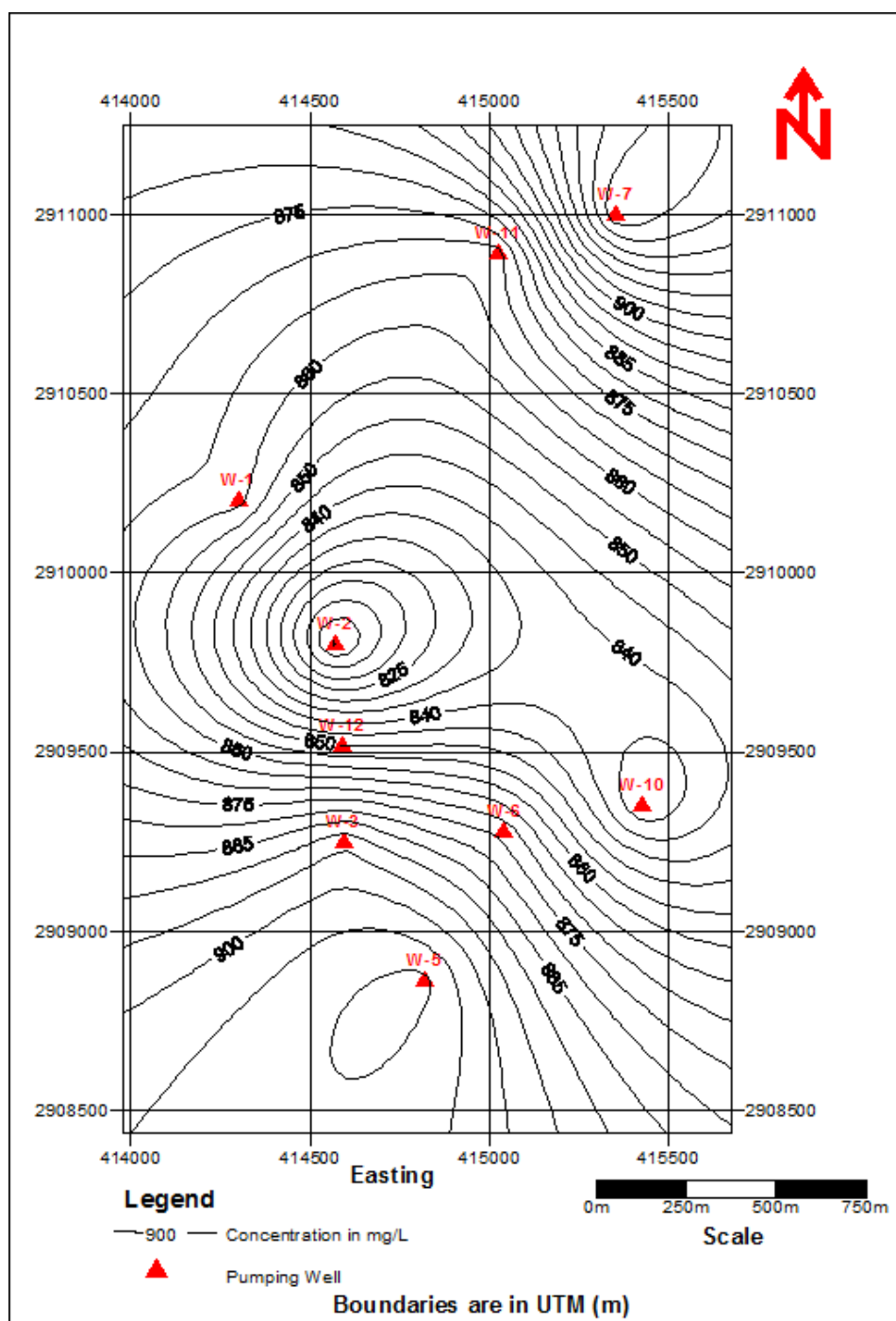


Figure 6.9: Sulphate concentration (mg/L) variation in the study area

6.2.2.7 COLIFORM BACTERIA AND E.COLI

Coliform bacteria are organisms normally found in the digestive tracts of livestock, humans, and birds (Hem, 1985). They are usually used as bacterial indicator species (Kehew, 2001). Coliform bacteria count in the collected groundwater samples ranges between 1.3×10^1 and 3.4×10^4 Most Probable Number (MPN) Index per 100 ml. Analysis for E.Coli yielded no-detection in all the sampled water. Coliform bacteria counts were found to be higher at the south and central part of the study area where the faculty housing and academic buildings are located (Figure 6.11). High bacteria counts in the sampled groundwater may be due to contamination from sewage that are poorly designed, improperly constructed, failing or located too close to the wells. The unconfined state of UER aquifer in the study area may have enhanced the transport of sewage into the groundwater.

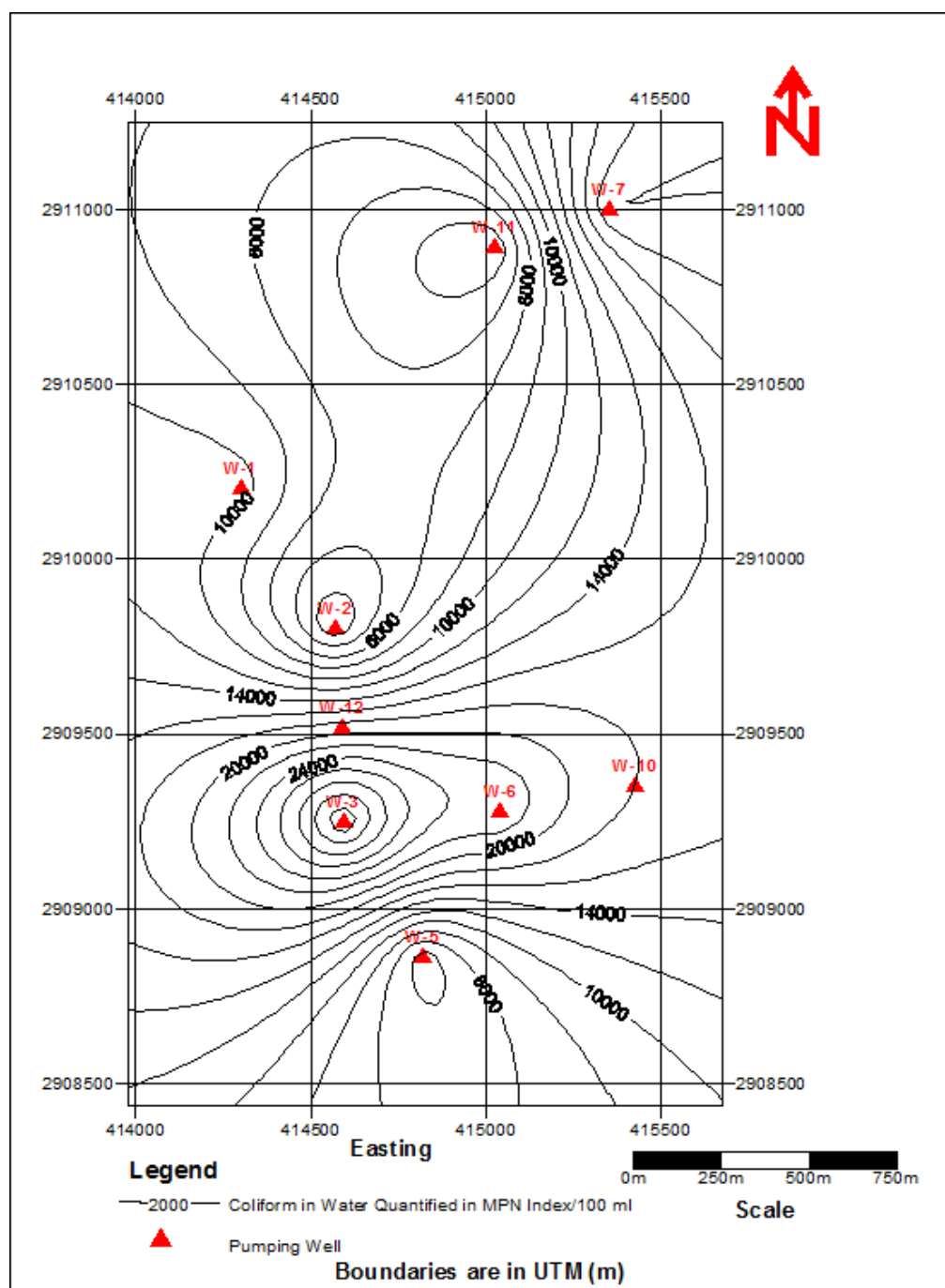


Figure 6.10: Distribution of coliform bacteria in the study area measured in Most Probable Number (MPN) Index per 100 ml

6.3 WATER QUALITY ANALYSES

6.3.1 CLASSIFICATION OF WATER BASED ON HYDROCHEMICAL DATA

Water classification has been done to understand the hydrochemical variation of the groundwater in the study area. Graphical methodologies were used to classify the water samples into homogeneous groups. Three methods are considered in this work and these include diagrams of Piper, Durov and Stiff. Rockworks Version 15 was used to generate the hydrochemical plots based on the groundwater chemistry of the study area.

6.3.1.1 PIPER DIAGRAM

Based on the four main cations (calcium, magnesium, and sodium + potassium) and the four main anions (bicarbonate, sulfate, chloride and nitrate), Piper (1944) proposed a trilinear diagram that permits the classification of waters, according to Langguth (1966) into seven types as shown in Figure 6.12. Major ions are plotted in the two basal triangles of the diagram as cation and anion percentages of milli-equivalent per liter. Total cation and total anion are each considered as 100 percent. The respective cation and anion locations for an analysis are projected into the diamond, which represents the total ion relationship. The central plotting field (diamond shaped) of the diagram is divided into seven areas and water is classified into seven types depending on the area in which the analyses fall. In this classification, alkali cation (Na^+ and K^+) are called primary constituents, and the alkaline earth cation (Ca^{2+} and Mg^{2+}) are called secondary constituents. The strong acid anions (SO_4^{2-} , Cl^- and NO_3^-) are treated as saline constituents, while CO_3^{2-} and HCO_3^- are termed as weak acids.

Groundwater in the study area fall in the g-sector of Langgurth division (Figure 6.13). The cation composition of the water ranges from Na-K dominated through a mix of Mg-Na+K dominated. The anion composition is chloride dominated. These indicate that groundwater in the study area is of alkaline type with prevailing sulphate and chloride levels.

6.3.1.2 DUROV DIAGRAM

Durov diagram is based on the percentage of the major ions in meq/L. Both the positive and the negative ion percentages total 100 %. The values of the cations are plotted on the triangle on the left side and the anions are plotted on the upper triangle and both are projected into the square of the main field. The advantage of this diagram is that it displays some possible geochemical processes that could affect the water genesis. Lloyd and Heathcoat (1985) classified the central square into 9 sectors, each signifying a certain process (Figure 6.14). Below is the summary of the classification of the divisions in Durov diagram as given by Lloyd and Heathcoat (1985):

Field (1): HCO_3^- and Ca^{2+} dominant, frequently indicates recharging waters in limestone, sandstone, and many other aquifers.

Field (2): This water type is dominated by Ca^{2+} and HCO_3^- . Association with dolomite is presumed if Mg^{2+} is significant. However, those samples in which Na is significant, an important ion exchange is presumed.

Field (3): HCO_3^- and Na^+ are dominant, indicates ion exchanged water, although the generation of CO_2 at depth can produce HCO_3^- where Na^+ is dominant under certain circumstances.

Field (4): SO_4^{2-} dominates, or anion discriminant and Ca^{2+} dominant, Ca^{2+} and SO_4^{2-} dominant, frequently indicates are charge water in lava and gypsiferous deposits, otherwise a mixed water or water exhibiting simple dissolution may be indicated.

Field (5): No dominant anion or cation indicates water exhibiting simple dissolution or mixing.

Field (6): SO_4^{2-} dominant or anion discriminant and Na^+ dominant; is a water type that is not frequently encountered and indicates probable mixing influences.

Field (7): Cl^- and Na^+ dominant are frequently encountered unless cement pollution is present. Otherwise the water may result from reverse ion exchange of Na-Cl waters.

Field (8): Cl^- dominant anion and Na^+ dominant cation, indicate that the ground waters be related to reverse ion exchange of Na-Cl waters.

Field (9): Cl^- and Na^+ dominant frequently indicate end-point waters.

Figure 6.15 shows the Durov diagram of the groundwater chemistry of the study area. According to Lloyd and Heathcoat (1985) hydrochemical classification using Durov diagram, groundwater in the study area is dominated by Ca^{2+} and CO_3^{2-} , with significant concentration of Na^+ and an important ion exchange presumed.

6.3.1.3 STIFF DIAGRAM

Figure 6.16 shows the Stiff diagram representation of the hydrochemical data of the study area. the horizontal distance from the vertical axis is based on the number of

milli-equivalent per liter of each anion and cation. As a standard, Ca, Mg, Na+K, Cl, SO₄ and HCO₃+CO₃ ions are considered for the diagram. All the analyzed groundwater samples have a similar signature. The Stiff diagram clearly indicates that the dominant cation is Na+K ion, while the dominant anion is Cl ion.

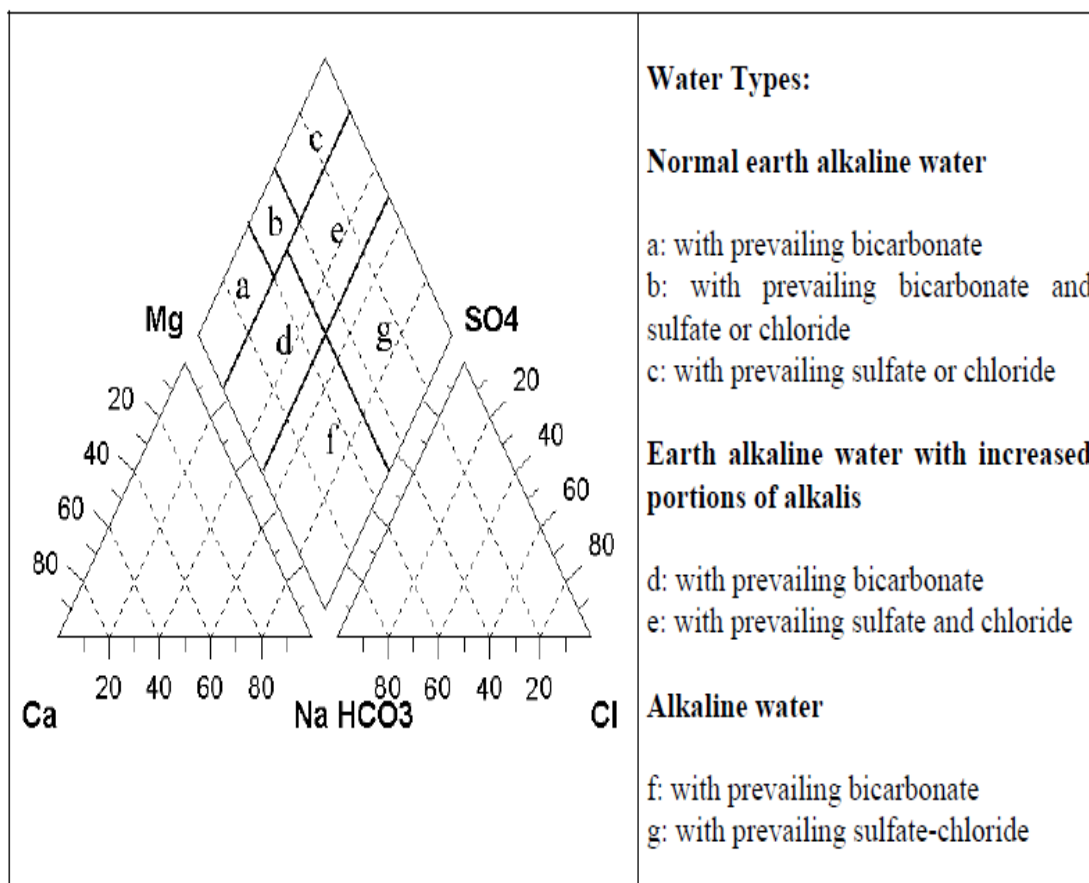


Figure 6.11: Piper trilinear diagram for hydrochemical facies modified by Langguth (1966)

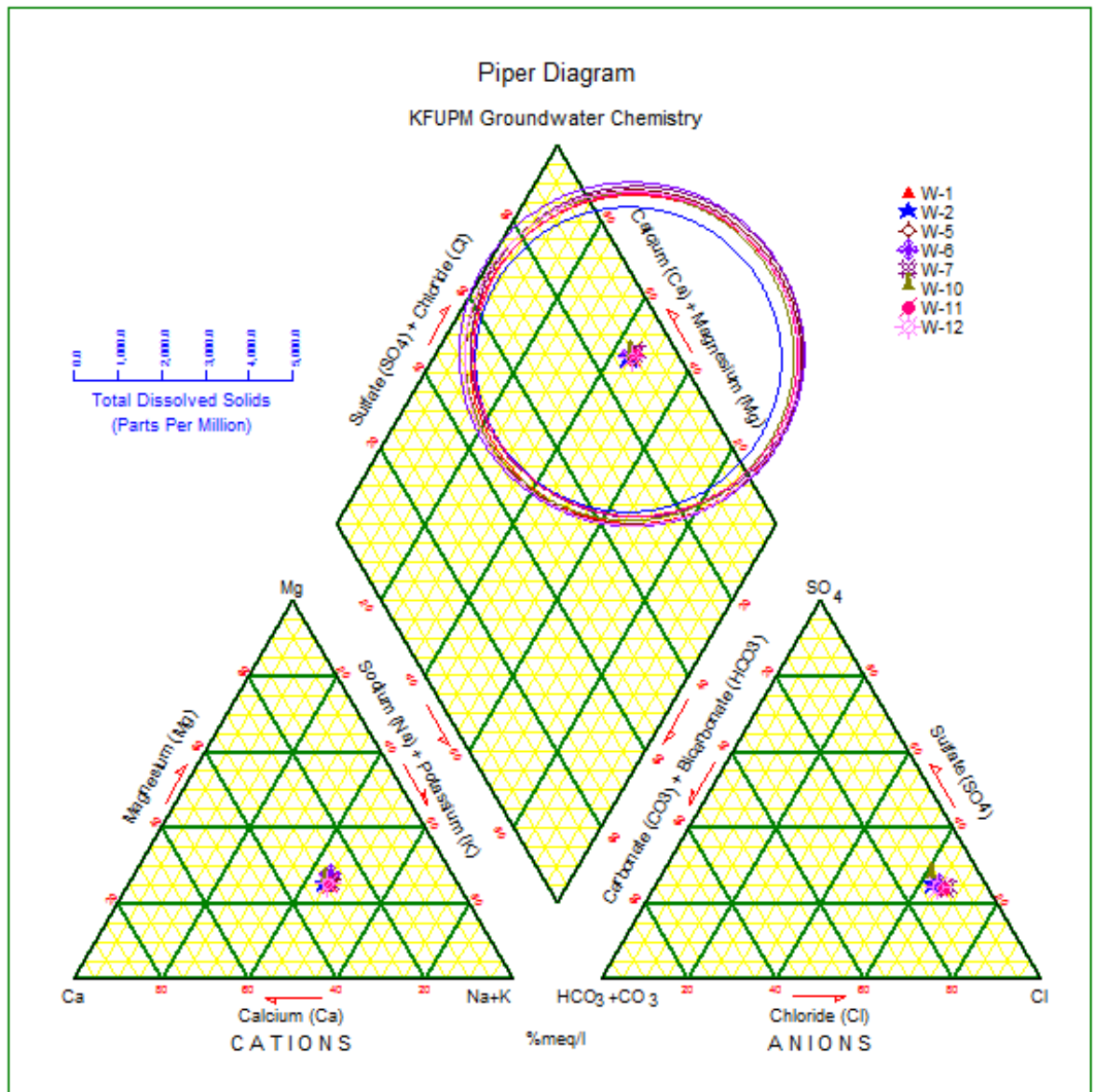


Figure 6.12: Piper diagram of groundwater samples collected from the study area

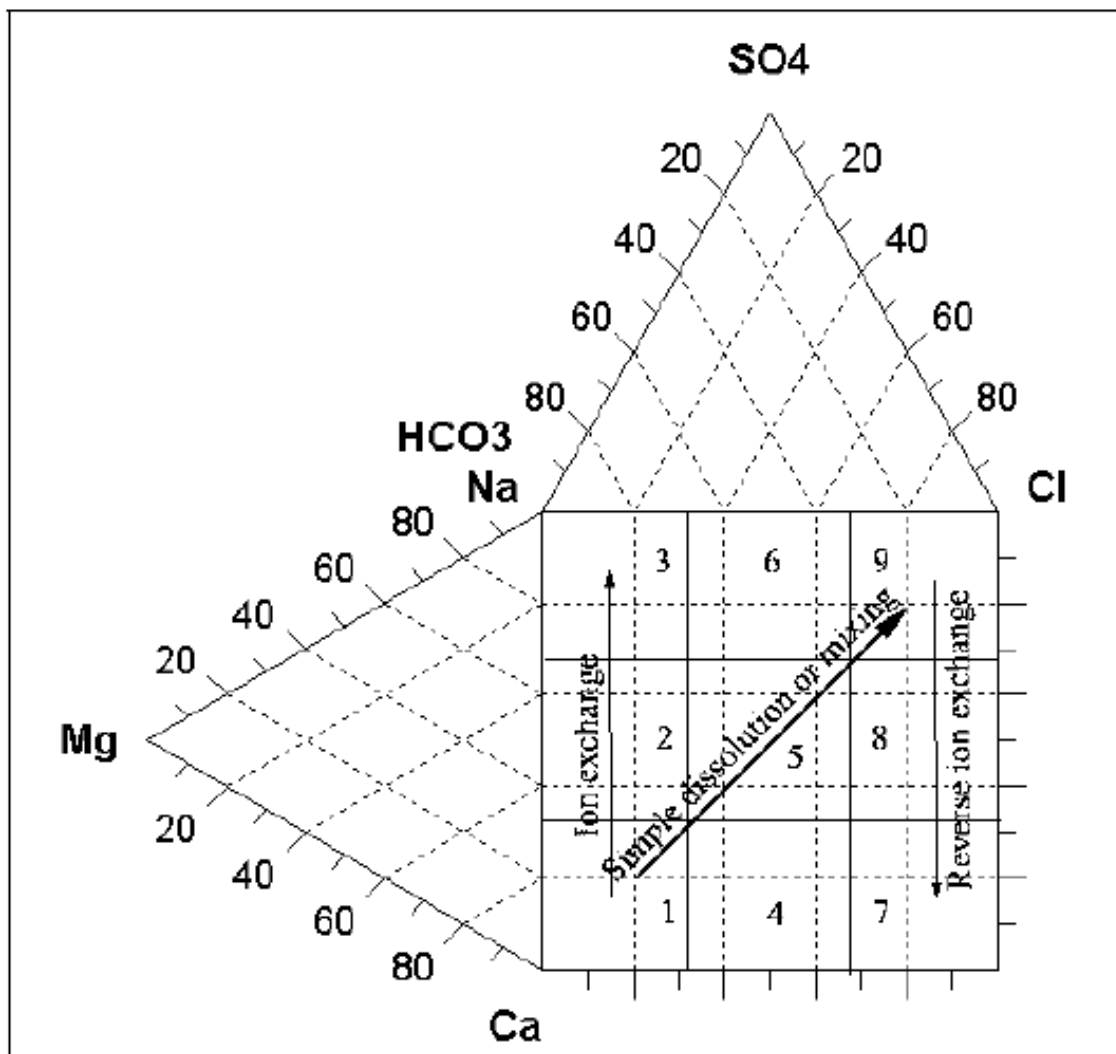


Figure 6.13: Index diagram for standard Durov diagram classification proposed by Lloyd and Heathcoat (1985)

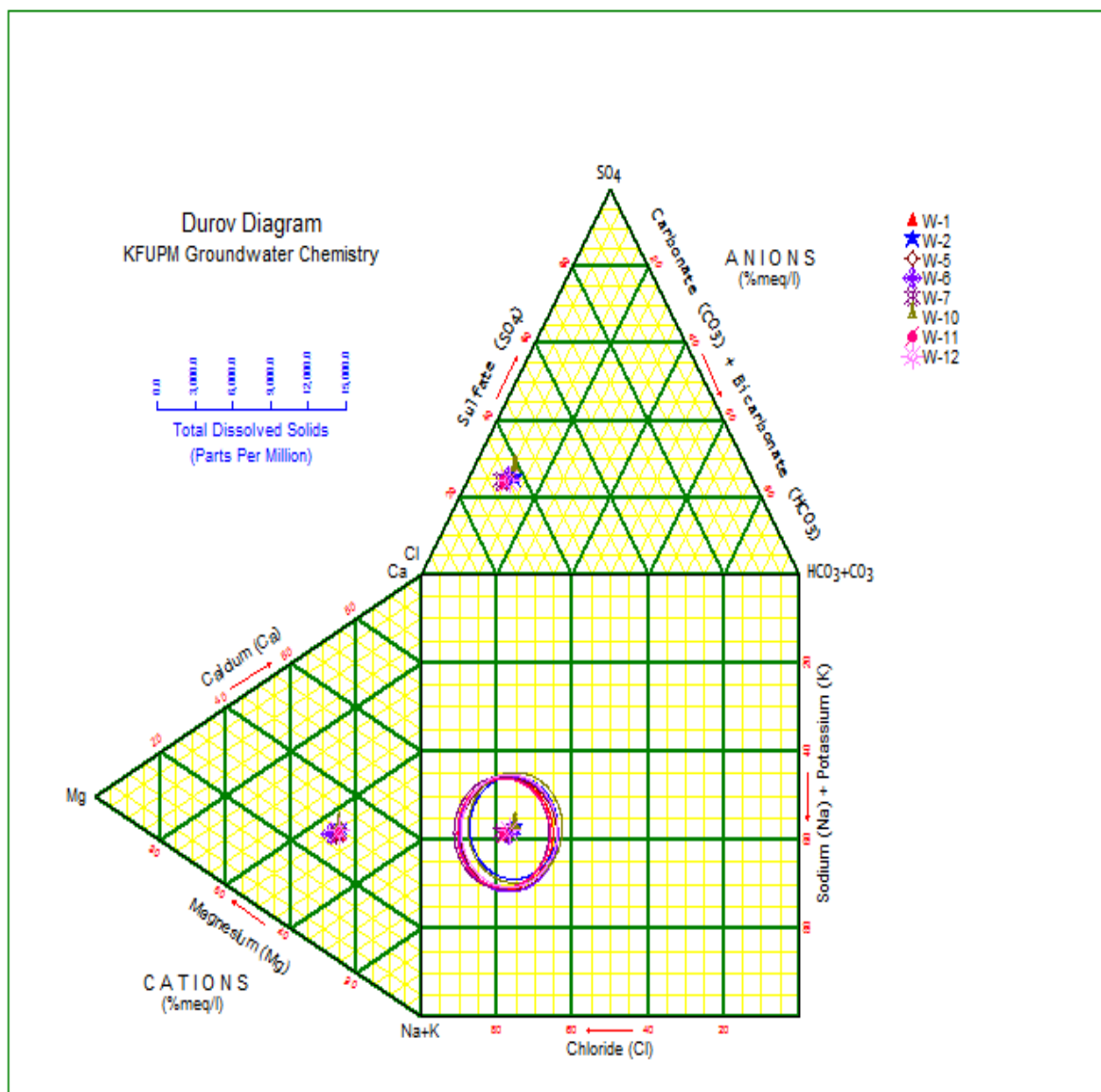


Figure 6.14: Durov diagram of groundwater samples of the study area

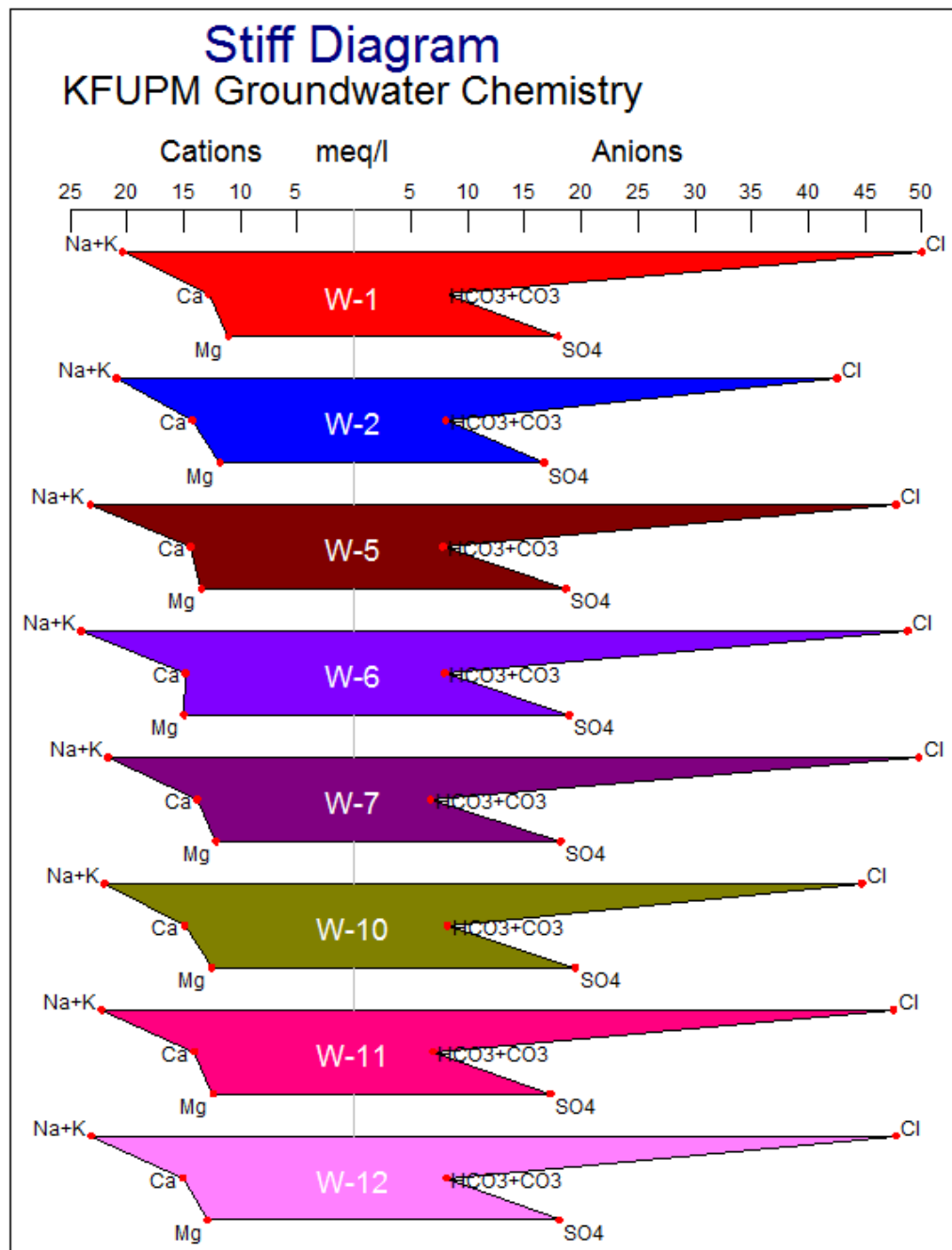


Figure 6.15: Stiff diagram of groundwater samples collected from the study area

6.4 WATER QUALITY STANDARDS

The primary use of water analyses in groundwater hydrology is for production of information concerning the water quality. The main objective of hydrogeochemical assessment is to determine groundwater suitability for different uses based on different chemical indices. In this research, assessment of suitability for drinking and irrigation was evaluated by comparing the hydrochemical parameters of groundwater in the study area with the prescribed specifications of US Environmental Protection Agency (EPA, 2004), World Health Organization (WHO, 2004) and Presidency of Meteorology and Environment (PME, 2003) – Saudi Arabian water quality standard (Table 6.4).

6.4.1 SUITABILITY FOR DRINKING

Drinking water requires high standards of physical, chemical and bacteriological purity. It should be electrically neutral and be fundamentally free from undesirable physical properties, cloudiness and objectionable odor and taste.

The first test conducted on the quality of water in the study area is comparison between the sum of concentrations of cations and anions in milliequivalent per liter (meq/L). The mg/L concentrations were converted to meq/L concentrations according to the following equation:

$$meq/L = \frac{mg/L}{formula\ weight/charge} \quad (6.1)$$

Given that water is electrically neutral, the ratio of the concentration sum of the cations to the anions should be unity. Table 6.5 gives the calculation based on the results of the groundwater chemistry of the study area. The range of acceptability of

Table 6.4: International standards for drinking water (values are in mg/L, unless indicated otherwise)

	International Standards		
	EPA, 2004	WHO, 2004	PME, 2003
TDS	500	1000	
EC(μ S/cm)		1500	500-1000
pH	6.5-8.5	<11	6-9
Sodium	20	200	
Calcium		200	75
Magnesium		150	30
Sulphate	250	500	250
Chloride	250	250	250
Nitrate	10	3	
Pb	0.015	0.01	0.01
Boron		0.3	
Iron	0.3		0.3
Zn	5	3	5
Mercury	0.002	0.01	0.001
As	0.05	0.01	0.1
Coliform Bacteria (per 100 ml)	0		
BOD			25

Table 6.5: Evaluation of electroneutrality of the groundwater in the study area

		Wells		W-1	W-2	W-5	W-6	W-7	W-10	W-11	W-12	Total(meq/L)
		Charges										
Cations (meq/L)	rCa++	12.8400	14.2550	14.4265	14.8675	13.8350	14.9590	14.0990	15.1015	114.3835		
	rK+	1.1194	1.1429	1.2270	1.2474	1.1505	1.1709	1.1628	1.2074	9.4283		
	rMg++	11.2233	11.9667	13.6317	15.1650	12.3192	12.7125	12.5833	13.0983	102.7000		
	rNa+	221.4400	227.5900	252.9250	262.1250	235.9000	239.4400	242.1650	252.0150	1933.6000		
	rFe+++	0.0000	0.0005	0.0010	0.0015	0.0000	0.0005	0.0000	0.0005	0.0040		
								Total Cation (meq/L)			2160.1158	
Anions (meq/L)	rF-	0.0461	0.0388	0.0371	0.0378	0.0473	0.0425	0.0411	0.0411	0.3317		
	rCl-	49.9155	42.4507	47.6620	48.6479	49.6338	44.6479	47.4366	47.6620	378.0563		
	rB-	0.0765	0.0655	0.0718	0.0703	0.0760	0.0705	0.0679	0.0714	0.5699		
	rNO ₃ -	0.0538	0.0255	0.0743	0.0396	0.0656	0.0655	0.0592	0.0266	0.4101		
	rSO ₄ --	8.9802	8.3667	9.3083	9.4906	9.0938	9.7396	8.6458	9.0417	72.6667		
	rHCO ₃ -	7.9567	8.0633	7.7967	7.9400	6.7133	8.2200	6.9733	8.1500	61.8133		
							Total Anion (meq/L)			513.8480		
							Cation/Anion ratio			4.2038		

cation/anion ratio is ± 0.05 . However, the cation/anion ratio of the groundwater in the study area equals 4.2038, which is clearly outside the acceptable range. This result indicates that the concentration of cations in groundwater in the study area is four times the concentration of anions. This further reflects that groundwater in the study area is impure.

The pH values of the groundwater in the study area fall within the allowable limits as specified by the international guidelines. Electrical conductivity (EC) drinking water guidelines present 500 – 1000 $\mu\text{S}/\text{cm}$ (PME, 2003) and 1500 $\mu\text{S}/\text{cm}$ (WHO, 2004) as desirable limits. WHO provides a guideline of 1000 mg/L for total dissolved solids (TDS). A comparison between the hydrochemical results in Table 6.2 and international standards in Table 6.4 reveals that groundwater in the study area exceeds the international regulation values or limits for drinking water for all the analyzed parameters. However, heavy metals were mostly undetectable and are therefore within the allowable limits.

According to EPA (2004) guideline, coliform bacterial count should be zero in drinking water. However, groundwater samples collected from study area show total coliform range of 1.3×10^1 and 3.4×10^4 MPN Index/100 ml.

6.4.1.1 HEALTH RISKS

One of the possible health implications that can result from consumption of groundwater resource at KFUPM can be that of hypertension resulting from daily and regular consumption of sodium-chloride containing water. According to Onugba et al. (1992), the presence of nitrate in groundwater sample may result in cyanosis or methemoglobinemia in infants under two years old. In addition to cyanosis, nitrate in

drinking water is also a probable factor in stomach cancer development (Forslund, 1986).

Intake of high level of sulphate in drinking water may result in dehydration and diarrhea in people not used to drinking water with high level of sulphate, with high sensitivity noticed in kids than adults (Tamil Nadu Report, 2008). Calcium have beneficial effects when ingested, however, very high concentrations of calcium may adversely affect the absorption of other essential minerals in the body. Laxative effect may result from consumption of magnesium in drinking water, especially where magnesium sulphate concentration is above 700 mg/L.

No health risk has been linked with consumption of coliform bacteria in drinking water. However, because coliform bacteria are commonly associated with sewage, the presence of coliform bacteria in drinking water indicates that other disease-causing organisms, such as pathogens, may be present.

6.4.2 SUITABILITY FOR IRRIGATION USE

Since groundwater in the study area is used for landscape irrigation, its suitability for irrigation purpose was assessed. The suitability of groundwater for irrigation is contingent on the effects on the mineral constituents of the water on both the plant and the soil. Parameters such as salinity hazard (electrical conductivity, EC), alkali hazard (sodium adsorption ratio, SAR) and magnesium hazard (MH) were used to assess the suitability of groundwater in the study area for irrigation purpose.

SAR and MH, proposed by Szabolcs and Darab (1964), are calculated according to the following equations (all concentrations are in meq/L):

$$SAR = \frac{Na}{\sqrt{(Ca + Mg)/2}} \quad (6.2)$$

$$MH = \frac{Mg}{Mg + Ca} \times 100 \quad (6.3)$$

Table 6.6 shows salinity and alkali hazards according to Richard (1954) classification, and magnesium hazard classified by Szabolcs and Darab (1964). The measured EC values and the calculated SAR and MH values for all the sampled wells are presented in Table 6.7.

Based on salinity hazard classification in Table 6.6, groundwater in the study area can be classified as unsuitable for irrigation purpose because the EC values for all the sampled wells are above the very high salinity hazard level of 2500 $\mu\text{S}/\text{cm}$. Water with alkali hazard index (SAR) of more than 26 is categorized as unsuitable for irrigation purpose based on Richard (1954) classification in Table 6.6. Groundwater samples from wells in the study area have alkali hazard which ranges between 62.85 and 67.65. For the fact that the calculated SAR values for the sampled water from all the wells in the study area are above 26, groundwater in the study area is unsuitable for irrigation use. However, magnesium hazard for all the wells, with a range of 46 to 50, falls within the permissible limit with respect to Szabolcs and Darab (1964) magnesium hazard classification. Therefore, groundwater in the study area is safe from magnesium hazard.

Table 6.6: Classification of salinity and alkali hazards (Richard, 1954) and magnesium hazard (Szabolcs and Darab, 1964)

Quality of water	EC ($\mu\text{S}/\text{cm}$)	SAR (eq/mole)	MH (%)
Excellent	<250	<10	
Good	250-750	10-18	
Doubtful	750-2250	18-26	
Unsuitable	>2250	>26	>50

Table 6.7: Measured EC values and calculated SAR and MH values of groundwater samples in the study area

Well Identification	EC ($\mu\text{S}/\text{cm}$)	SAR (eq/mole)	MH (%)
W-1	5440	63.83	47
W-2	5760	62.85	46
W-5	6090	67.52	49
W-6	5850	67.65	50
W-7	5510	65.24	47
W-10	5470	64.37	46
W-11	5740	66.29	47
W-12	6340	67.11	46

CHAPTER 7

RESULTS AND DISCUSSIONS

It is obvious that with the fast developments and expansions currently going on in KFUPM, the abstraction level will not remain at the rate of increase as proposed in Alternative Scheme II. Certainly, an increase in abstraction rate will occur, but the possibility of employing conservative measures as proposed in Alternative Scheme II should not be overlooked.

It is also very clear from historical changes in water level and salinity in the study area from 1967 until now, that serious negative impact has been put on the aquifer. Although the decline in water level in the aquifer during the last 45 years is limited (between 8-12m), the increase in groundwater salinity in the aquifer is from 2,800 mg/L to 4,200 mg/L. This indicates clearly that Umm Er Radhuma aquifer in the study area is seriously exhausted. Therefore, rate of abstraction should be carefully revised to reduce the rate of increase in salinity level for the sustainability of the aquifer.

Any increases in abstraction rates definitely are harmful for the sustainable development of aquifers. Notwithstanding, Alternative Scheme II still presents the best management measure as evident in the model results.

CHAPTER 8

CONCLUSIONS AND RECOMMENDATIONS

8.1 CONCLUSIONS

- (1.) At local scale, significant variations in hydraulic parameters were found. The general trend was such that the Umm Er Radhuma aquifer was highly transmissive along structural highs and not as transmissive at slopes.
- (2.) Groundwater quality of UER aquifer in the study area shows absolutely no variations in terms of ionic concentration and types of ions present in the water.
- (3.) The general trend of the increase in TDS is from the south and southwest to the north and northeast (towards the Arabian Gulf).
- (4.) Total abstraction from UER aquifer in the study area increased from 2.4 MCM in 1967 to 13.9 MCM in 2010, which represents an increase of about 480 %. Due to excessive pumping from UER, the average TDS level increased from 2,800 mg/L in 1967 to 4,200 mg/L in 2010 and the average decline in water level was approximately 8.5 m.

- (5.) Three different Alternative Development Schemes were formulated and analyzed to predict future responses of the calibrated model of the Groundwater Flow Model and Solute Transport Model for the planning period 2011 to 2030 (inclusive of both years):
- (I.) Alternative Scheme I assumed 600 liters per capita per day and an increase of 10% in the pumping over the 20-year planning period for irrigation water use. The results indicate that decline in water level would be about 5.4 m and the salinity level would be around 5,600 mg/L by year 2030.
 - (II.) Alternative Scheme II assumed conservative measures: 300 liters per capita per day and a decrease of 20% in pumping over the 20-year planning period for irrigation water use. The results indicate that decline in water level would be about 3m and the salinity level would be around 4,550 mg/L by year 2030.
 - (III.) Alternative Scheme II assumed continuation of the present trend of abstraction over the 20-year planning period. The results indicate that decline in water level would be about 4.1 m and the salinity level would be around 5,300 mg/L by year 2030.
- (6.) Analyses of the major anions and cations of groundwater in the study area reveal Na+K as the dominant cation. The order of abundance of the anions is $\text{Cl}^- > \text{SO}_4^{2-} > \text{HCO}_3^-$. Based on these analyses, groundwater in the study area can be classified as alkaline water with prevailing sulphate-chloride.

(7.) Hydrochemical assessments by comparison with international and local standards reveal that groundwater in the study area is unsuitable for drinking purpose. Richard (1954) salinity and alkali hazard classifications reveal that groundwater samples in the study area are not suitable for irrigation purpose. However, magnesium hazard classification by Szabolcs and Darab (1964) indicates that groundwater samples in the study area are within magnesium hazard permissible limits. These findings indicate that salinity is the principal concern in the groundwater of the study area. High salinity in the groundwater can be attributed to overexploitation and high evaporation rate in the study area.

8.2 RECOMMENDATIONS

The results of the study show that alternative II is the best alternative to protect the quality and water level of the aquifer. This shows that water conservation by reduction of 20% in irrigation water use over the 20-year planning period is essential for protection of long-term groundwater quality and level in the study area. It is recommended that studies of water conservation for irrigation purposes should be investigated. For example, use of treated wastewater could be a good source to green the University in order to preserve the UER for more important purposes. Replacement of grasses with granites in some parts of the campus could also serve as an alternative option.

The impact of employing the implementation of domestic water conservation measures, which was initiated by the Ministry of Water and Electricity, should be evaluated. It would seem that implementing these would be beneficial because more than 90% of domestic water in KFUPM is pumped from groundwater. Further,

construction of new groundwater well may be beneficial if the new well is located in the south of the study area, where cones of depression are relatively minimal. Any plan to locate a new well in the northeast of the study area is strongly discouraged.

Residents and staffs should make every effort to conserve water and to use it only for those activities identified as appropriate, such as: laboratory usage, cooking, operation of central air-conditioning units, house cleaning, personal hygiene, general kitchen use and campus fire extinguisher system. Specifically, residents and staffs can help rationalize water consumption by acting upon the advice contained in Section 4.1 of KFUPM Water Usage and Conservation Regulations (2000), which are summarized as follows:

- (I.) It should be ascertained that taps are off before leaving home.
- (II.) Regular check of leaks both inside and outside home and in the laboratories should be conducted and any report leak should be reported immediately.
- (III.) Water should not be allowed to run continuously while washing, shaving or brushing
- (IV.) Bucket of water should be used in washing cars and floors instead of hose pipe
- (V.) Fruits and vegetables should be cleaned in water-filled containers rather than under running water
- (VI.) Frozen food should be thawed in good time to avoid defrosting it under running water
- (VII.) Careful and frequent checks should be made on garden irrigation
- (VIII.) Children should not be allowed to play with irrigation facilities

- (IX.) Before leaving on vacation, residents should ask a fellow member of the staff or faculty to look after the house while he is away so that leaks or other potentially damaging occurrences can be detected and reported to the Maintenance Department.
- (X.) Supervisors should take the lead by reminding employees of the vital need to conserve water and to report any instances of leakage or damage to the water supply network to the Maintenance Department.

REFERENCES

1. Abderrahman, W. A. and M. Rasheeduddin 1994 Future Groundwater Conditions under Long-term Water Stresses in an Arid Urban Area, Water Resources Management, 8, pp. 245-264.
2. Abderrahman, W. A., Abdalla S. E., Ibrahim M. A. and Eqnaibi S. E., 2007 Management of Groundwater in Urban Centers: a case study of Dammam Metropolitan Area. The Arabian Journal for Science and Engineering, Vol. 32, pp. 49-63.
3. Abu-El-Sha'r, W. Y. and Hatamleh, R. I., 2007 Using Modflow and MT3D Groundwater flow and Transport Models As a Management Tool for the Azraq Groundwater System. Jordan Journal of Civil Engineering, Volume 1, No. 2, pp. 153 – 172.
4. Al-Amoud A. I., 2010 Guiders' Manual to Estimate Water Requirements for Crops in Saudi Arabia. Submitted to King Abdullah City for Science and Technology (KACST), Riyadh.
5. Al-Fares, A.A., Bouman, M., Jeans, P. 1998 A New Look at the Middle to Lower Cretaceous Stratigraphy, Offshore, Kuwait. – GeoArabia, v. 3, no. 4:543-560.
6. Alhajjar, B.J., Chesters, G., and Harkin, JM., 1990 Indicators of Chemical Pollution from Septic Systems, Groundwater, vol. 28, No.4, pp.559-568
7. Al-Hassoun, Saleh A. 1996 Prediction of the Effect of Pumping on Al-Wasia Well Field. Eng. Sci. (1), pp. 25 – 37.
8. American Public Health Association (APHA), 1995 Standard Methods for Examining Water and Waste Water Analysis, 20th edition. Washington, DC, USA.
9. Anderson, M. P., and Woesner, W.W., 1992 Applied groundwater modeling, Academic Press, San Diego, California, 381p
10. Backiewicz, W., D. M. Milne, and M. Noori, 1982 Hydrogeology of Umm Er Radhuma aquifer, Saudi Arabia, with reference to fossil gradients, Quarterly Journal. of Engineering Geology, v. 15, pp. 105-126.
11. Bahroudi, A., 2003 The Effect of Mechanical Characteristics of Basal Decollement and Basement Structures on Deformation of the Zagros Basin – Comprehensive Summaries of Uppsala Dissertations from the Faculty of Science and Technology, 836:43.

12. Bayer, H.J., Hoetzel, H., Jado, A.R., Roscher, B., Voggenreiter, W., 1988 Sedimentary and structural evolution of the northwest Arabian Sea margin – Tectonophysics, 153:137-151.
13. Beaumont, P., 1977 Water Development in Saudi Arabia. Geog. Jour. 143:42 – 60.
15. Bureau De Recherche Geologiques et Mineres (BRGM), 1977 Al-Hassa Development Project: Groundwater Resources Study and Management Program: Unpublished report to Ministry of Agriculture and Water, Riyadh, Saudi Arabia, 4 Vols.
16. Campus Water Utilization Committee Report, KFUPM, 2000 Water Usage & Conservation Regulations for the KFUPM Campus, pp. 11-13
17. Cavalier, C., Al Salatt, Y., 1970 Geological Description of the Qatar Peninsula. – Bureau de Recherches Géologiques et Minières, Paris.
18. Eccleston, B.L., Pike, J.G., Harhash, I., 1981 The Water Resources of Qatar and their Development – Ministry of Industry and Agriculture Technical Report, 5.
19. Edgell, H.S., 1990b Evolution of the Rub'al Khali desert - Journal of King Abdel Aziz University. – Earth Science, Special Issue, Earth Science, 3:109-126; Jeddah.
20. El-Asa'Ad, M., 1983a Lithostratigraphy of the Aruma Formation in Central Saudi Arabia – in Abed, A.M., Khaled, H.M. (Eds.), Geology of Jordan, Proceedings of the first Jordanian Geological Conference. – Jordanian Geologists Association: 72-86.
21. El-Asa'Ad, M., 1983b Bio- and chronostratigraphy of the Aruma Formation in Central Saudi Arabia – in Abed, A.M., Khaled, H.M. (Eds.), Geology of Jordan, Proceedings of the first Jordanian Geological Conference. – Jordanian Geologists Association: 87- 111.
22. Environmental Protection Agency (EPA) US, 2004 2004 Edition of the Drinking Water Standards and Health Advisories, Office of water, US Environmental Protection Agency, EPA 822-R-04-005
23. Flack, J. E., 1981 Residential Water Conservation, Journal of the Water Resources Planning and Management Division, (ASCE), Vol. 107, No WR1, PP. 85-95.
24. Forslund, J., 1986 Groundwater quality today and tomorrow. World Health Statist. Quart. 39p.

25. Gesellschaft für Technische Zusammenarbeit (GTZ), 2006 Investigations of updating groundwater mathematical model(s) for the Umm Er Radhuma and overlying aquifers submitted to Ministry of Water and Electricity, Saudi Arabia. Volume 11, pp. 1-67
26. Government of Tamil Nadu Water Resources Department, 2008 Sulphate in groundwater. Tamil Nadu Report, State Ground & Surface Water Resources Data Center, Chennai, India
27. Groundwater Development Consultants (GDC), 1980 Umm Er Radhuma Study: Bahrain Assignment: Demeter House, Station Road, Cambridge, CBI 2RS, Unpublished report to Ministry of Agriculture and Water, Riyadh, Saudi Arabia.
28. Hem, J. O., 1985 Study and the interpretation of chemical characteristics of natural water, (3rd ed), USGS WSP 2254, Washington, D.C pp 263.
29. Hoetzi, H., 1995 Groundwater recharge in an arid karst area (Saudi Arabia) – in ADAR, E., Leibundgut, C. (Eds.), Application of Tracer in Arid Zone Hydrology. – 232:195-207; Vienna.
30. Hoetzi, H., Job, C., Moser, H., Rauert, W., Stichler, W., Zoetl, J.G., 1980 Isotope methods as a tool for Quaternary studies in Saudi Arabia – Arid-Zone Hydrology: Investigations with Isotope Techniques: 215-235; Vienna.
31. Hoetzi, H., Wohnlich, S., Zoetl, J.G., Benischke, R., 1993 Verkarstung und Grundwasser im As Summan Plateau (Saudi Arabien) – Steir. Z. Hydrogeologie, 44:5-158.
32. Italconsult, 1969 Water and agricultural development studies for area IV., Eastern Province, Saudi Arabia: Unpublished report to Ministry of Agriculture and Water, Riyadh, Saudi Arabia.
33. Kehew, A.E., 2001 Applied chemical hydrogeology, Printice Hall Inc, NJ, USA.
34. King Fahd University of Petroleum and Minerals (KFUPM), 2009 Groundwater Study for the Dammam-Khobar-Dhahran Metropolitan Area Unpublished Report prepared for Al-Hejailan for Engineering Consultants, Khobar, Saudi Arabia.
35. Lloyd, J. W. & Heathcoat, J. A., 1985 Natural inorganic Hydrochemistry in Relation to Groundwater, Groundwater. An Introduction, Oxford University Press, New York, pp. 131-133
36. Mathhes, G., 1982 The properties of Groundwater, John Wiley & Sons, New York. 397p

37. Ministry of Agriculture and Water (MAW), 1988 Climatic Atlas of Saudi Arabia, Riyadh.
38. Kresik, N., 1997 Quantitative Solution in Hydrogeology and Groundwater Modeling. Lewis Publishers, Boca Raton, pp. 303-330.
39. Onugba, A.; Blavoux, B.; Guirand, R. and Travis, Y., 1992 Nitrate pollution of groundwater in Gongola State, Nigeria. Journal of Mining and Geology, Vol. 28, No. 2, pp. 317 – 323.
40. Powers, R.W., 1968 Arabie Seoudite – Lexique stratigraphique Internationale, 3, 10b:1- 177.
41. Powers, R. W., Ramirez L. F., Redmond C. D., and Elberg E. L., 1966 Geology of the Arabian Peninsula, U.S. Geological Survey, Professional Paper 560-D, New York, USA, 147 p.
42. Presidency of Meteorology and Environment (PME), 2003 Environmental Protection Standards, Document No. 1409-01, Ministry of Defense and Aviation Kingdom of Saudi Arabia.
43. Richards L. A, 1954 Diagnosis and improvement of saline alkali soils: Agriculture, vol 160. Handbook 60, US Department of Agriculture, Washington DC
44. Sadiq, A. M., Nasir, S.J., 2002 Middle Pleistocene karst evolution in the State of Qatar, Arabian Gulf – Journal of Cave and Karst Studies, 64:132-139.
45. Shampine, W.J., Dincer, T., Noory, M., 1979 An evaluation of isotope concentrations in the groundwater of Saudi Arabia – Isotope Hydrology, 2:443-463; Vienna.
46. Szabolcs I., Darab C., 1964 The influence of irrigation water of high sodium carbonate content of soils. In: Proceedings of 8th International Congress of Isss, Trans, vol II, pp. 803–812
47. Wagner, W., Geyh, M. A., 1999 Application of Environmental Isotope Methods for Groundwater Studies in the ESCWA Region – Geol. Jahrbuch Reihe C, 67:129
48. Weijermars, R., 1999 Quaternary Evolution of Dahat Zulum (Half Moon Bay) Region Eastern Province, Saudi Arabia – GeoArabia, v. 4, no. 1:71-90; Manama.
49. Whybrow, P. J., McClure, H. A., 1981 Fossil mangrove roots and paleoenvironments of the Miocene of eastern Arabia – Palaeogeography, Palaeoclimatology, Palaeoecology, 32:213-225.

50. World Health Organization (WHO), 2004 Guidelines for Drinking Water Quality, Vol. 1 Recommendations (3rd edn). WHO, Geneva.
51. Ziegler, M. A., 2001 Late Permian to Holocene Paleofacies Evolution of the Arabian Plate and its Hydrocarbon Occurrences – GeoArabia, v. 6, no. 3:445–504; Manama.

APPENDICES

**Appendix A: History of groundwater wells at KFUPM provided by KFUPM
Maintenance Department**

PRODUCTION HISTORY DATA							
Well	Easting	Northing	Year drilled	Year cancelled	Total Depth (m)	Static Water Level(m)	Capacity (m ³ /day)
W-1	414299.91	2910207.29	1967	Still Existing	146	1967: 70.12 1990: 76.00	2180
W-2	414569.39	2909808.62	1974	Still Existing	121	59.45	2180
W-3	414592.98	2909252.47	1974	Still Existing	117	58.00	5451
W-4	414221.82	2908686.19	1976	2003	110	1976: 55.18 1984: 57.00	5451
W-5	414819.14	2908867.26	1978	Still Existing	155	61.00	2180
W-6	415042.87	2909283.51	1978	Still Existing	154	1978: 50.30 1989: 54.50	5451
W-7	415353.67	2911004.70	1979	Still Existing	150	1979: 39.93 1990: 49.00	5451
W-8	414299.09	2910769.49	No Data	No Data	No Data	No Data	No Data
W-9	414297.79	2910361.96	1967	2003	120	69.00	4361
W-10	415427.70	2909355.29	1995	Still Existing	120	52.00	5451
W-11	415026.14	2910895.04	2004	Still Existing	150	55.00	4361
W-12	414427.00	2909510.00	1998	Still Existing	120	60.00	5451

Appendix B: Faculty (including families) and student on-campus population at KFUPM from year 2003 to year 2010 provided by KFUPM Faculty Housing Department and Student Housing Unit, respectively

Year	Population of Faculty (including Families) on Campus	Population of Students on Campus
2003	4051	4297
2004	4136	4379
2005	4248	4506
2006	4113	4627
2007	4119	4821
2008	4082	4951
2009	4211	4971
2010	4535	5175

VITAE

Tajudeen Iwalewa was born in Lagos, Nigeria. He completed his high school education at Boys' Academy, Lagos, Nigeria. He joined the University of Jos, Nigeria, in year 2000 and graduated with a B.Sc. (Hons) in Geology and Mining. He worked in the industry for a couple of years before joining the Earth Sciences Department, King Fahd University of Petroleum and Minerals (KFUPM), Dhahran, Saudi Arabia, in year 2009. At KFUPM, he participated in a number of research projects in the areas of groundwater studies and marine EIA. Under the supervision of Dr. Mohammad Makkawi, he graduated with a M.S. in Environmental Science from KFUPM.